Valdis V. Liepa
University of Michigan
November 1980

Interaction Application Memos

Memo 35

Scale Model Measurements of the F-16A

ABSTRACT

Frequency domain data are presented for the surface currents and charges measured in an anechoic chamber on F-16A models to simulate the aircraft response in free space environment. Models 1/48 and 1/32 in scale were measured over the frequency range 118 to 4400 MHz, simulating 2.46 to 91.7 MHz full scale. A total of 78 measurements are presented. These include eight test points measured on the 1/48 and 1/32 scale models and three excitations chosen to correspond to those used in the ATHAMAS I (HPD) and ATHAMAS II (VPD) full scale measurements.

CONTENTS

PREFACE

The author is indebted to C. Bickley, D. Brown and R. Wang who assisted with the measurements, J. Travis who supervised the measurements and was responsible for the scheduling, W. Rasey who typed the manuscript and, last but not least, W. Prather of AFWL/NTMOP for his support and encouragement.

SECTION I

INTRODUCTION

The data presented here were obtained for the Air Force Weapons Laboratory and TRW Systems to determine the surface response extrapolation function [1] for the F-16A aircraft. The test points and excitation conditions were therefore chosen to correspond to those of the full scale measurements made in the ATHAMAS I (Horizontally Polarized Dipole) and ATHAMAS II (Vertically Polarized Dipole) simulators at Kirtland AFB.

Data are presented for eight locations or test points on the aircraft under three different excitation conditions: (i) top incidence, E parallel to the fuselage; (ii) top incidence, E perpendicular to the fuselage; and (iii) nose-on incidence, E vertical. The measured quantities are the axial surface current density component J_a, the circumferential surface density component J_c, and the normal electric field component E_n. Of the 72 measurement situations possible, 39 were selected, and since the measurements were made on two different size scale models, a total of 78 data sets were generated. The results are presented in the form of amplitude and phase plots as functions of the full scale frequency, and have been furnished to the AFWL and TRW in digital form on punched cards for further analysis.

---

1. Carl E. Baum, "Extrapolation Techniques for Interpreting the Results of Tests in EMP Simulators in Terms of EMP Criteria," AFWL Sensor and Simulation Note 222, 1977.

SECTION II

MODELS

The two scale models of the F-16A aircraft that were selected were 1/48 scale (Scalecraft SC-4010) and 1/32 scale (Minicraft 100). Each came in the form of a plastic kit with a complement of armament that was full apart from the B-61 weapon. The models were good scale replicas of the F-16A, but did require some modification to make them electrically equivalent to the aircraft used in the full scale tests at AFWL. These modifications included cutting back the nose to STA:F60 to simulate the non-metallic radome, adding a metallic pitot tube, and modelling the radar antenna on the smaller model (the larger one had the radar antenna included in the kit). The cockpit canopies were also removed, since this is non-conducting on the actual aircraft. Both models had Sidewinder missiles (included in the kits) on each wing tip, but from the sketches and photographs supplied by AFWL it was necessary to construct models of the B-61 weapon and pylon that were attached under the right wings only.

After the models were assembled and the above modifications made, the joins and any surface imperfections were filled in with auto body putty, which was then filed and sanded to a smooth surface. Apart from the radome and canopy, the entire aircraft was regarded as metallic, and several coats of silver paint (Dupont No. 4817) were applied to the models to make them conductive. Finally, the lengths

and wingspans of the models were very carefully measured to determine the scale factors to be used in translating the measured frequencies to the full scale ones. The scale factors are listed in Table 1. Figure 1 gives pertinent aircraft dimensions used in preparation of the models.

Table 1

F-16 Model Scale Factors

Model	Length (cm)	Wing Span (cm)	Fuselage Scale*	Wing Span Scale*
Large (L)	46.14	31.39	1/32.70	1/31.89
Small (S)	30.78	20.82	1/49.01	1/48.09

*The scale factors are based on full scale dimensions of overall length 15.085 m and width 10.008 m, including Sidewinder missiles.

Models such as those used here are seldom perfect replicas of the full scale aircraft. As seen from Table 1, the scale factors derived from the fuselage length and the wingspan differ slightly, and though we could use the average to process the data, it is possible to obtain more accurate results by using the scale factor for that portion of the structure which supports the measured field. Thus, for the axial current on top of the fuselage (top incidence, E parallel to fuselage), the fuselage scale factor was used in processing the data, whereas for the circumferential current on top of the fuselage (top incidence, E perpendicular to fuselage) the scale factor derived from the wingspan is appropriate.

Figure 2 is a photograph of the large (1/32) model, and Figure 3 is a closeup showing the bulkhead, radar and pitot tube. The diameter of the pitot tube is not to scale. We initially used a wire that did have the right diameter, but it was so fragile that it kept getting bent when the model was handled. It is not felt that the larger diameter has a measurable effect on the electromagnetic response of the aircraft.

SECTION III

MEASUREMENTS AND DATA

3.1 Facility and Instrumentation

The measurements were made in the Radiation Laboratory's anechoic chamber, a facility especially designed, constructed, and instrumented for this type of surface field measurement. The measurement procedures were similar to those used in previous programs [2 through 7] apart from changes resulting from the continued upgrading of the facility and the measurement techniques.

---

2. Valdis V. Liepa, "Sweep Frequency Surface Field Measurements," University of Michigan Radiation Laboratory Report No. 013378-1-F; Sensor and Simulation Note 210, 1975.

3. Valdis V. Liepa, "Surface Field Measurements on Scale Model EC-135 Aircraft," University of Michigan Radiation Laboratory Report No. 014182-1-F; Interaction Application Memo 15, 1978.

4. Valdis V. Liepa, "Surface Field Measurements on Scale Model E-4 Aircraft," University of Michigan Radiation Laboratory Report No. 014182-2-F; Interaction Application Memo 17, 1978.

5. Valdis V. Liepa, "Surface Field Measurements on Scale Model F-111 Aircraft," University of Michigan Radiation Laboratory Report No. 014449-1-T; Interaction Application Memo 13, 1977.

6. Valdis V. Liepa, "Current and Charge Measurements on Scale Model E-3A Aircraft," University of Michigan Radiation Laboratory Report No. 015814-1-F; Interaction Application Memo 29, 1978.

7. Valdis V. Liepa, D. M. Brown, F. E. Lenning, R. L. Turcotte, "Measurements of Surface Fields on Scale Model E-4B Aircraft," University of Michigan Radiation Laboratory Report No. 016708-1-F, Interaction Application Memo 33, 1979.

Figure 4 shows a block diagram of the facility as it exists now. When these measurements started the instrumentation and procedures were as described in [7], but as the program progressed, numerous changes were made. These include extending the low frequency operation from 125 MHz to 118 MHz, increasing the number of frequency bands from 3 to 4, and incorporating a calculator-controlled switching of the power amplifiers and low pass filters. The last two changes reduced the "between band" jumps evident in previously obtained data [5,6]. We have also experimented with rectangular data recording instead of the standard phase/log recording which produces ambiguities near ±180 degrees, but this change was not made because of the limited dynamic range of the amplitude recording that this new procedure has.

3.2 Measurements

Current and charge measurements were made at eight locations on the model as indicated in Fig. 5. On the fuselage the locations are identified by a station number given in terms of the full scale distance in inches from the bulkhead (STA:F60). Thus, F239T is 179 inches from the bulkhead. The wing stations were located on the line bisecting the wing at a distance (in inches) given by the station number measured perpendicularly from the center line of the fuselage. Table 2 lists the station numbers of the test points and describes their locations.

The measurements were made for three different illuminations each having a prescribed polarization referenced to the fuselage of the aircraft (see Fig. 6). In our measurements the directions of

TABLE 2

DESCRIPTION OF MEASUREMENT LOCATIONS

Test Point	Stations	Location
1	F76T	Upper Surface, Forward of Canopy FS = 76 WL = Top Surface BL = 0 (centerline)
2	F239T	Upper Surface, Behind Canopy FS = 239 WL = Top Surface BL = 0 (centerline)
3	W352R	Upper Surface, Right Wing FS = 352 WL = Top Surface BL = 96 (right)
4	F488B	AFT Fuselage, Bottom FS = 488 WL = Bottom Surface BL = 0 (centerline)
6	F76RS	FWD Avionics Bay, Right Side FS = 76 WL = 88 BL = Right Surface
7	F100B	FWD Fuselage, Bottom Surface FS = 100 WL = Bottom Surface BL = 0 (centerline)
8	W352B	Lower Surface, Left Wing FS = 352 WL = Lower Surface BL = 96 (left)
9	F257B	Mid-Fuselage, Bottom Surface FS = 257 WL = Bottom Surface BL = 0 (centerline)

illumination and polarization are often referred to as orientations since these are fixed relative to the chamber and can be changed only by suitably orienting the model. Figure 6 also shows the direction of the measured current on the top and bottom of the aircraft. In all cases the component J_c is perpendicular to J_a. The data presented are normalized relative to the incident field, i.e., J/H_o for the surface current data and E_n/E_o for the charge data. The phase is referenced to that of the incident field at the station where the measurement was made, based on the $e^{i\omega t}$ time convention.

All of the current and charge measurements were made using miniature surface-mounted probes [8]. To mount the probes, holes were drilled in the model and the probe lead passed through to the other side. When not in use a hole was taped over with conductive adhesive copper tape (see Figs. 2 and 3) and as far as we can ascertain, the taping had no effect on the measurements.

3.3 Data

The data presented were measured in the anechoic chamber with the model supported by a styrofoam pedestal using specially prepared styrofoam supports to orient the model appropriately in relation to the incident field.

For each measurement situation the data were obtained using both models over either three or four bands of frequencies, depending on the system in use at the time. The bands of data were then combined to give single data sets for the large (L) and small (S) scale models. Because different numbers of sampling points were used

8. Valdis V. Liepa, D. L. Sengupta, J. E. Ferris, and T.B.A. Senior, "Surface Field Measurements with Image and Ground Planes," University of Michigan Radiation Laboratory Report No. 014449-1-F; Sensor and Simulation Notes, Note 224, 1977.

in each frequency band, and because the measured frequencies were divided by the model scale factors to obtain the full scale frequencies, the sampling rate is not uniform throughout the data plots, nor was it uniform in the data delivered to AFWL and TRW. For the data recorded over three frequency bands, 187 points were used in Band 1 (118 to 1100 MHz), 122 in Band 2 (950 to 2200 MHz), and 144 in Band 3 (2000 to 4400 MHz). For the four band recording, 90 points were used in Band 1 (118 to 546 MHz), 95 in Band 2 (550 to 1000), 116 in Band 3 (1000 to 2100 MHz) and 138 in Band 4 (3100 to 4400 MHz). Thus, with some overlap, 453 data points were recorded with the three band system, and 439 with the four band system. However, due to the occasional failure of the network analyzer to properly lock onto the signal, a few (perhaps half a dozen) points were sometimes omitted from a data set. The result is that a data set generally contains about 430 data points regardless of the system. For any particular data set the exact number of points and the frequency range covered are given, with other information, in line 5 of a data file (see Table 4). Typically, the full scale frequency range for the F-16A obtained using the small (1/48) model is 2.46 to 91.7 MHz, and using the large (1/32) model, 3.7 to 137.5 MHz.

Table 3 summarizes the cases for which data have been obtained and gives the figure numbers where the plots for each case can be found. The figure numbers are the same as those of the data files with the letter 'S' (small model) or 'L' (large model) specifying the particular model used for the measurement. The (digital) data files are also identified in the first line of the data set.

TABLE 3

F-16A SCALE MODEL MEASUREMENT MATRIX

EXCITATION		1 OVERHEAD E||FUS			2 OVERHEAD E⊥FUS			3 NOSE-ON E-VERT	
Test Pt.	component / station	J_A	J_C	Q	J_A	J_C	Q	J_A	Q
1	F76T	F01		F02	F03		F04	F05	F06
2	F239T	F07		F08	F09	F10		F11*	F12
3	W352T	F13	F14	F15	F16			F17	
4	F488B	F33		F34		F35	F36	F37	F38
6	F76RB			F39					
7	F100B	F28		F29	F30			F31	F32
8	W352B	F24	F25		F26			F27	
9	F257B	F18		F19	F20	F21		F22	F23

Note: Each measurement has two data sets, one measured on the small model (S) and one on the large model (L).

*Data set F11L is inconsistent with that of F11S and is believed to be inaccurate. Do not use F11L.

Plots of the data are given in the following section. In addition to the plots the data has also been furnished to AFWL and TRW in digital form on punched cards and is stored on IBM compatible magnetic tape at the University of Michigan. The format used for the data is as follows:

Line	1	FILENAME (4A4)
	2	Comments (18A4)
	3	Comments (18A4)
	4	TITLE used in plotting (18A4)
	5	FMIN, FMAX, AMPMIN, AMPMAX, PHASEMIN, PHASEMAX, NN (4F8.3, 2F8.2, I5)
	6	F(1) AMP(1) PHASE(1) F(2) AMP(2) PHASE(2) F(3) AMP(3) PHASE(3) 3(2F8.3, F8.2)
	↑	
	data	
	↓	..... F(NN) AMP(NN) PHASE(NN)

where NN is the number of data points in the set. Table 4 is an example of a typical data file for the F-16A.

TABLE 4

SAMPLE DATA FILE

```
LIST F-16A

>      1      F-16A
>      2      F16,S,F239T,3,JA,J14,B1,02/13/80,JT
>      3      SCALE FACTOR=49.01
>      4      SAMPLE DATA FOR F-16A MEASUREMENTS
>      5         2.612   89.827    1.045    2.626  -186.76   176.53   435
>      6         2.612    1.882     0.65    2.710    1.802    -4.61   2.808    1.827    -6.48
>      7         2.906    1.888    -2.75    3.003    1.829    -3.51   3.101    1.784    -0.57
>      8         3.199    1.899    -2.04    3.297    1.806    -2.00   3.395    1.765    -1.37
>      9         3.493    1.690    -1.53    3.591    1.668     0.11   3.689    1.727     0.95
>     10         3.787    1.756     1.79    3.885    1.777     2.53   3.983    1.837    -1.13
>     11         4.081    1.783    -3.09    4.179    1.639    -1.15   4.277    1.761    -1.11
>     12         4.375    1.791     1.93    4.473    1.792     0.27   4.570    1.793     1.32
>     13         4.668    1.777     1.06    4.766    1.837     0.80   4.864    1.805     0.75
>     14         4.962    1.810     0.79    5.060    1.888    -0.06   5.158    1.821    -1.22
>     15         5.256    1.781    -3.27    5.354    1.829    -2.43   5.452    1.665    -3.68
>     16         5.550    1.675    -1.43    5.648    1.668     2.52   5.746    1.749     1.86
>     17         5.844    1.825     3.11    5.942    1.768    -0.24   6.040    1.791    -0.49
>     18         6.138    1.780    -1.34    6.235    1.730    -0.79   6.333    1.700    -0.24
>     19         6.431    1.710     1.20    6.529    1.708     2.15   6.627    1.734     4.20
>     20         6.725    1.822     5.85    6.823    1.863     4.60   6.921    1.922     4.25
>     21         7.019    1.921     2.90    7.117    1.937     1.65   7.215    1.939     1.30
>     22         7.313    1.960     2.05    7.411    1.968     2.20   7.509    2.022     1.15
>     23         7.607    2.044    -0.10    7.705    2.095    -0.86   7.802    2.069    -3.01
>     24         7.900    2.054    -4.06    7.998    1.988    -5.71   8.096    1.854    -5.77
>     25         8.194    1.849    -2.92    8.292    1.918    -1.38   8.390    1.960    -2.73
>     26         8.488    2.002    -1.89    8.586    2.020     1.26   8.684    2.038    -4.30
>     27         8.782    2.057    -5.16    8.880    2.052    -6.42   8.978    2.037    -6.78
>     28         9.076    2.005    -8.64    9.174    2.339     5.80   9.272    2.323     9.33
>     29         9.370    1.950    -8.73    9.467    2.356     9.50   9.565    2.159     9.44
>     30         9.663    2.105    12.97    9.761    1.817   -10.90   9.859    2.044    19.83
>     31         9.957    1.848    -7.95   10.055    1.827    -8.82  10.153    1.866    -9.50
>     32        10.251    1.863    26.93   10.349    1.801   -10.65  10.447    2.216    29.27
>     33        10.545    1.802   -10.02   10.643    2.000    27.60  10.741    2.150    33.51
>     34        10.839    2.191    35.02   10.937    1.726   -14.07  11.034    1.680   -14.26
>     35        11.132    1.640   -14.16   11.230    1.607   -13.66  11.328    1.579   -13.66
>

>    135        73.716    1.856   167.17   74.058    1.911   168.12   74.401    1.966   166.48
>    136        74.744    1.919   165.73   75.087    1.974   168.57   75.429    2.044   165.72
>    137        75.772    1.989   164.36   76.115    1.970   165.41   76.458    2.044   166.26
>    138        76.801    2.047   163.41   77.143    1.981   164.36   77.486    2.040   164.21
>    139        77.829    2.033   163.67   78.172    2.078   163.94   78.515    2.084   162.11
>    140        78.857    2.052   161.69   79.200    2.058   161.08   79.543    2.036   159.58
>    141        79.886    2.022   159.88   80.228    2.032   159.50   80.571    2.009   159.32
>    142        80.914    1.991   158.56   81.257    1.959   159.40   81.600    2.009   159.26
>    143        81.942    1.972   157.73   82.285    1.935   157.91   82.628    1.935   158.80
>    144        82.971    1.953   158.10   83.314    1.908   157.11   83.656    1.856   157.64
>    145        83.999    1.822   158.37   84.342    1.813   159.52   84.685    1.860   161.28
>    146        85.028    1.864   159.44   85.370    1.806   160.22   85.713    1.819   160.90
>    147        86.056    1.775   160.10   86.399    1.751   161.00   86.741    1.721   162.10
>    148        87.084    1.771   163.72   87.427    1.781   163.73   87.770    1.727   164.26
>    149        88.113    1.742   165.58   88.455    1.773   166.41   88.798    1.777   166.14
>    150        89.141    1.801   166.26   89.484    1.801   166.09   89.827    1.781   167.82
#END OF FILE
#
```

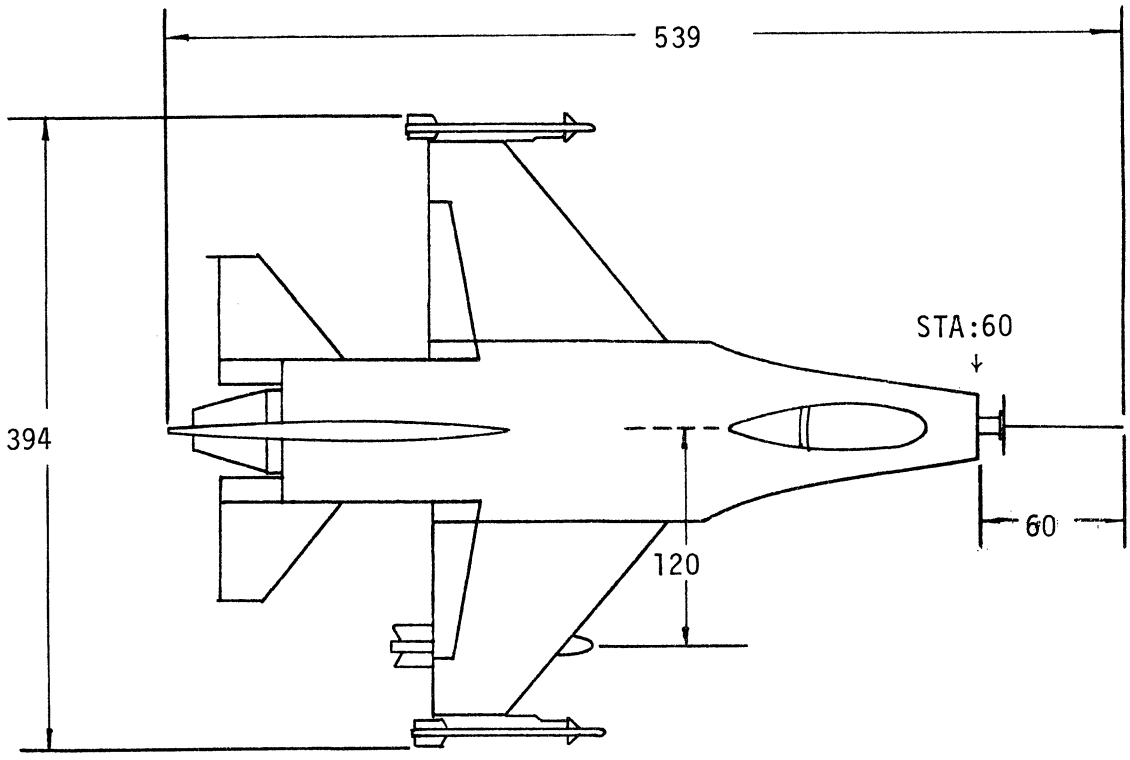

Dimensions in inches (full scale)

Notes: (1) Radome and plastic canopy removed.

(2) Radar and pitot tube simulated.

(3) Sidewinder missiles at each wing tip.

(4) B-61 plus pylon, right wing only.

Fig. 1: Pertinent Aircraft Specifications.

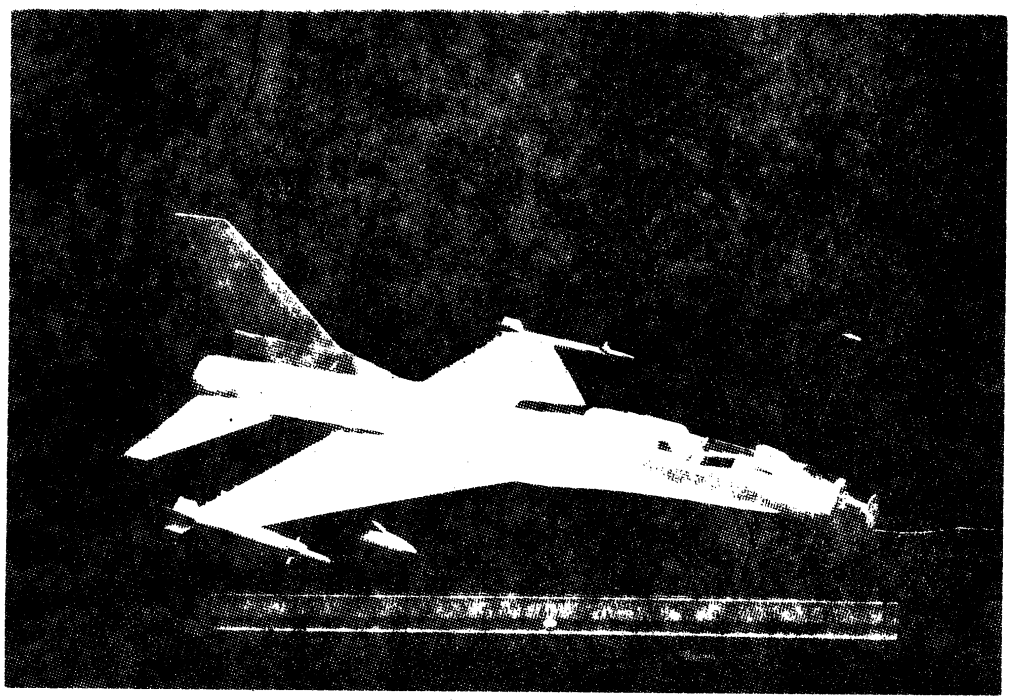

Fig. 2: Photograph of the Large Model (1/32 Scale).

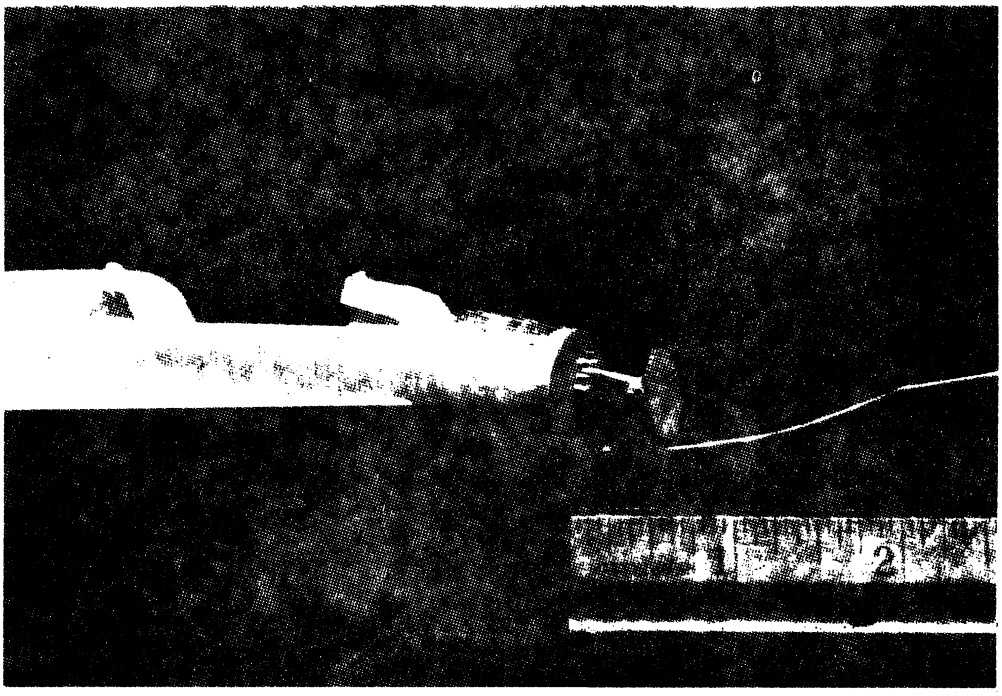

Fig. 3: Closeup of the Bulkhead Showing Radar and Pitot Tube.

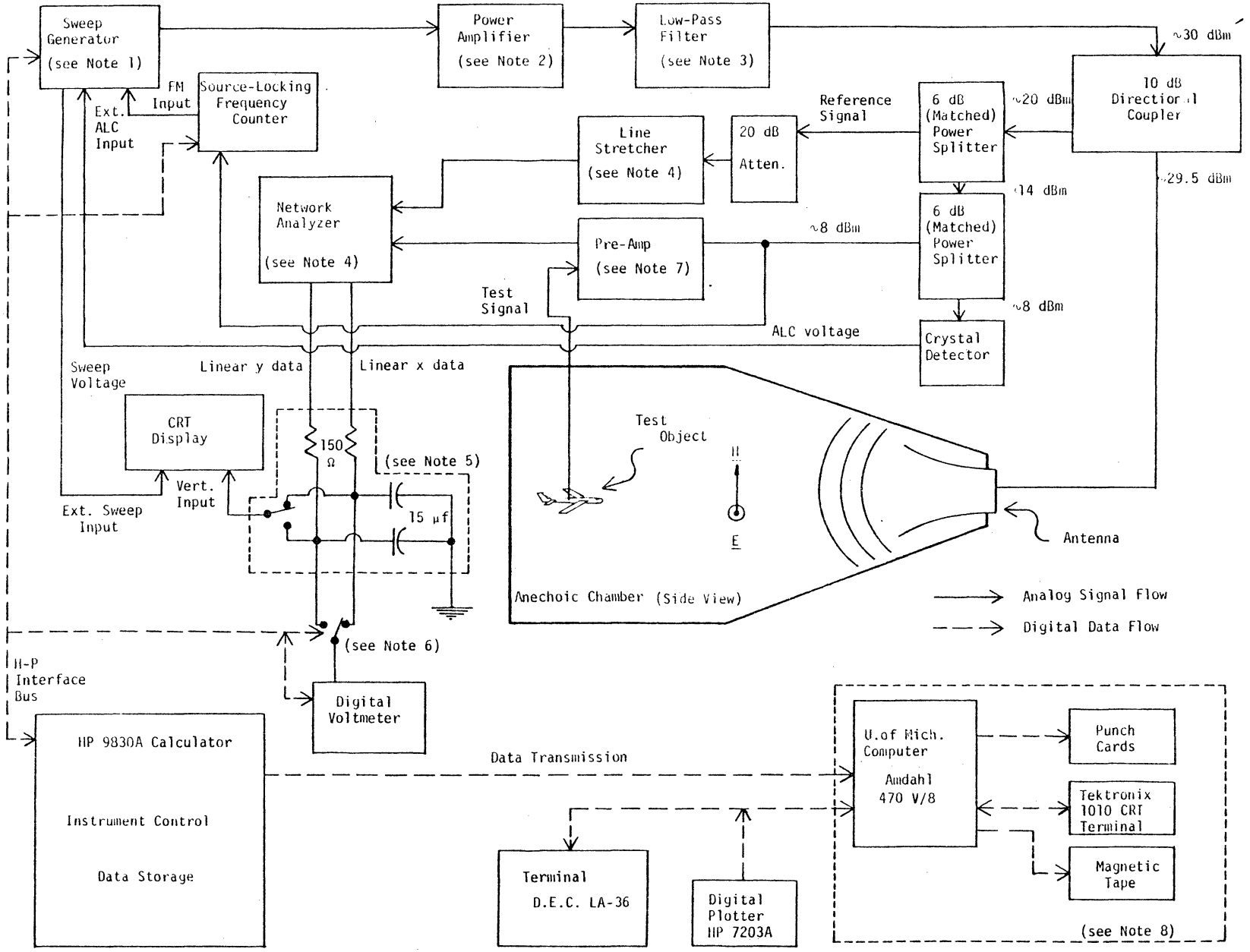

Fig. 4 : Block Diagram of the Present Facility.

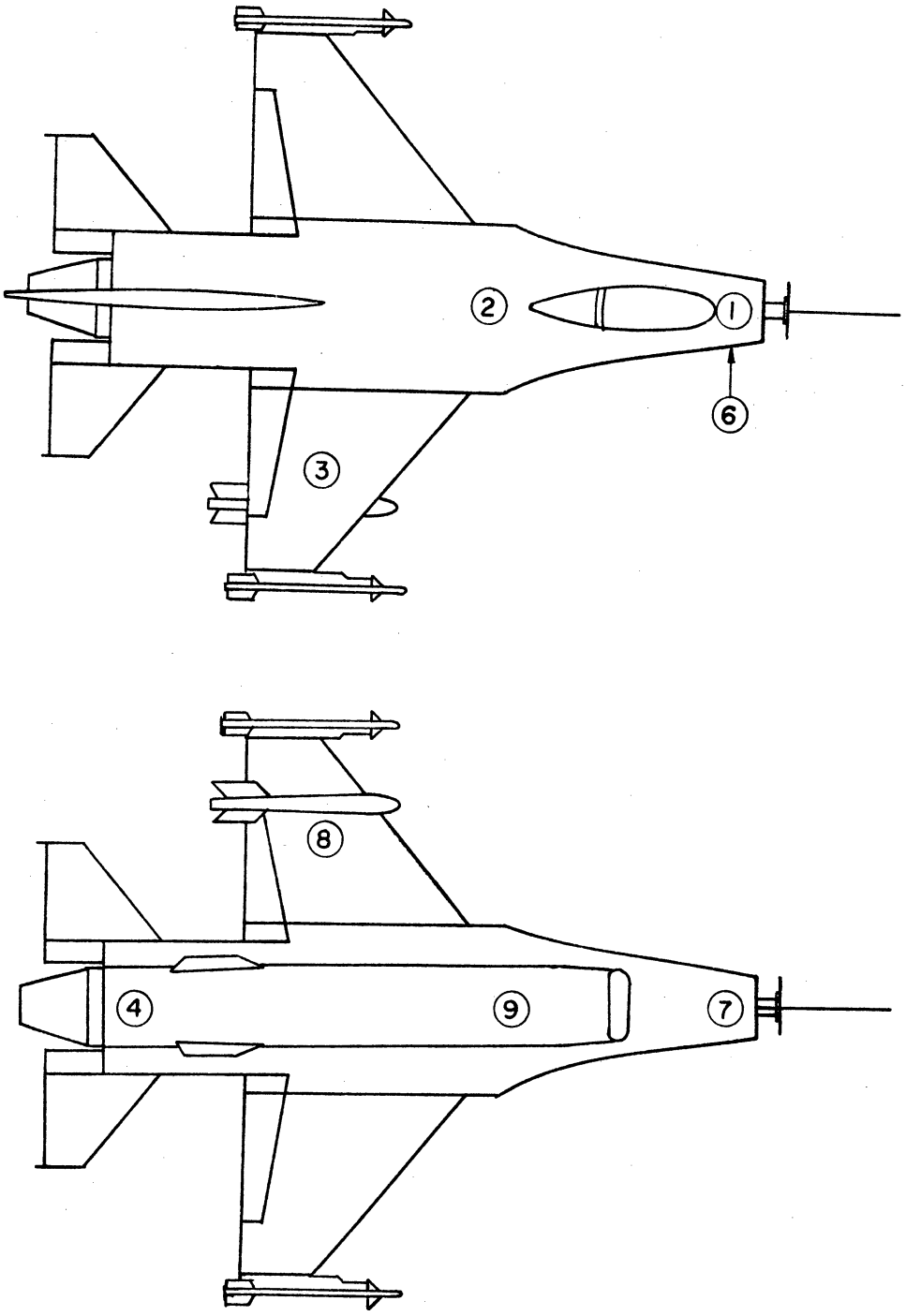

Fig. 5: Location of Measurement Stations. (See Table 2 for details.)

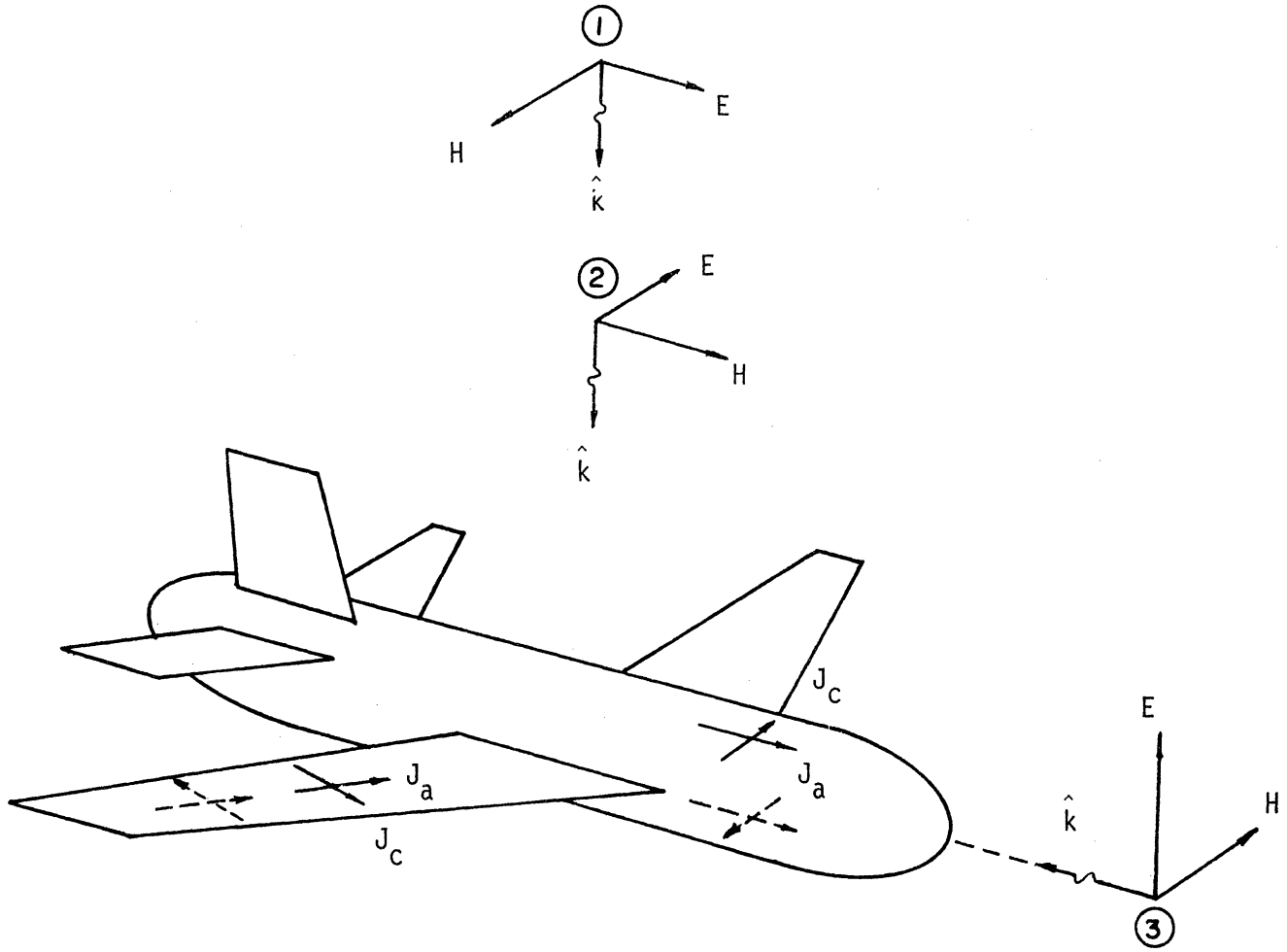

① E parallel to fuselage, top incidence.

② E perpendicular to fuselage, top incidence.

③ E vertical, nose-on.

Note: Dashed lines indicate bottom surface current components.

Fig. 6: Illumination Directions (Orientations) and the Measured Current Components.

SECTION IV

DATA

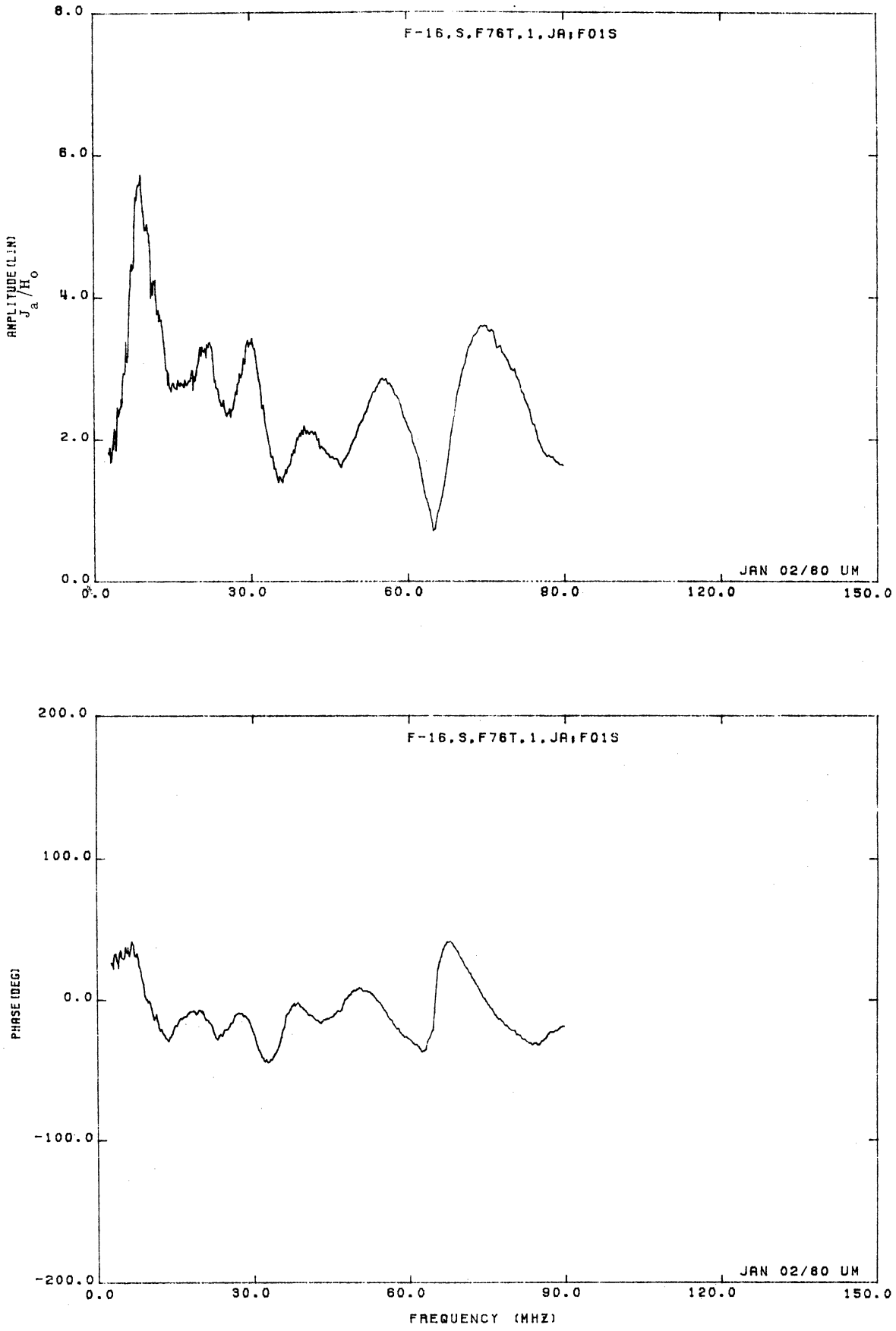

Figure 01S. Axial Current at STA:F76T, Excitation 1, 1/48 Model.

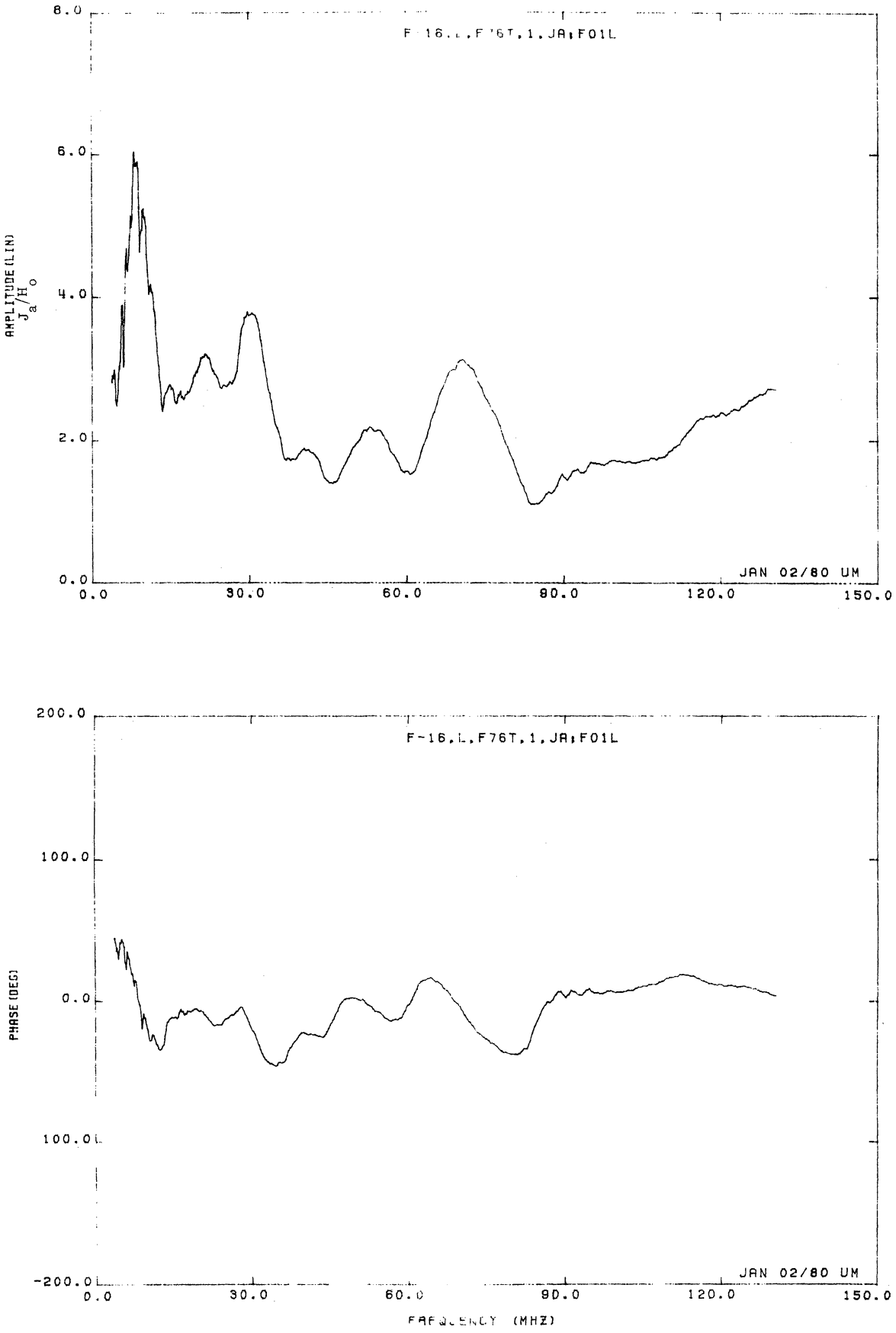

Figure 01L. Axial Current at STA:F76T, Excitation 1, 1/32 Model.

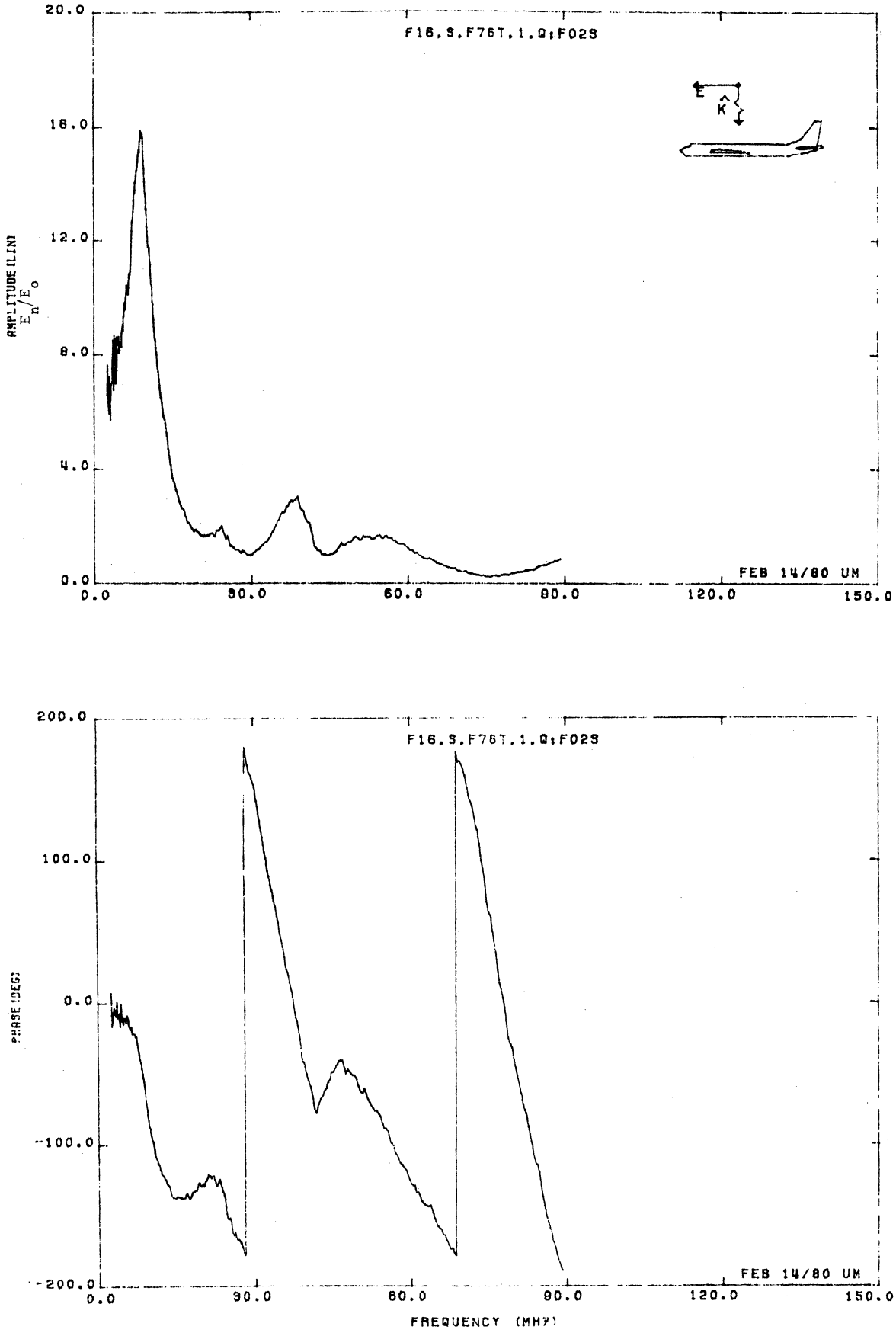

Figure 02S. Normal Electric Field at STA:F76T, Excitation 1, 1/48 Model.

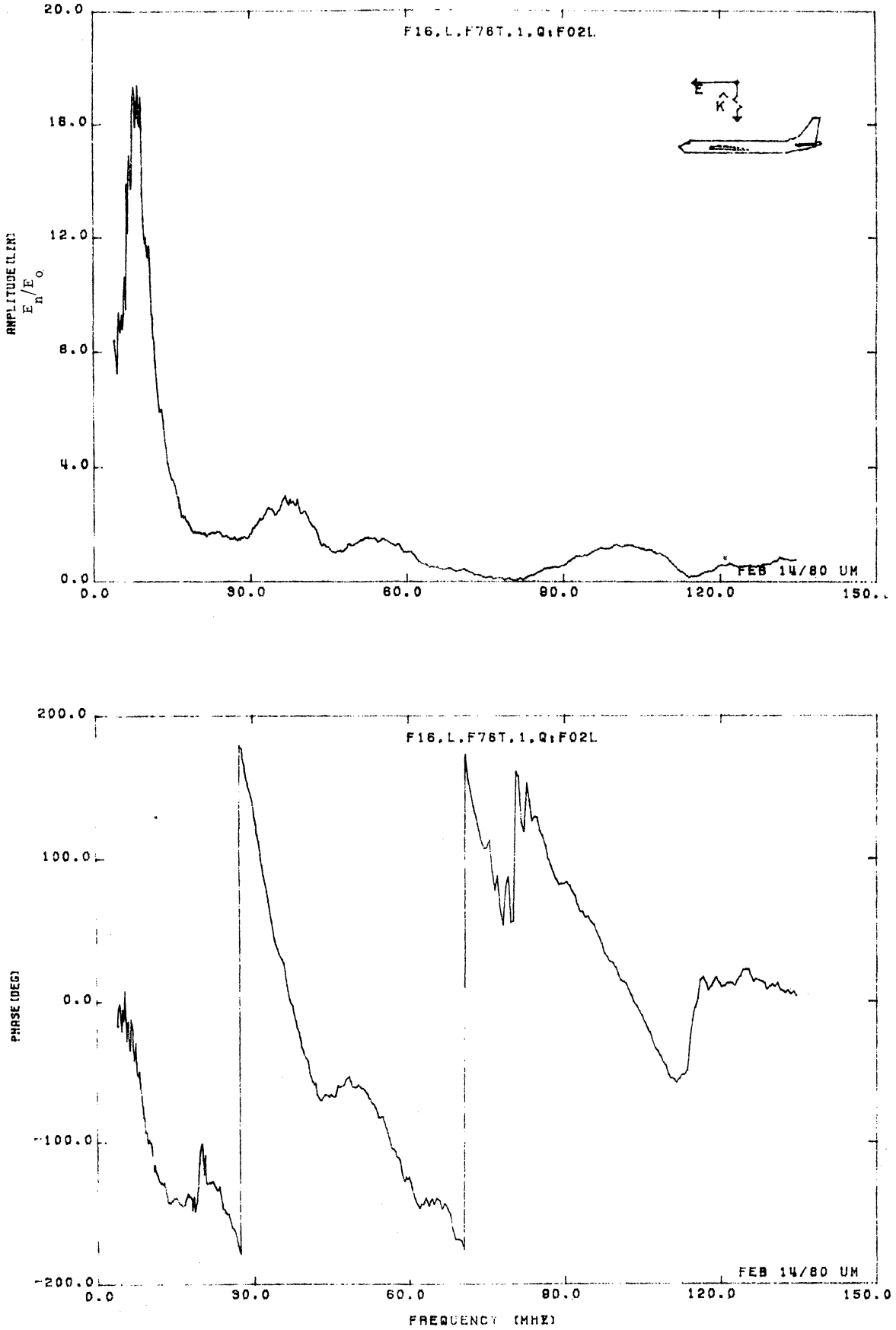

Figure 02L. Normal Electric Field at STA;F76T, Excitation 1, 1/32 Model.

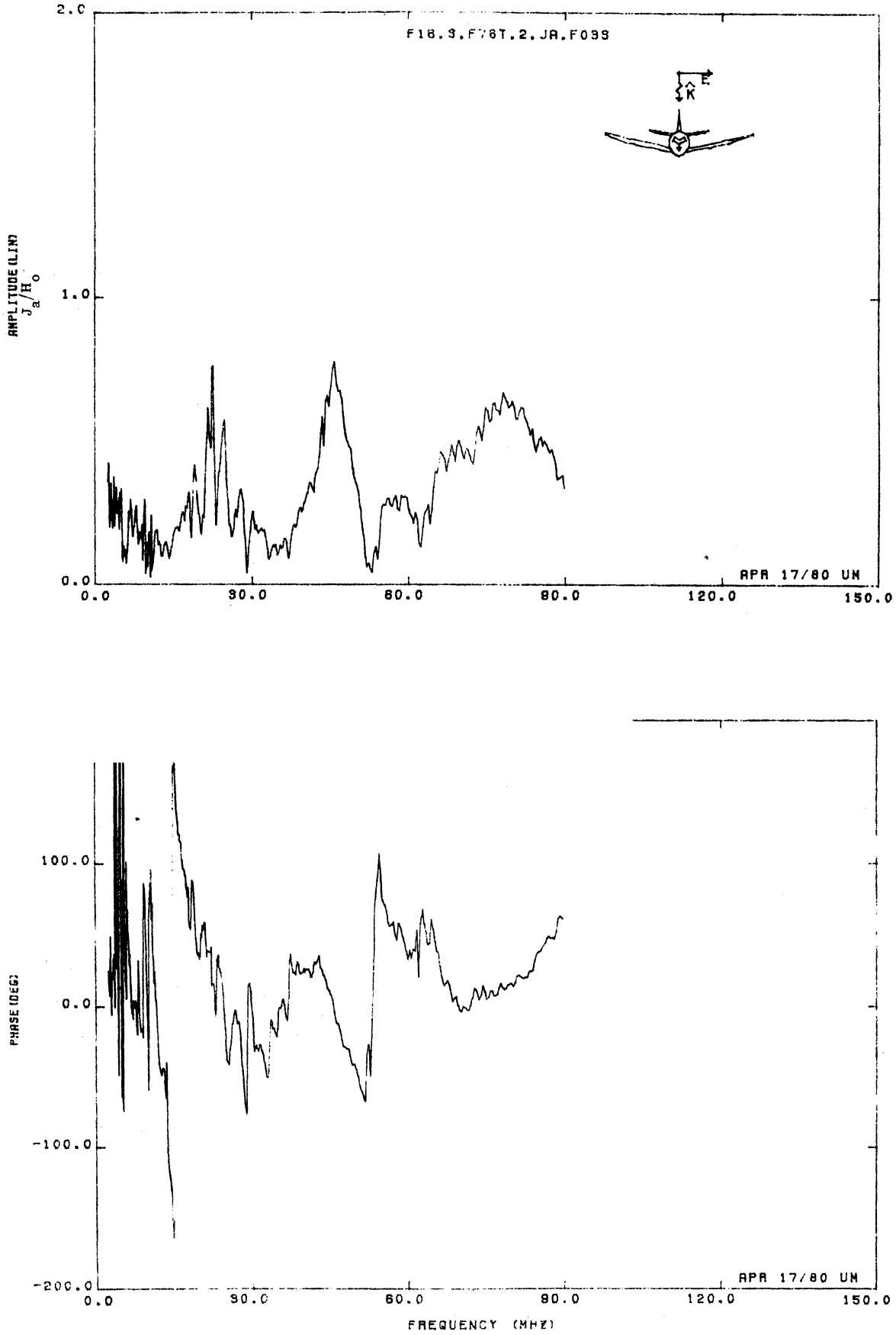

Figure 03S. Axial Current at STA:F76T, Excitation 2, 1/48 Model.

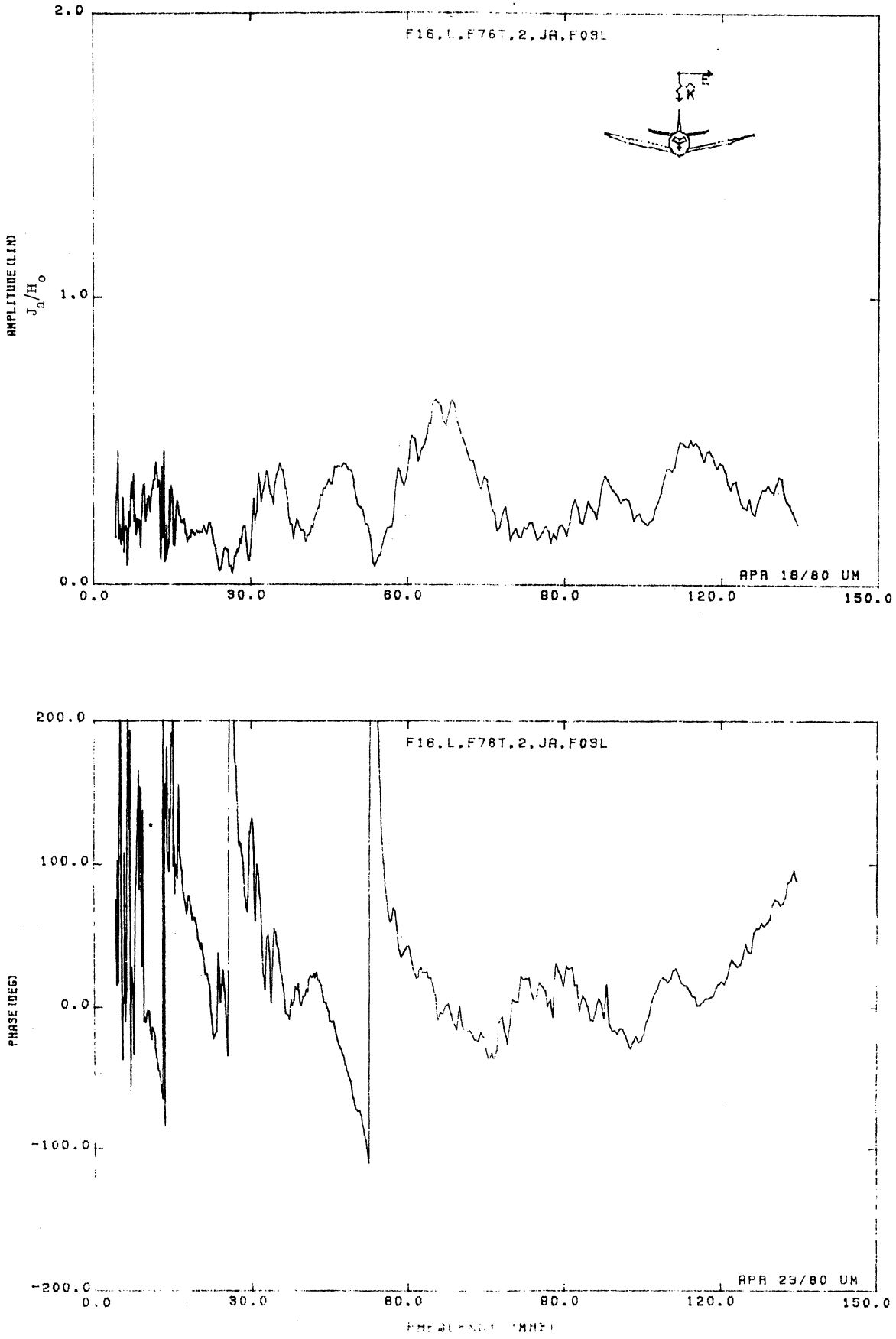

Figure 03L. Axial Current at STA:F76T, Excitation 2, 1/32 Model.

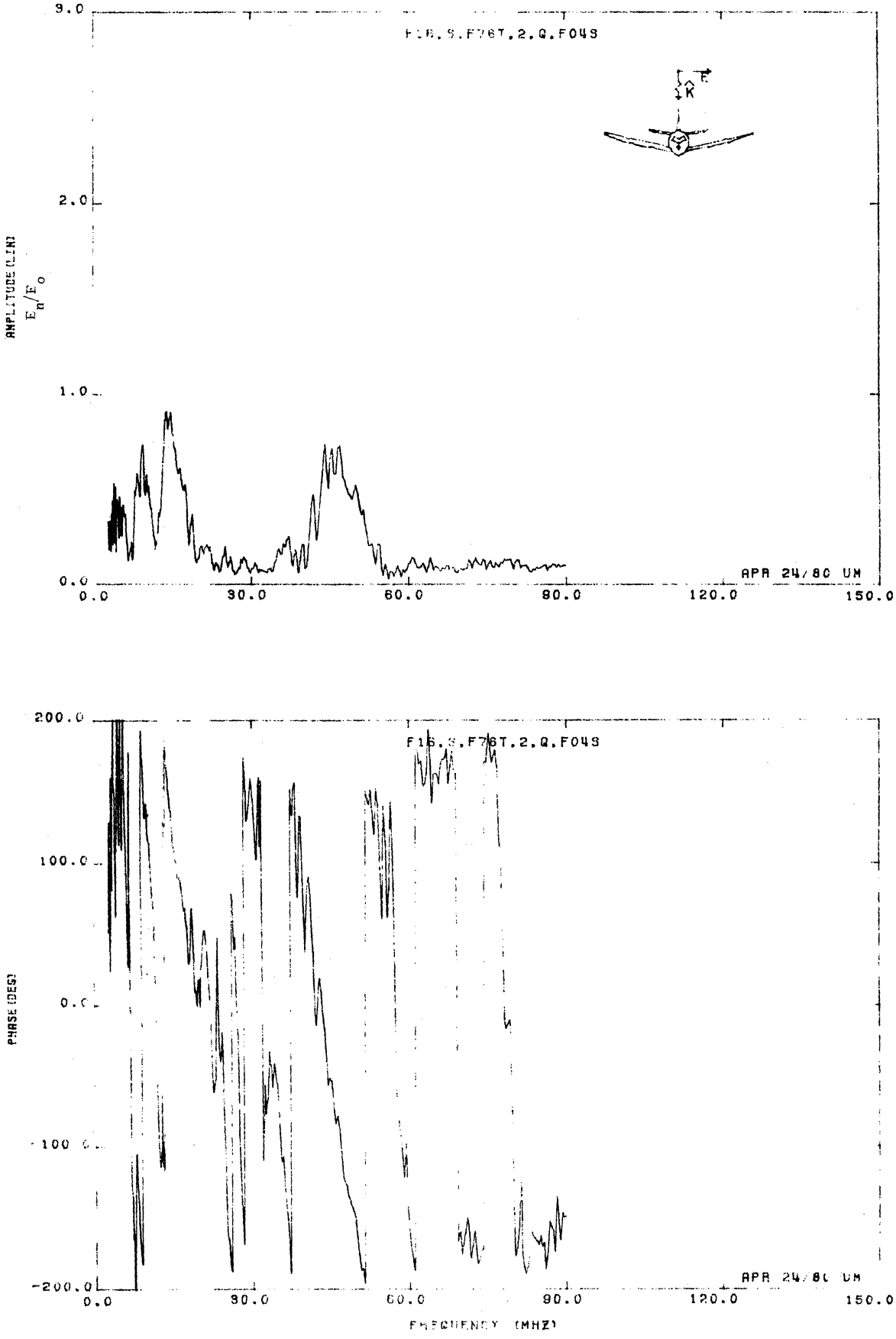

Figure 04S. Normal Electric Field at STA:F76T, Excitation 2, 1/48 Model.

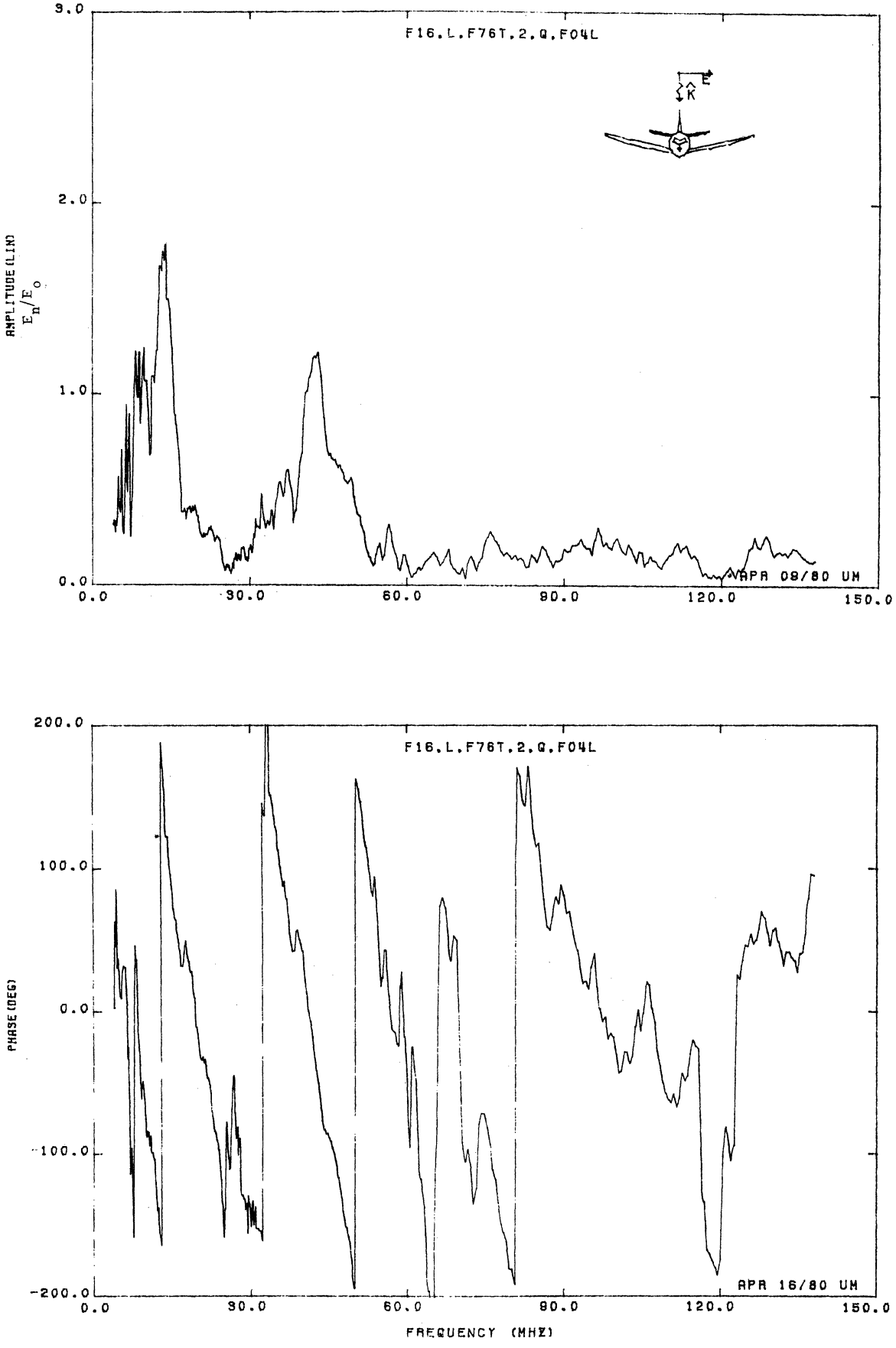

Figure 04L. Normal Electric Field at STA:F76T, Excitation 2, 1/32 Model.

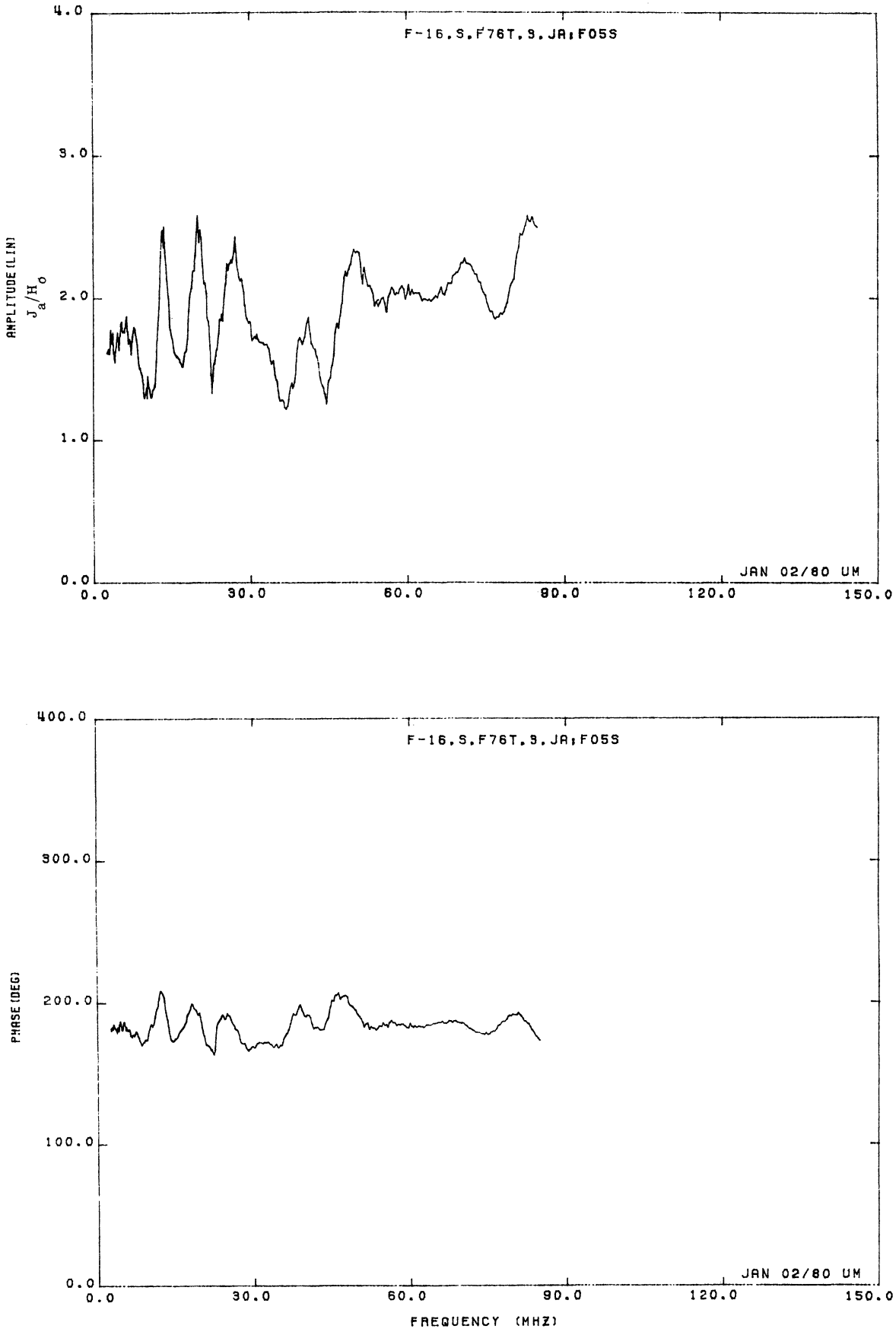

Figure 05S. Axial Current at STA:F76T, Excitation 3, 1/48 Model.

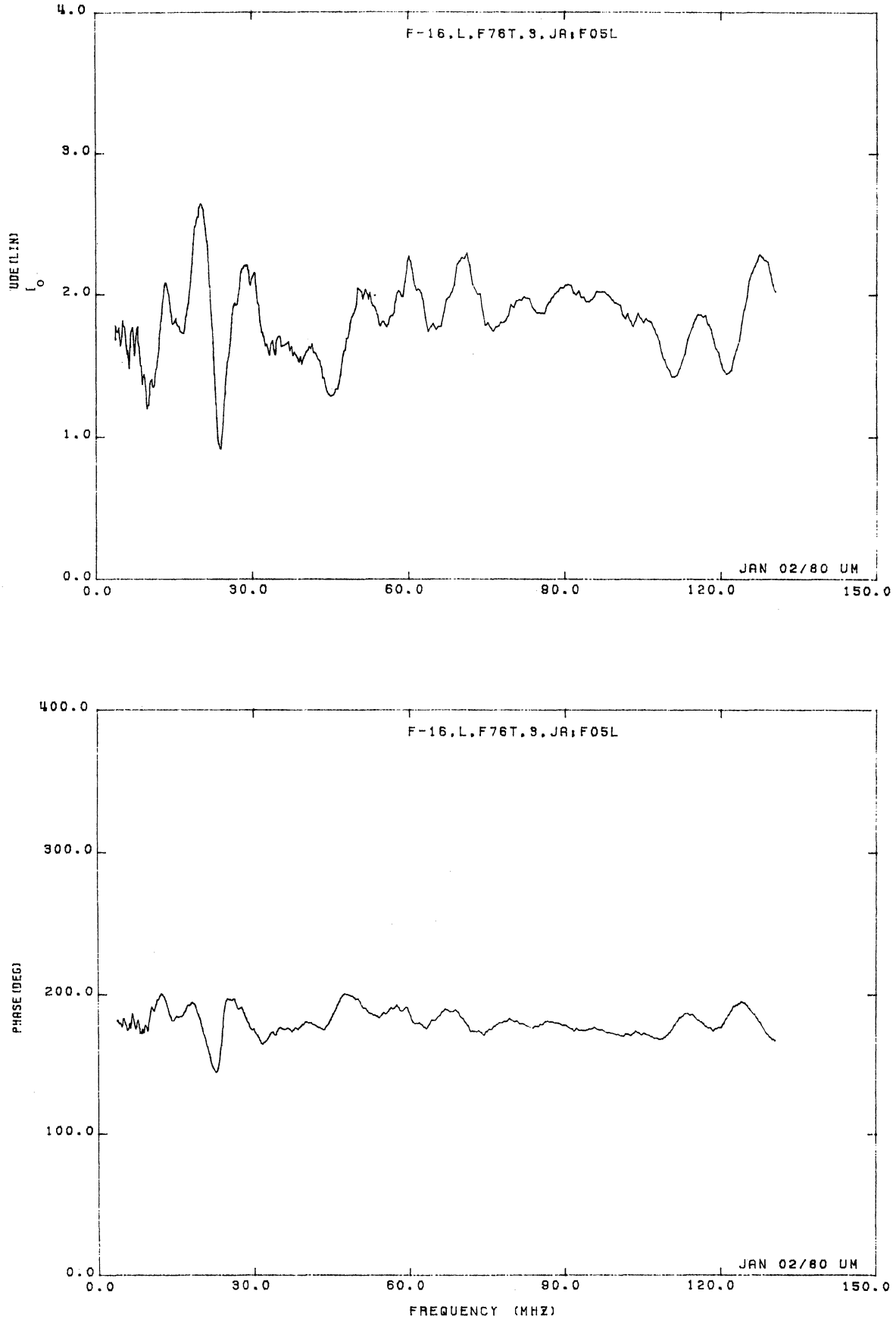

Figure 05L. Axial Current at STA:F76T, Excitation 3, 1/32 Model.

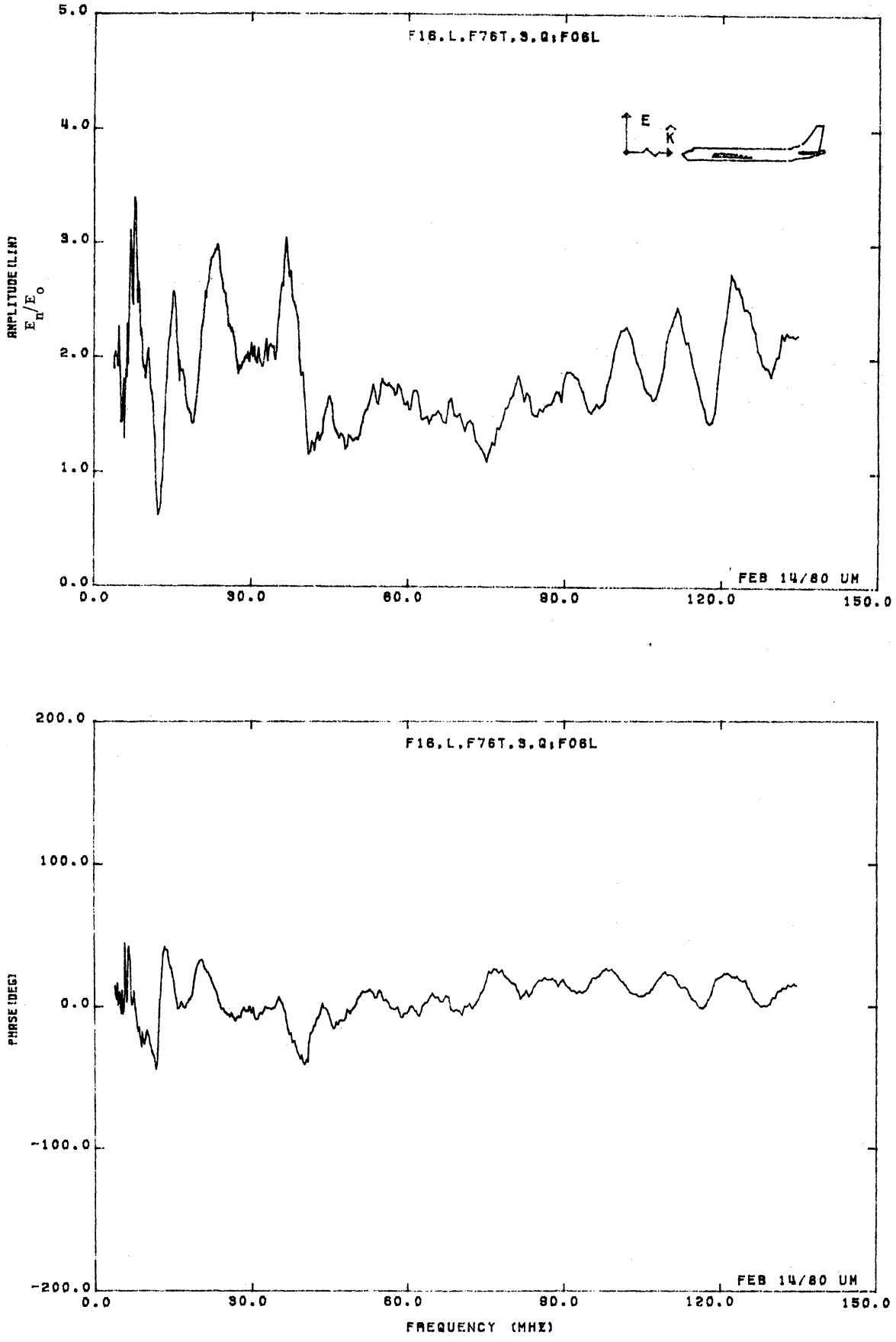

Figure 06L. Normal Electric Field at STA:F76T, Excitation 3, 1/32 Model.

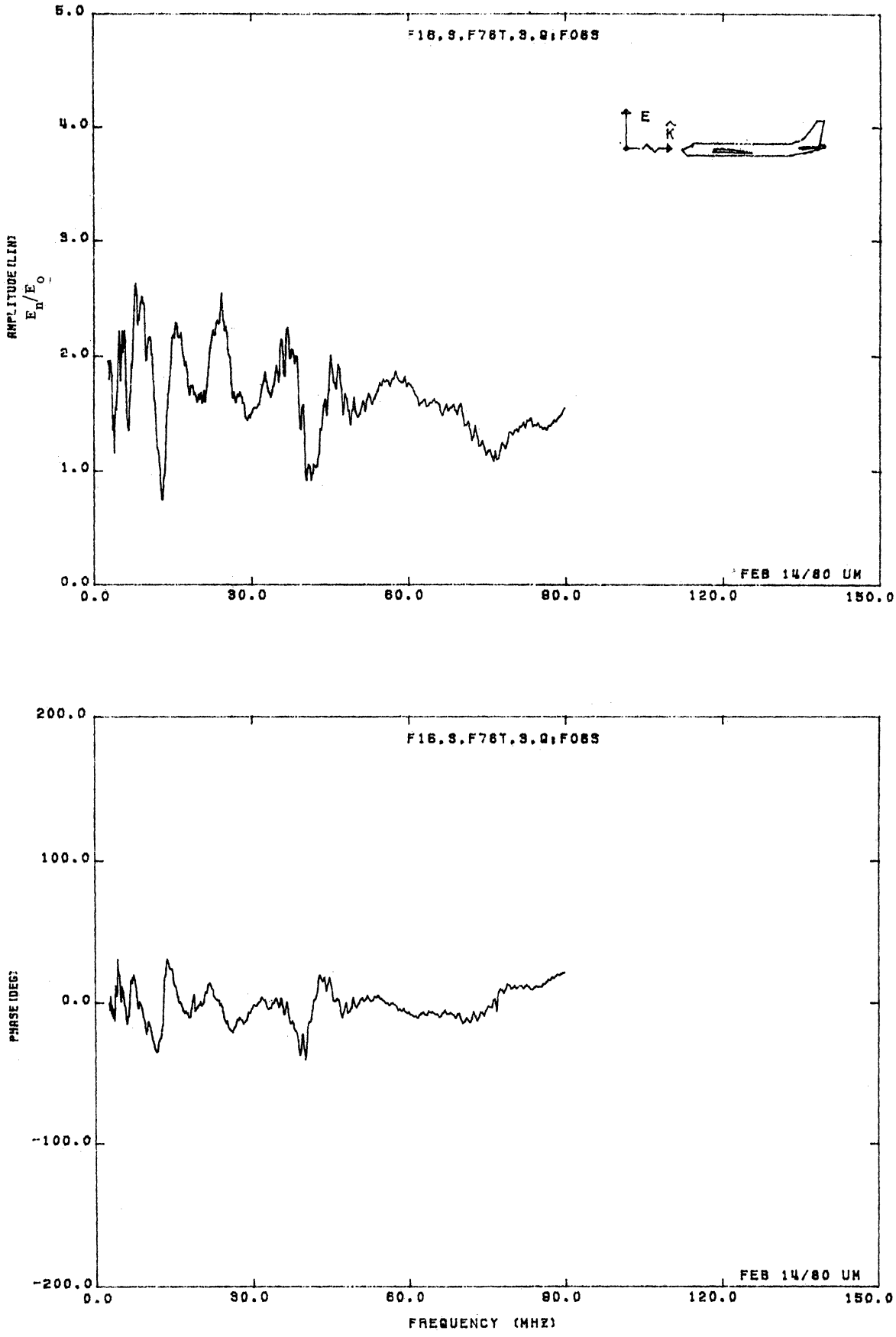

Figure 06S. Normal Electric Field at STA:F78T, Excitation 3, 1/48 Model.

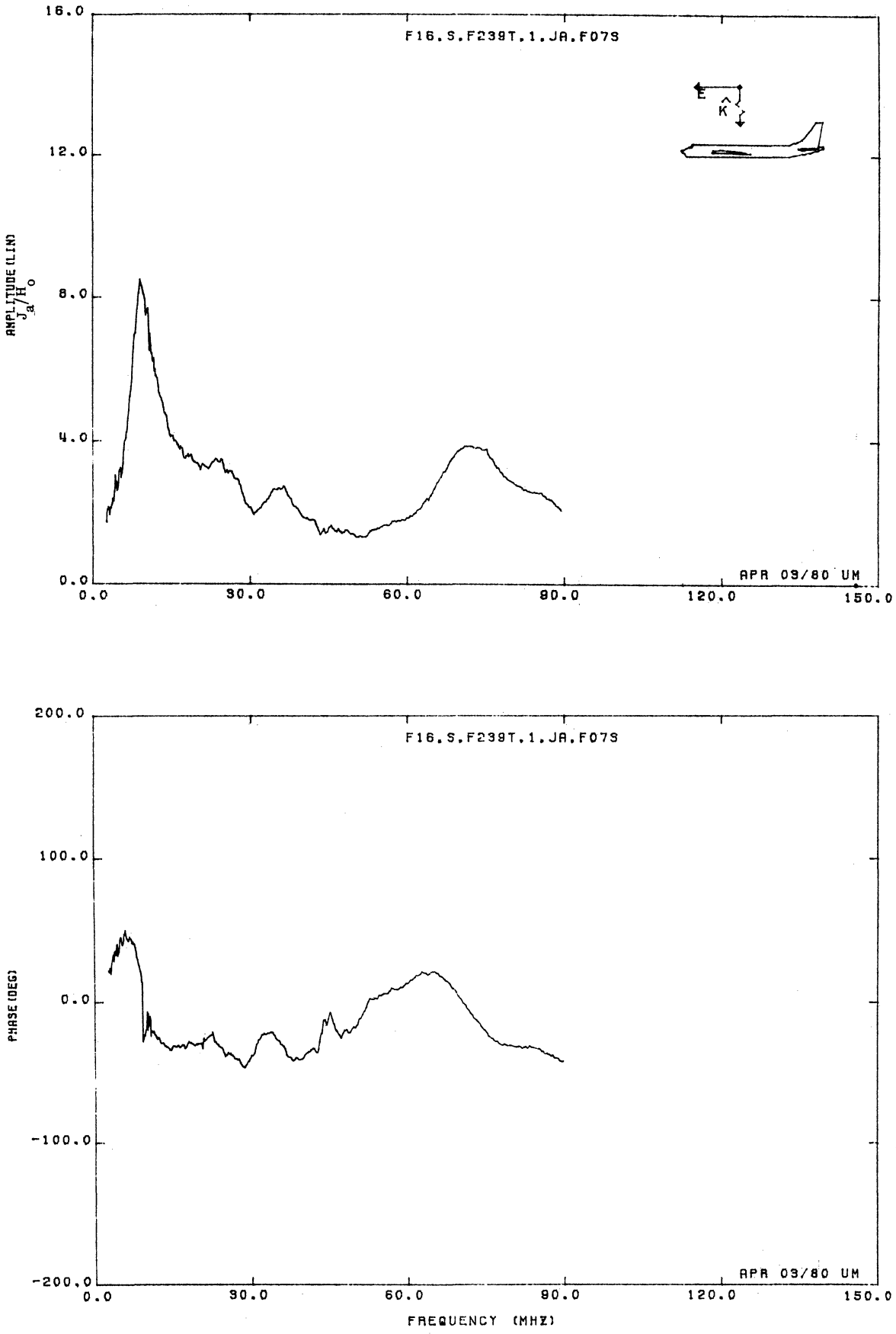

Figure 07S. Axial Current at STA:F239T, Excitation 1, 1/48 Model.

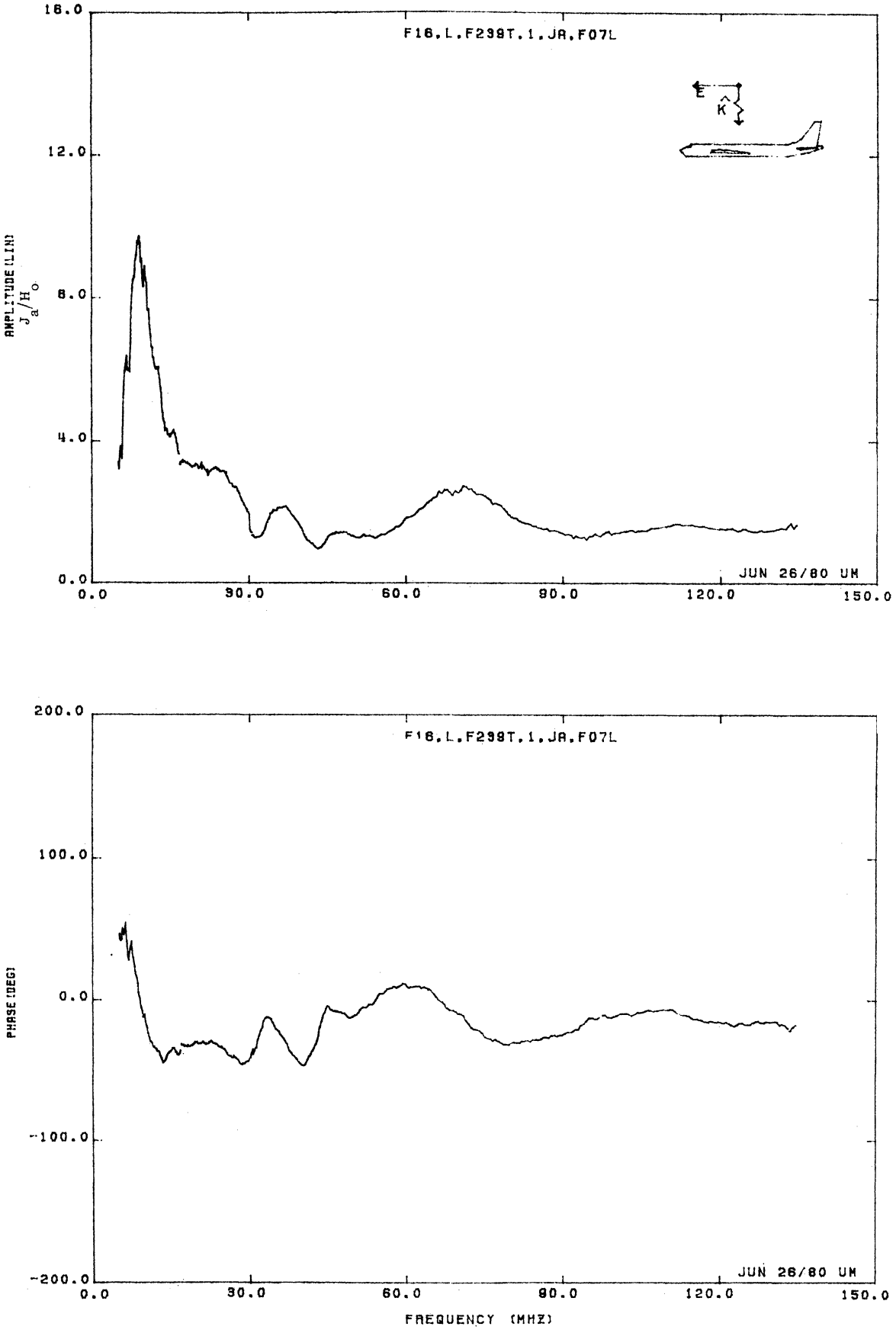

Figure 07L. Axial Current at STA:F239T, Excitation 1, 1/32 Model.

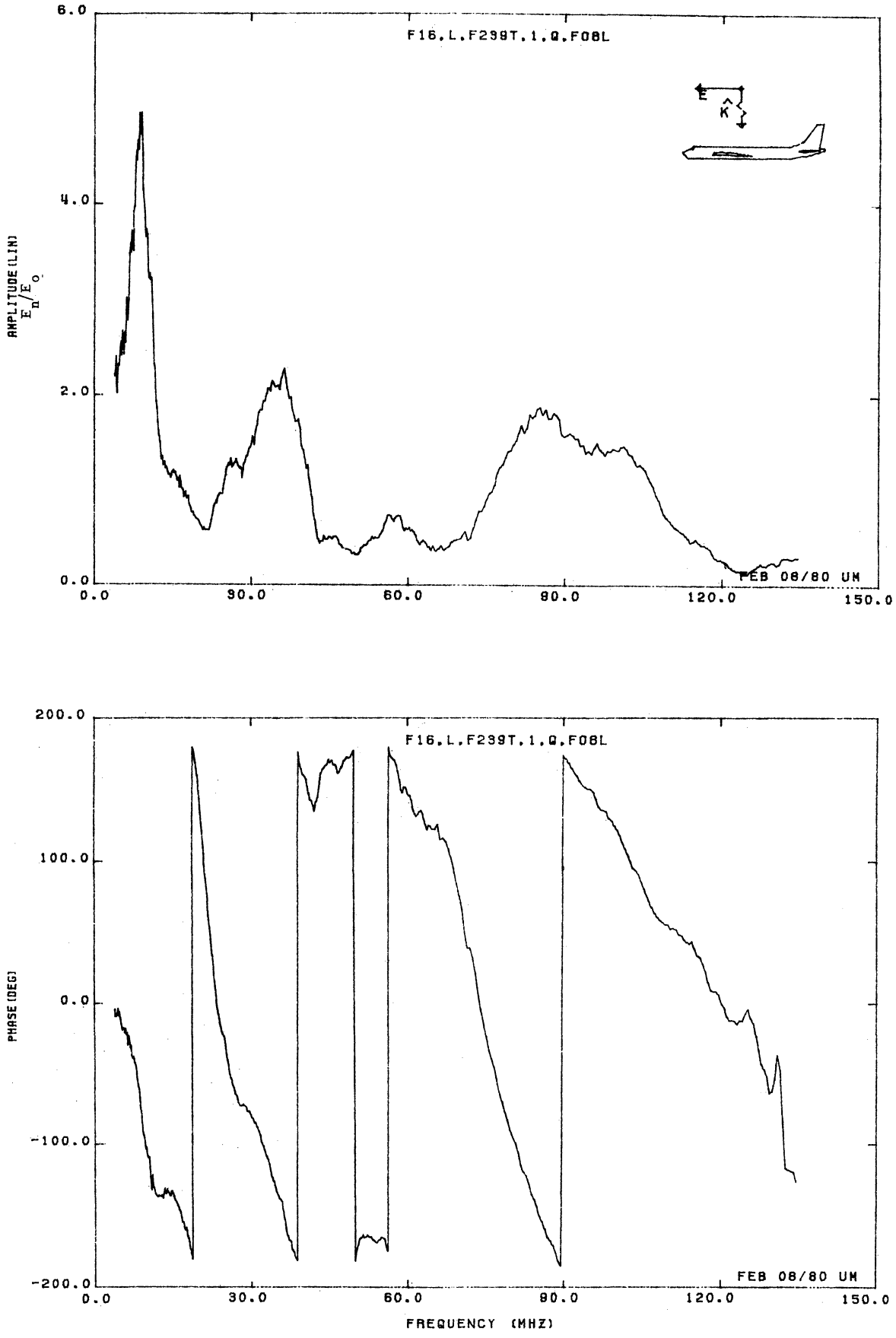

Figure 08L. Normal Electric Field at STA:F239T, Excitation 1, 1/32 Model.

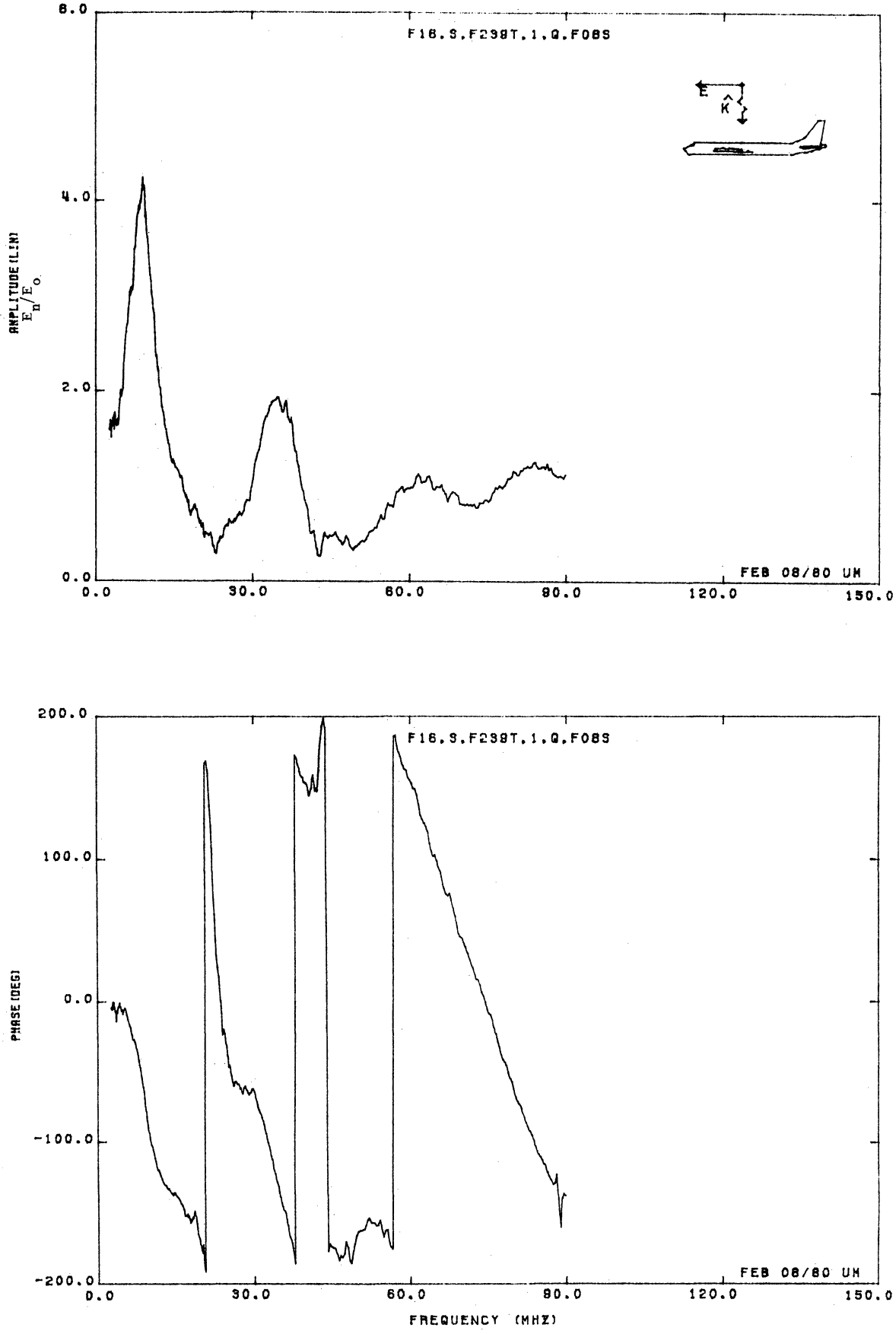

Figure 08S. Normal Electric Field at STA:F239T, Excitation 1, 1/48 Model.

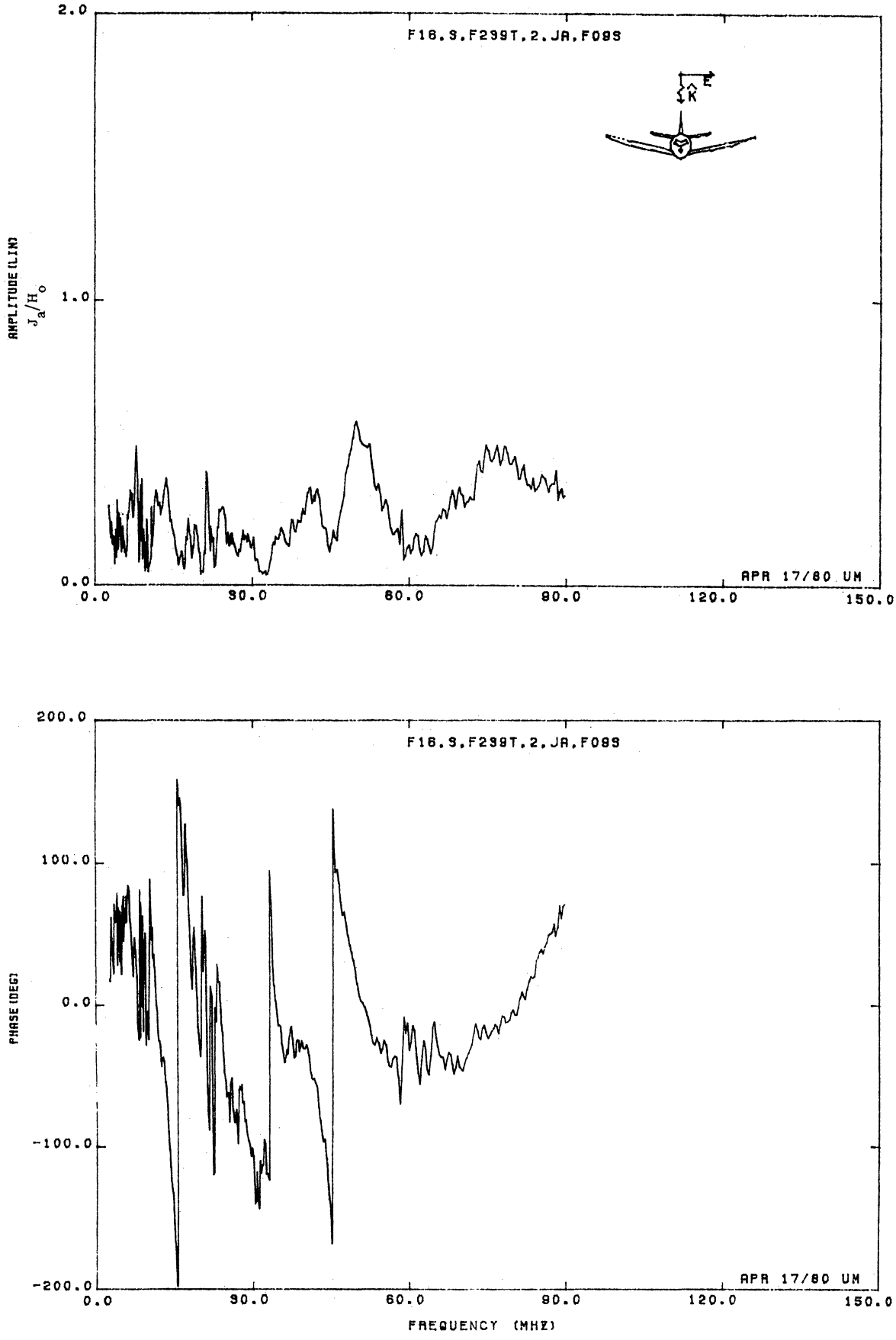

Figure 09S. Axial Current at STA:F239T, Excitation 2, 1/48 Model.

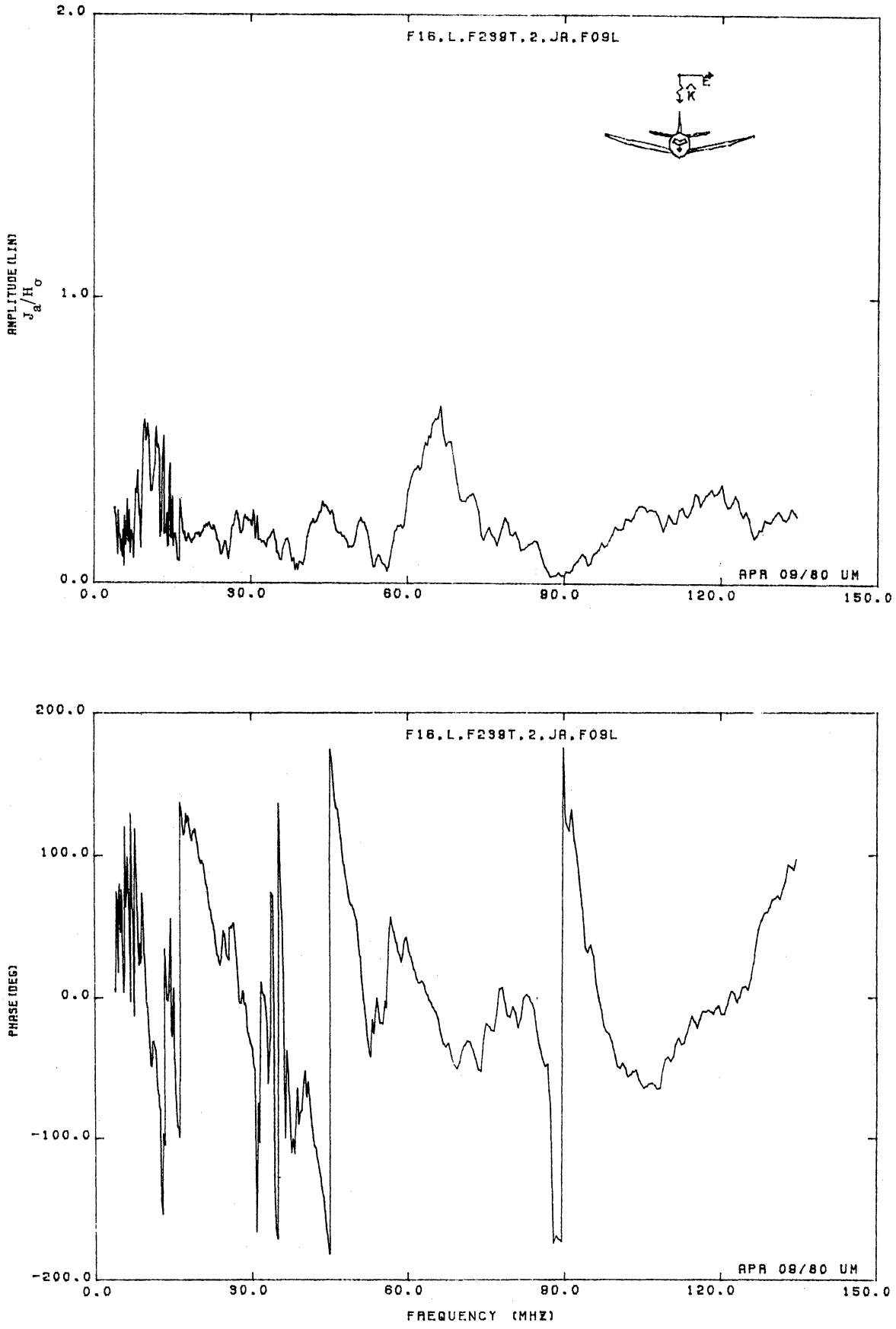

Figure 09L. Axial Current at STA:F239T, Excitation 2, 1/32 Model.

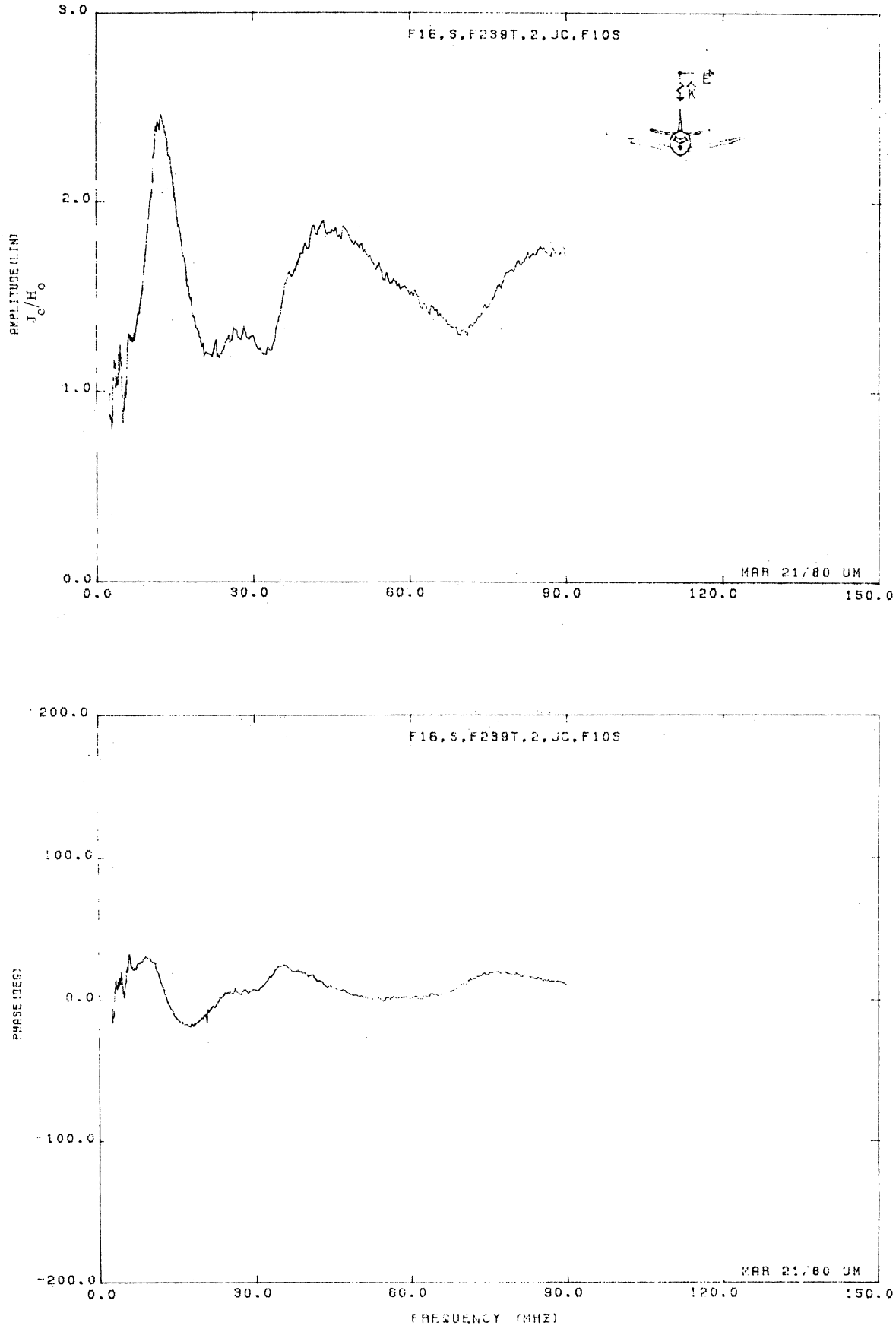

Figure 10S. Circumferential Current at STA:F239T, Excitation 2, 1/48 Model.

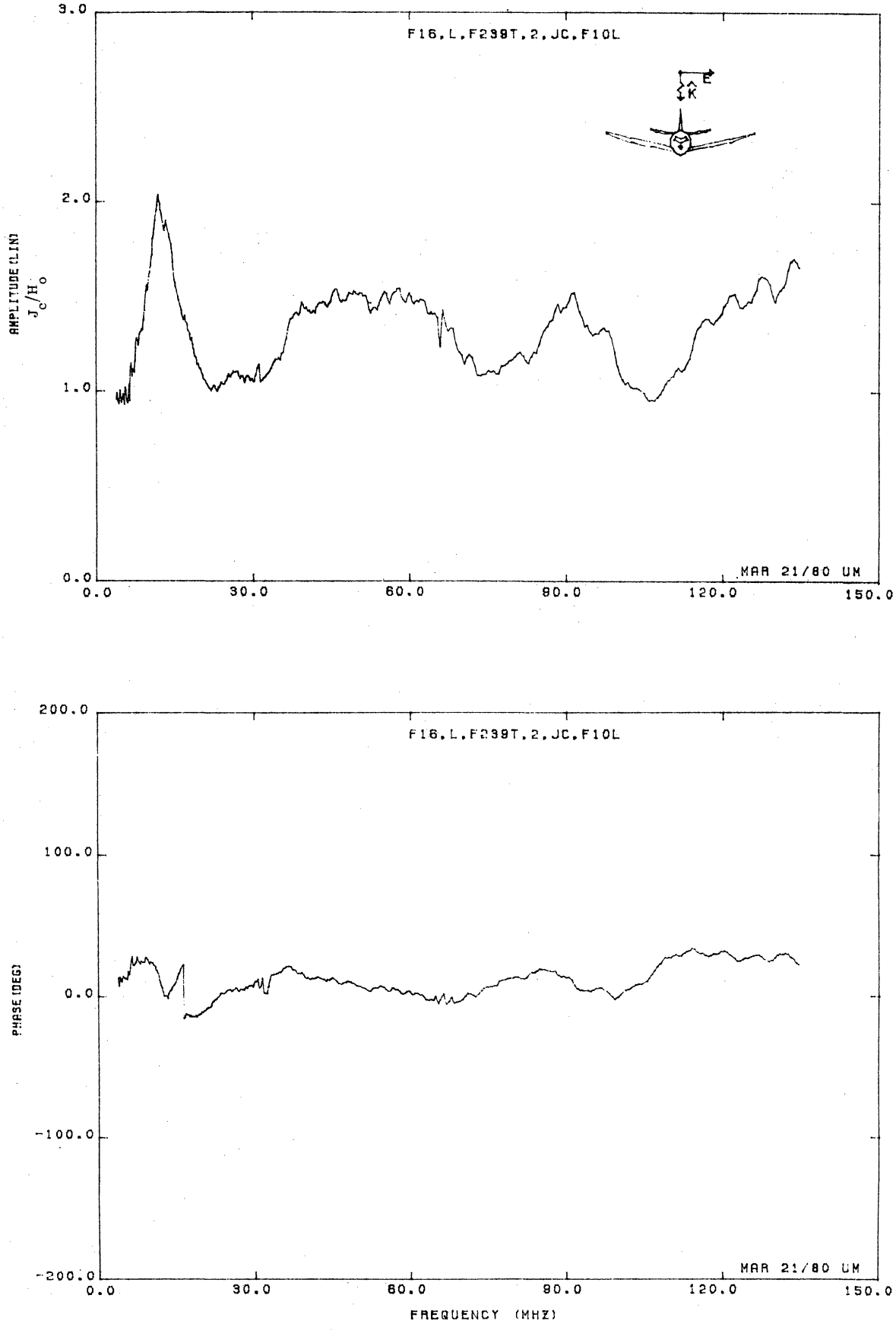

Figure 10L. Circumferential Current at STA:F239T, Excitation 2, 1/32 Model.

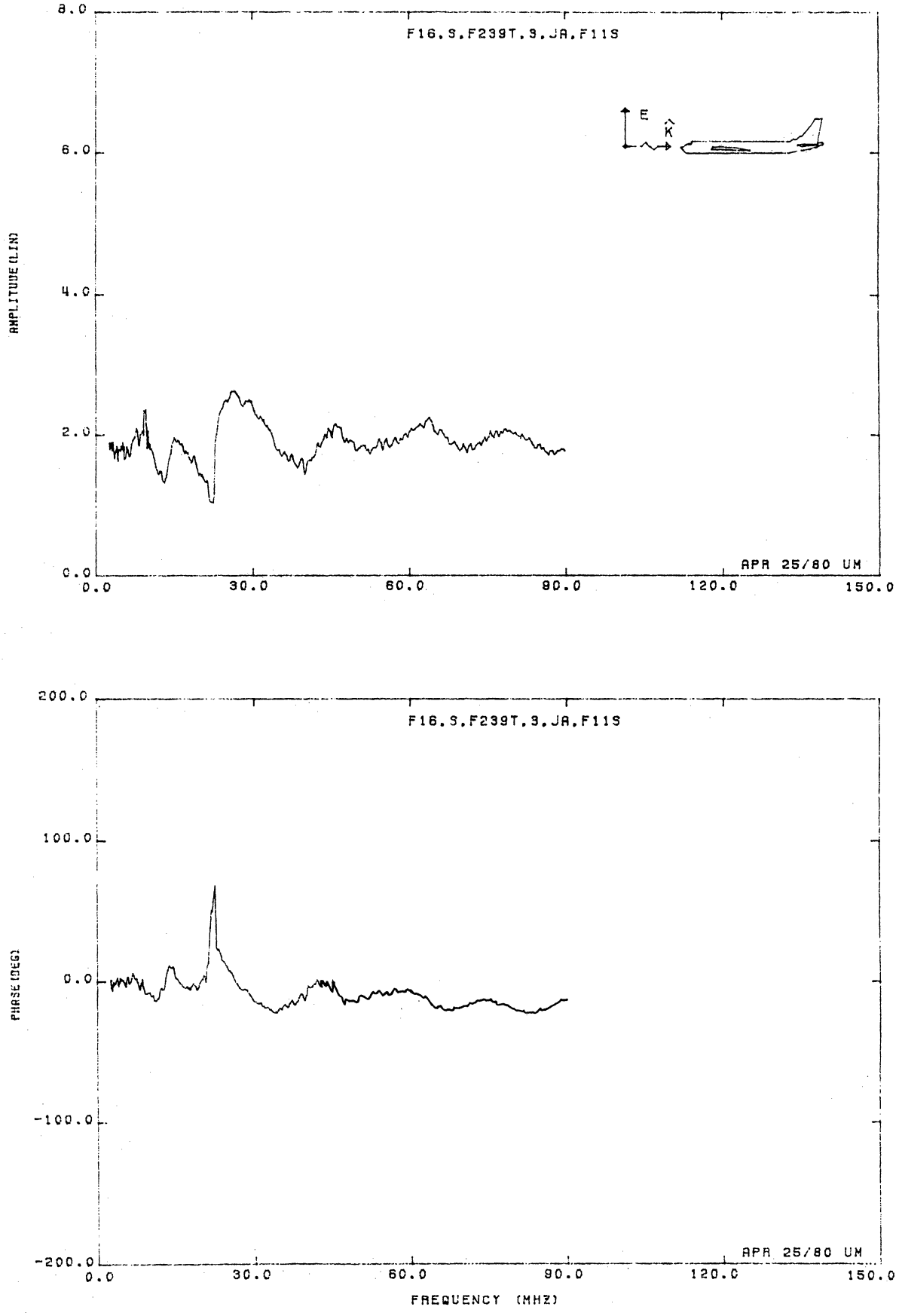

Figure 11S. Axial Current at STA:F238T, Excitation 3, 1/48 Model.

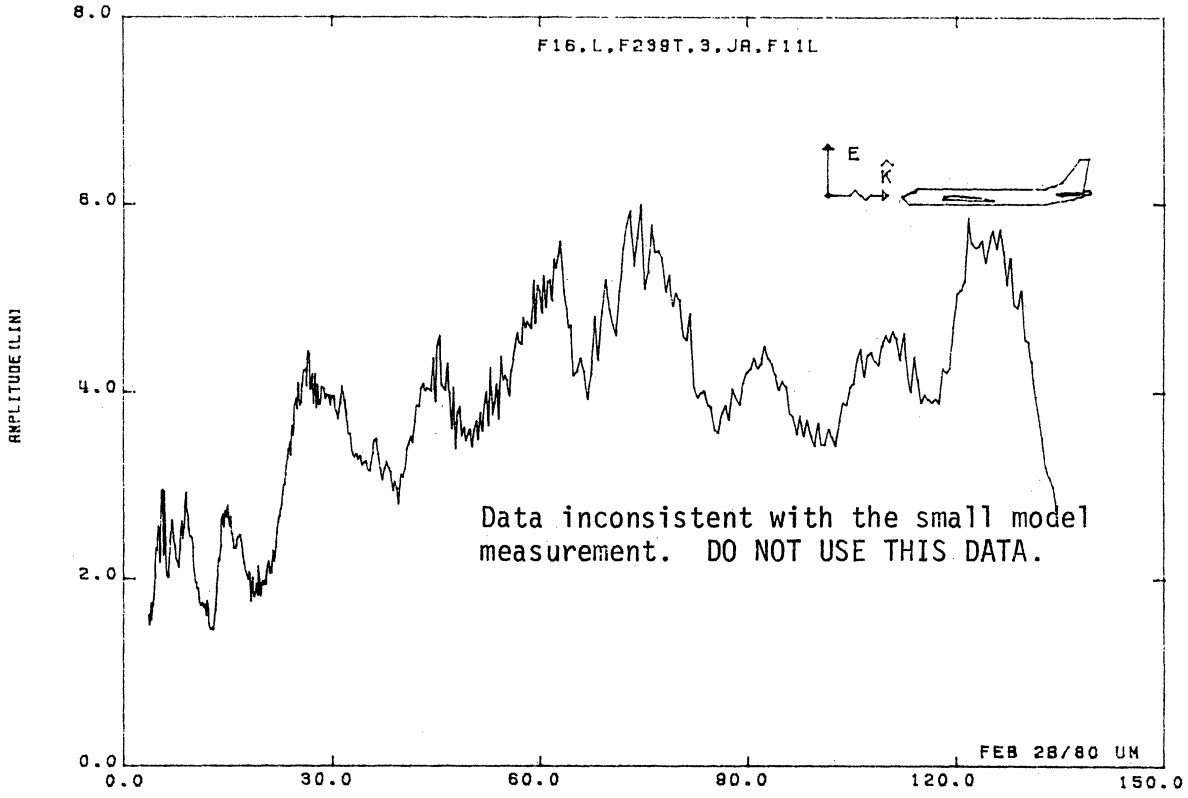

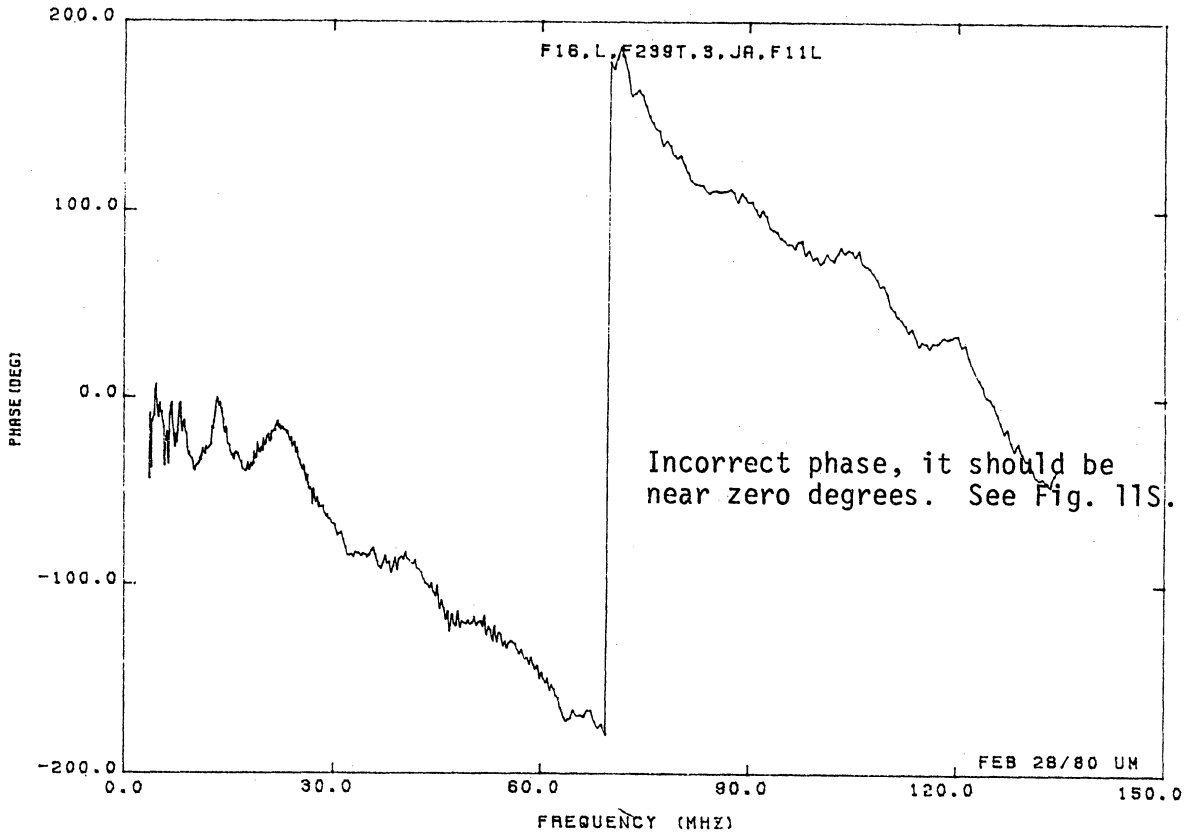

Figure 11L. Axial Current at STA:F239T, Excitation 3, 1/32 Model.

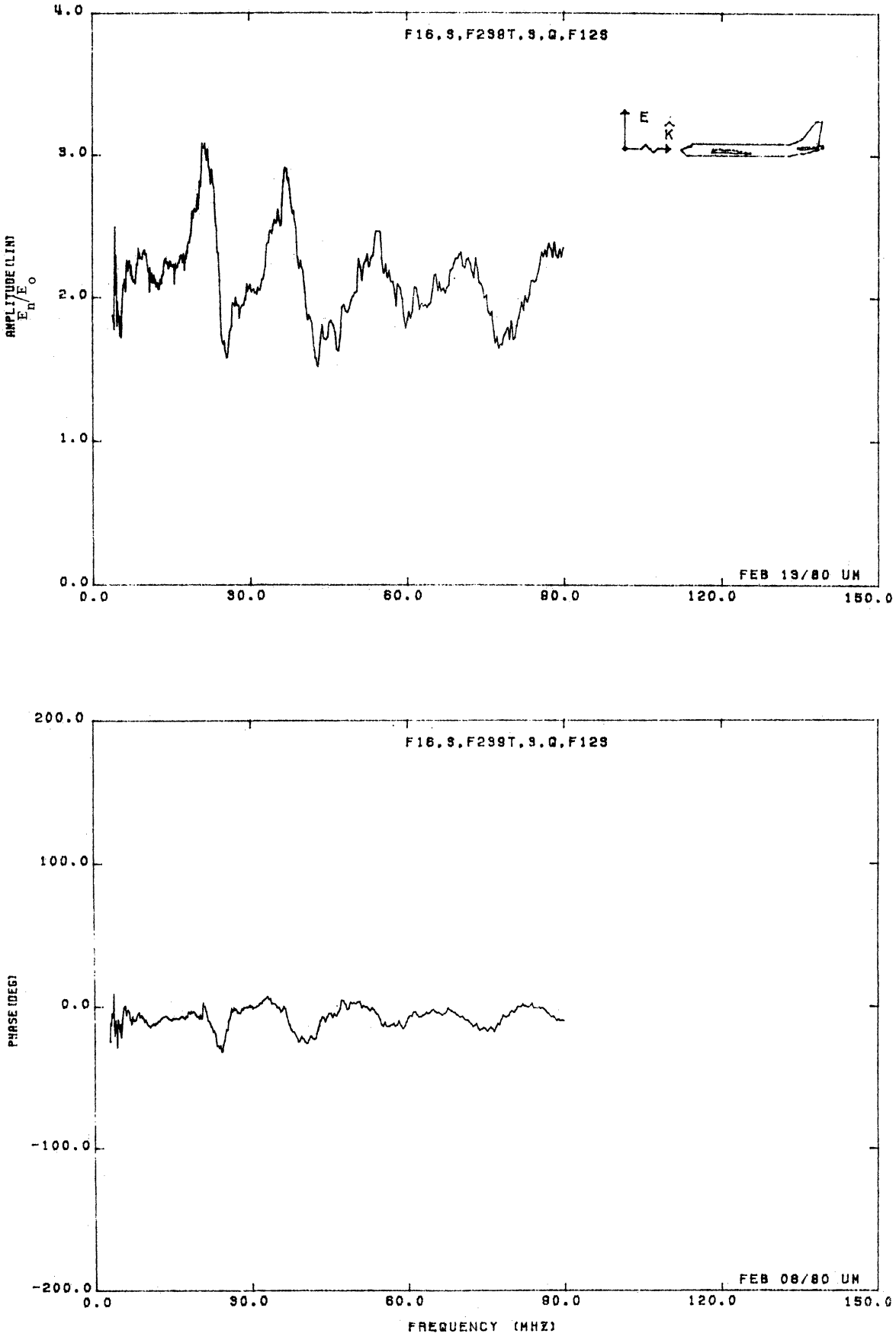

Figure 12S. Normal Electric Field at STA:F239T, Excitation 3, 1/48 Model.

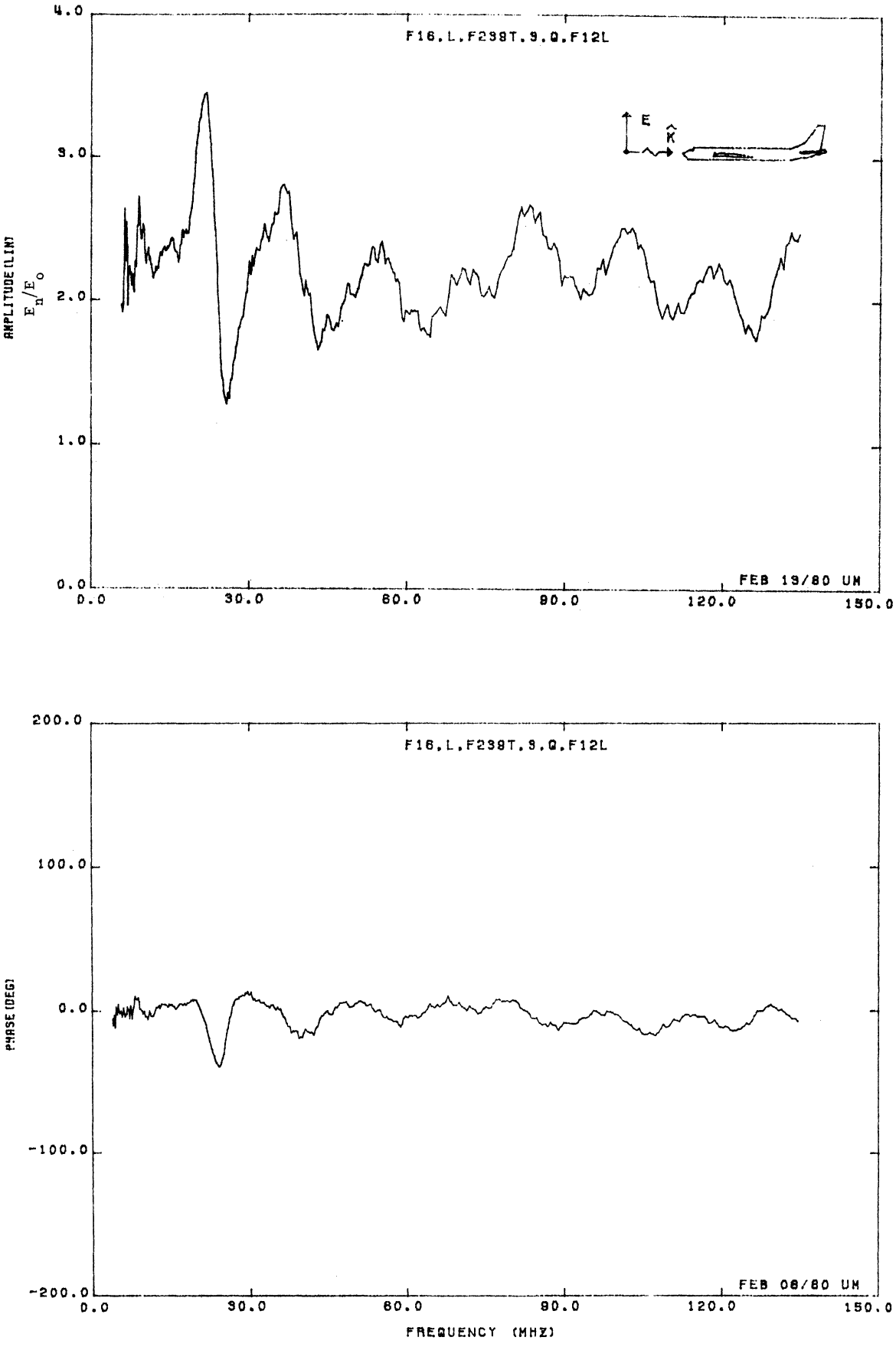

Figure 12L. Normal Electric Field at STA:F239T, Excitation 3, 1/32 Model.

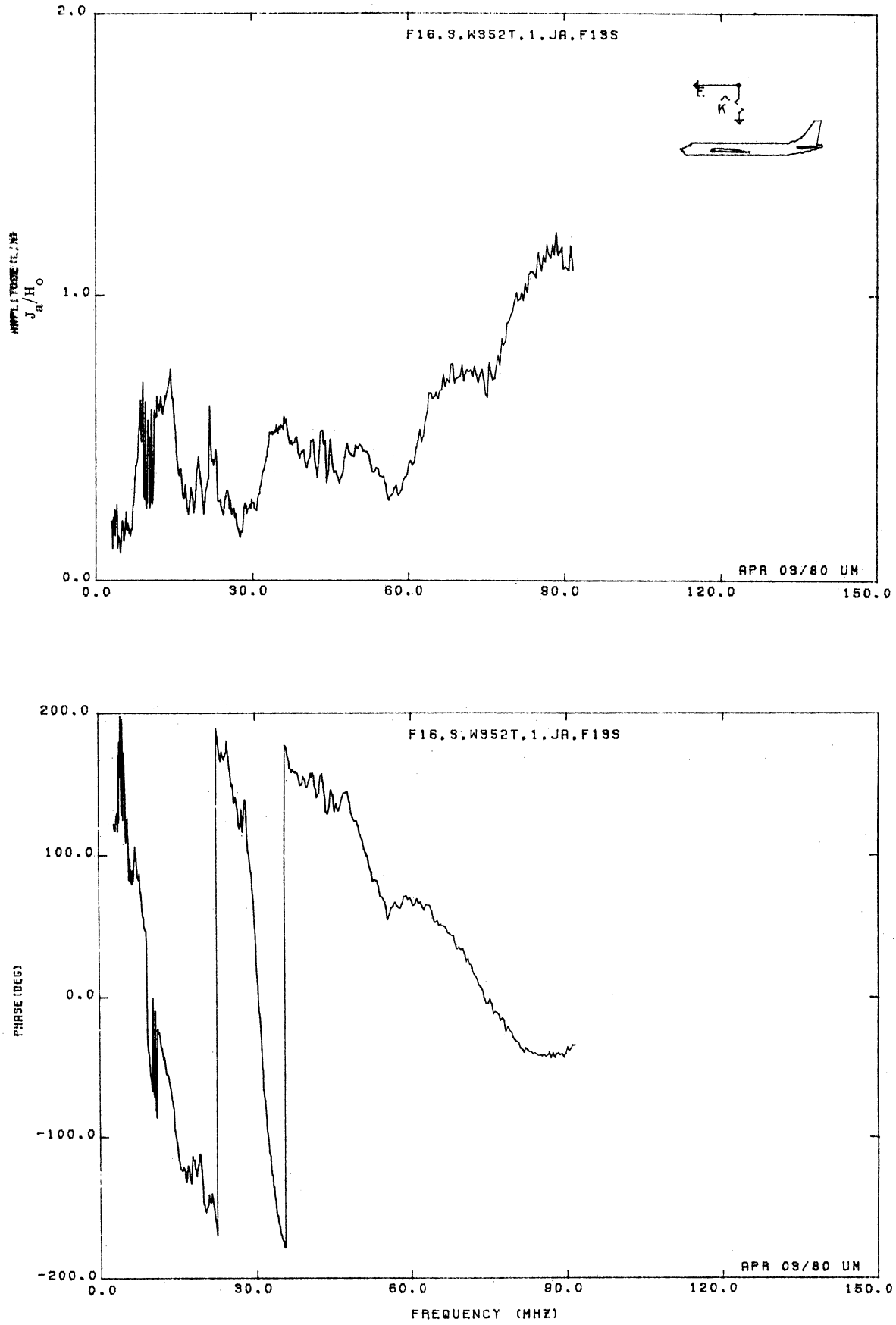

Figure 13S. Axial Current at STA:W352T, Excitation 1, 1/48 Model.

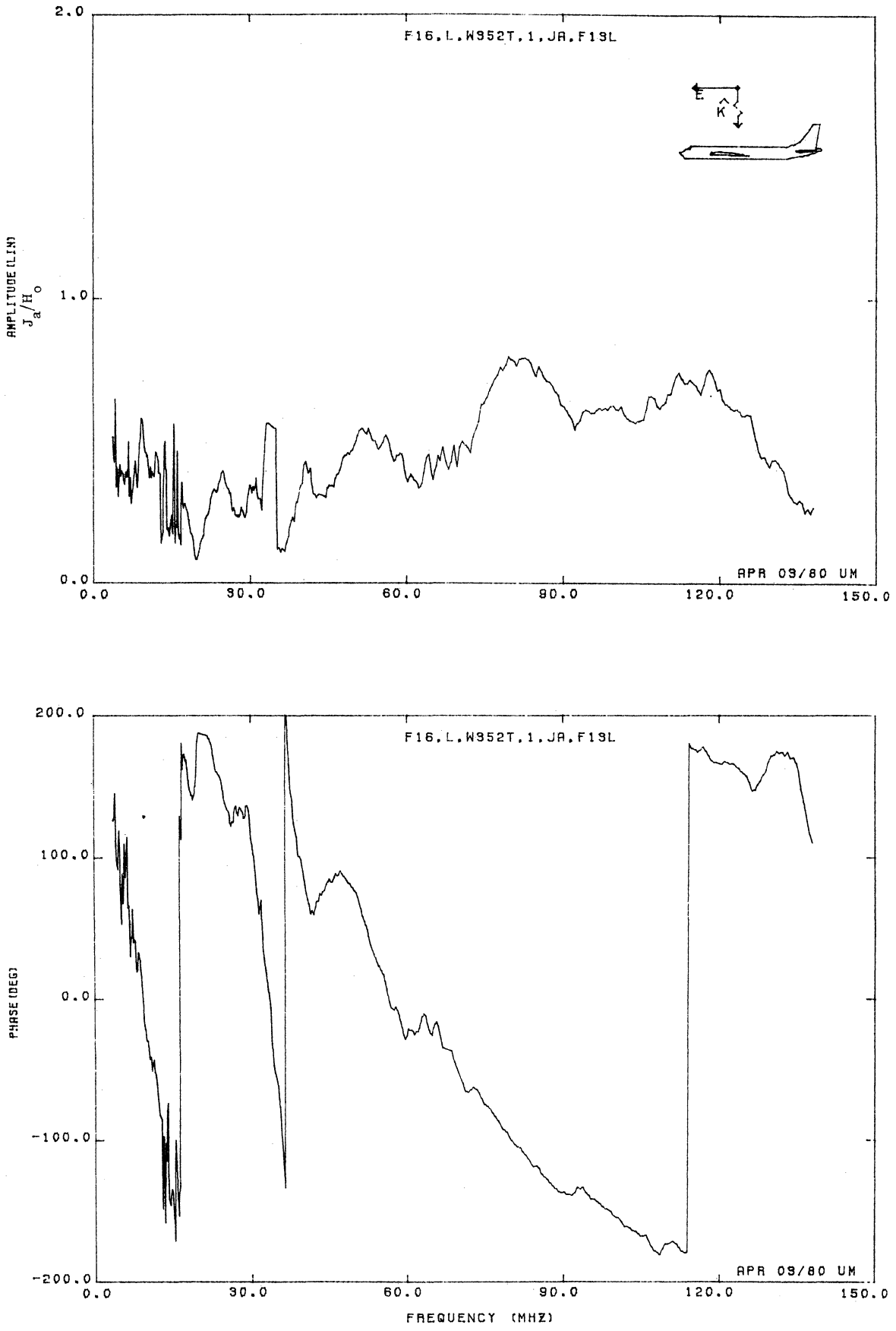

Figure 13L. Axial Current at STA:W352T, Excitation 1, 1/32 Model.

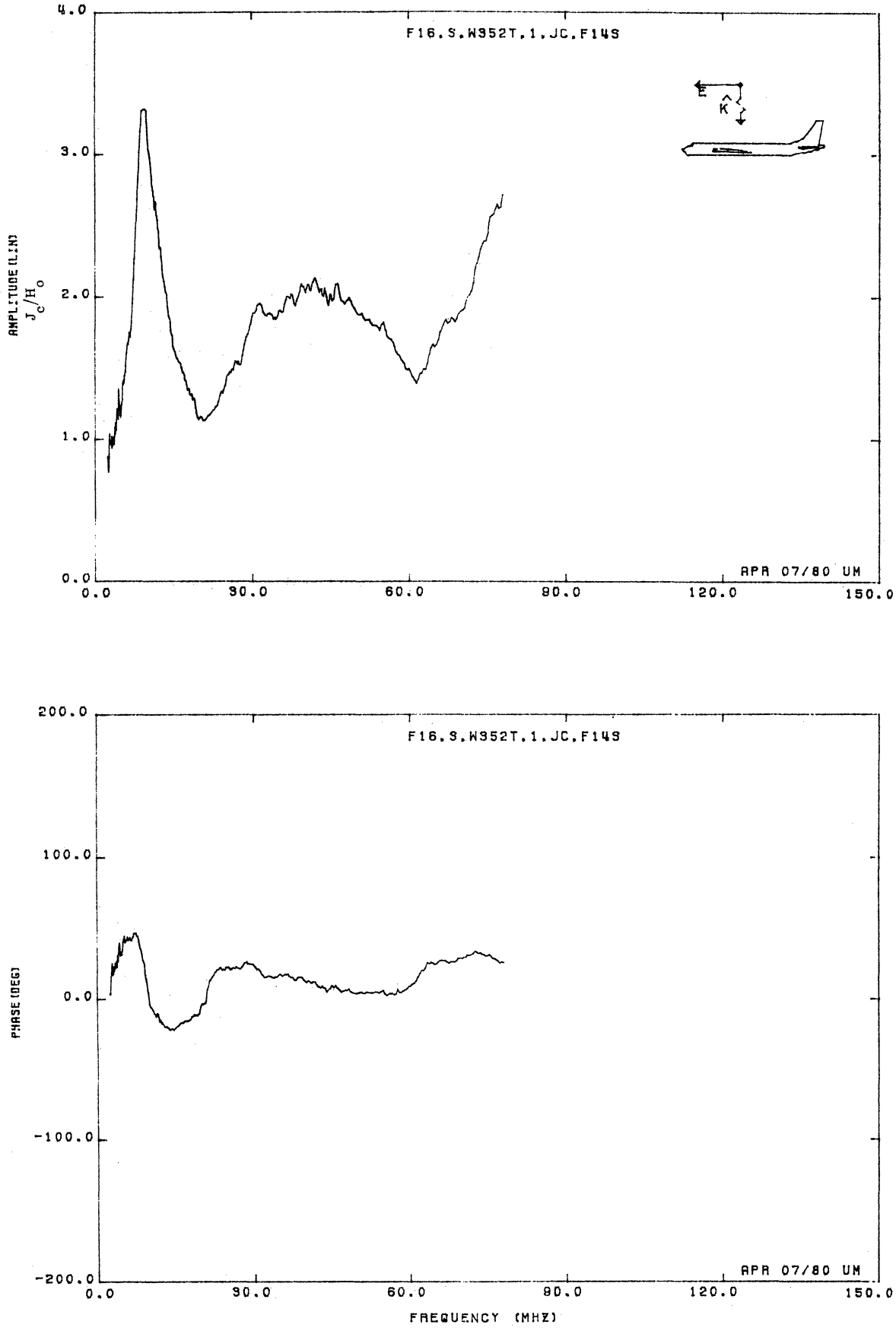

Figure 14S. Circumferential Current at STA:W352T, Excitation 1, 1/48 Model.

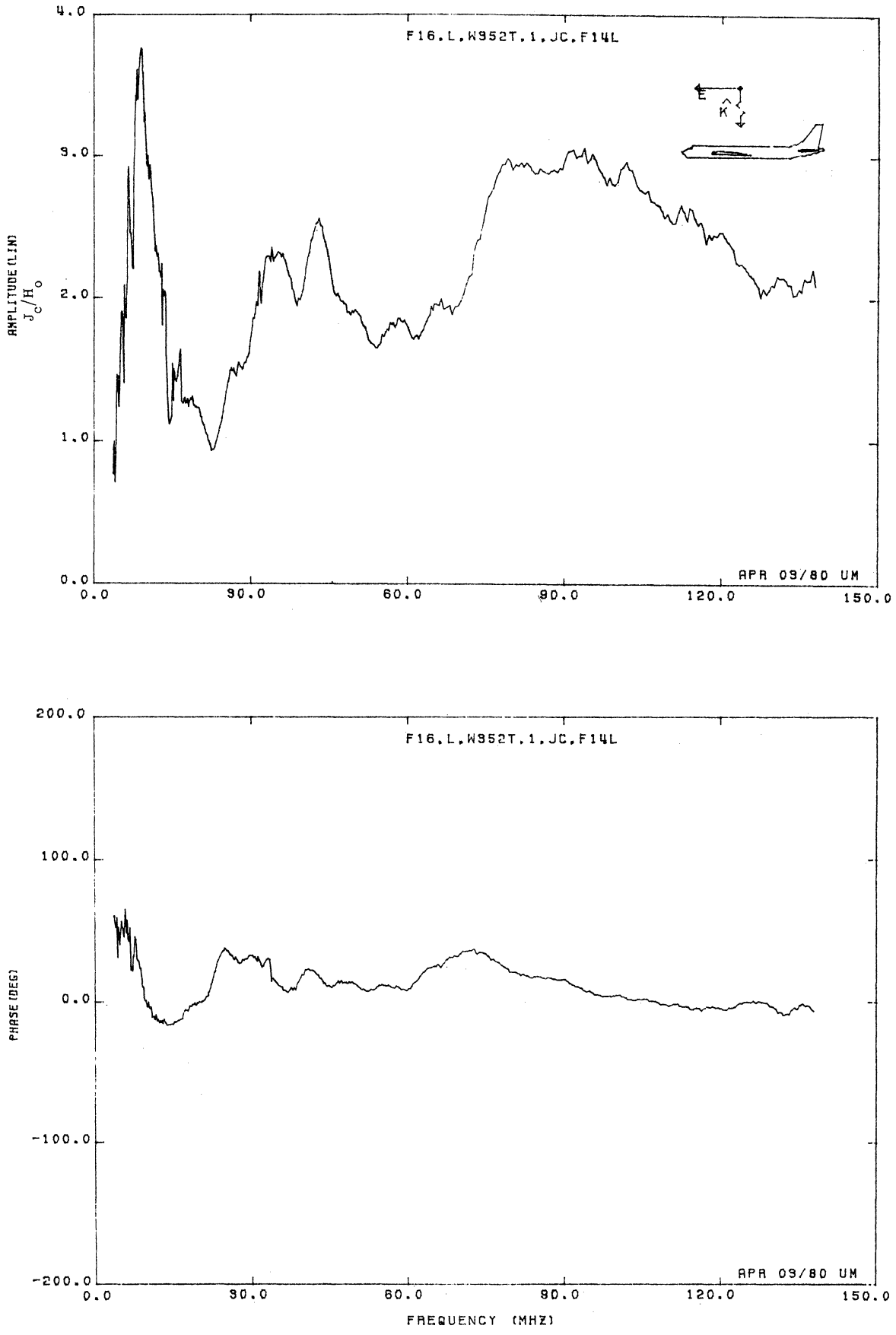

Figure 14L. Circumferential Current at STA:W352T, Excitation 1, 1/32 Model.

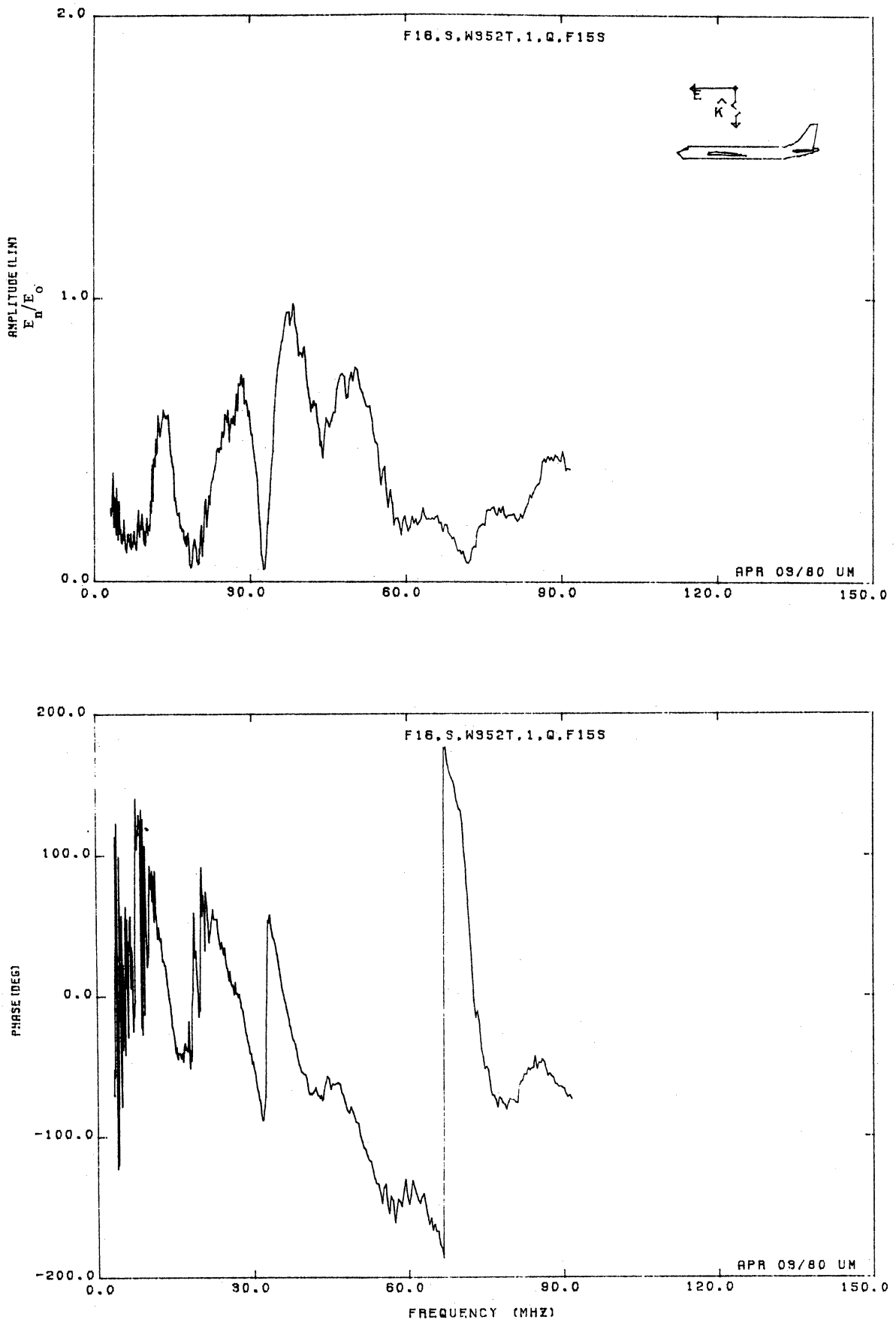

Figure 15S. Normal Electric Field at STA:W352T, Excitation 1, 1/48 Model.

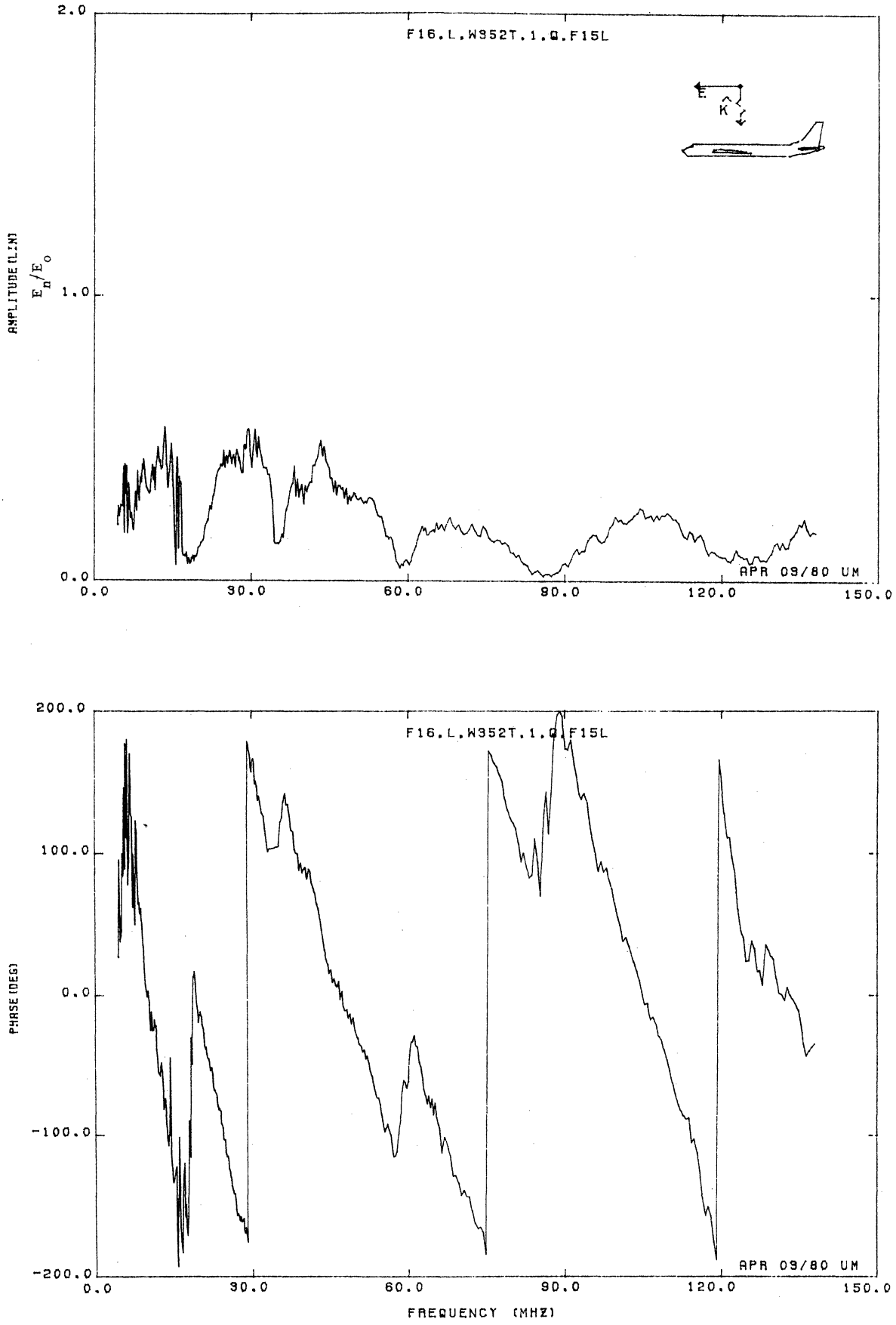

Figure 15L. Normal Electric Field at STA:W352T, Excitation 1, 1/32 Model.

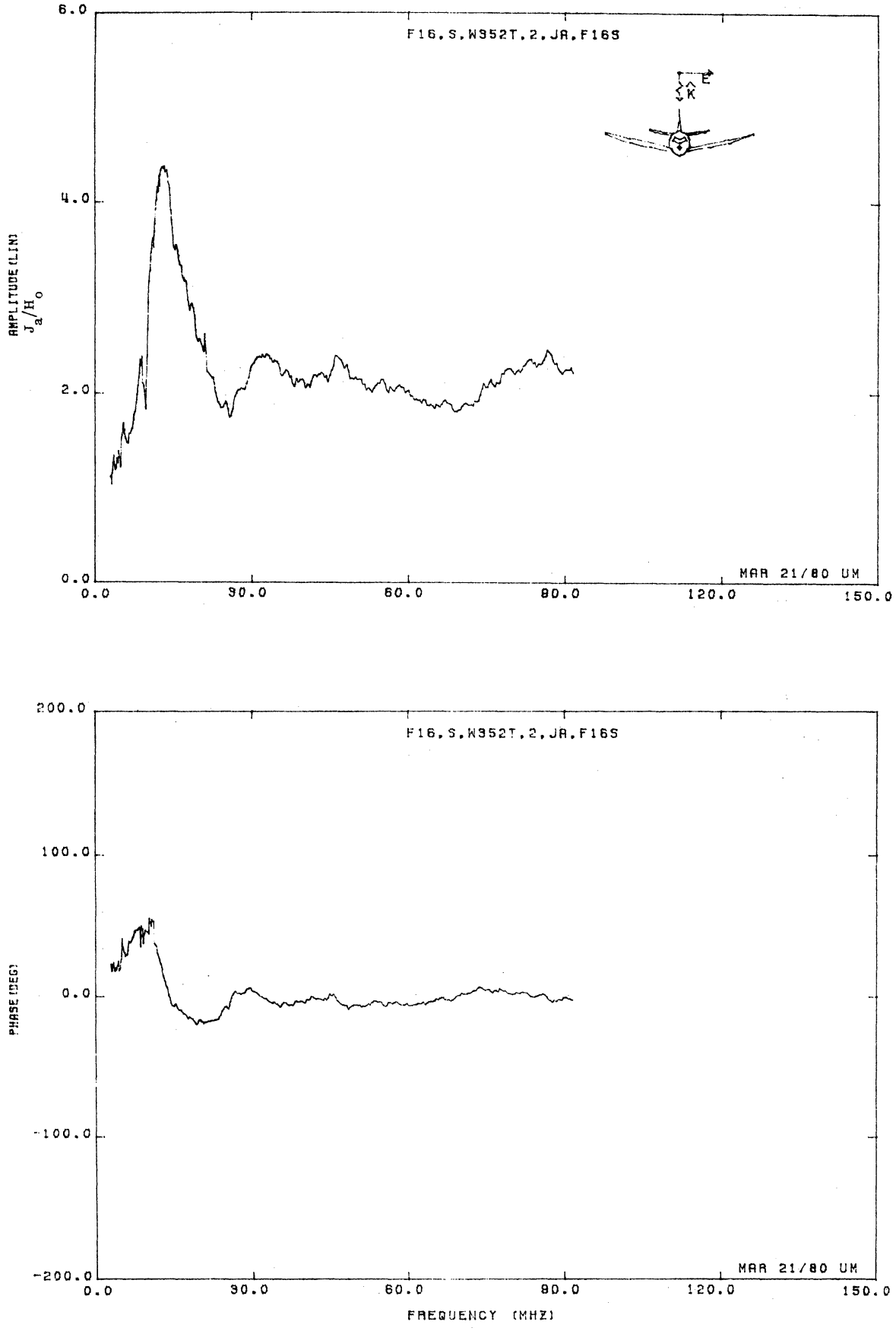

Figure 16S. Axial Current at STA:W352T, Excitation 2, 1/48 Model.

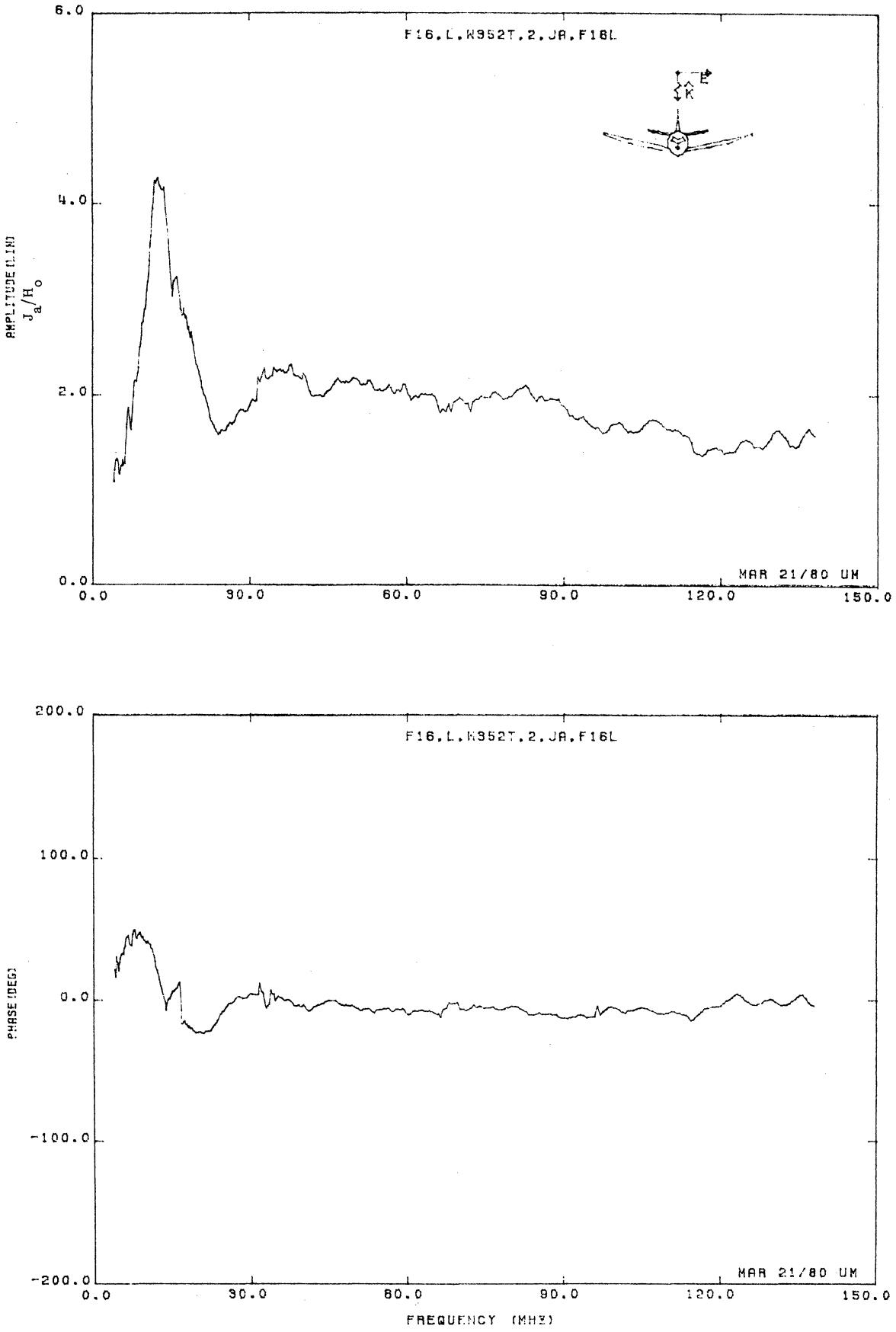

Figure 16L. Axial Current at STA:W352T, Excitation 2, 1/32 Model.

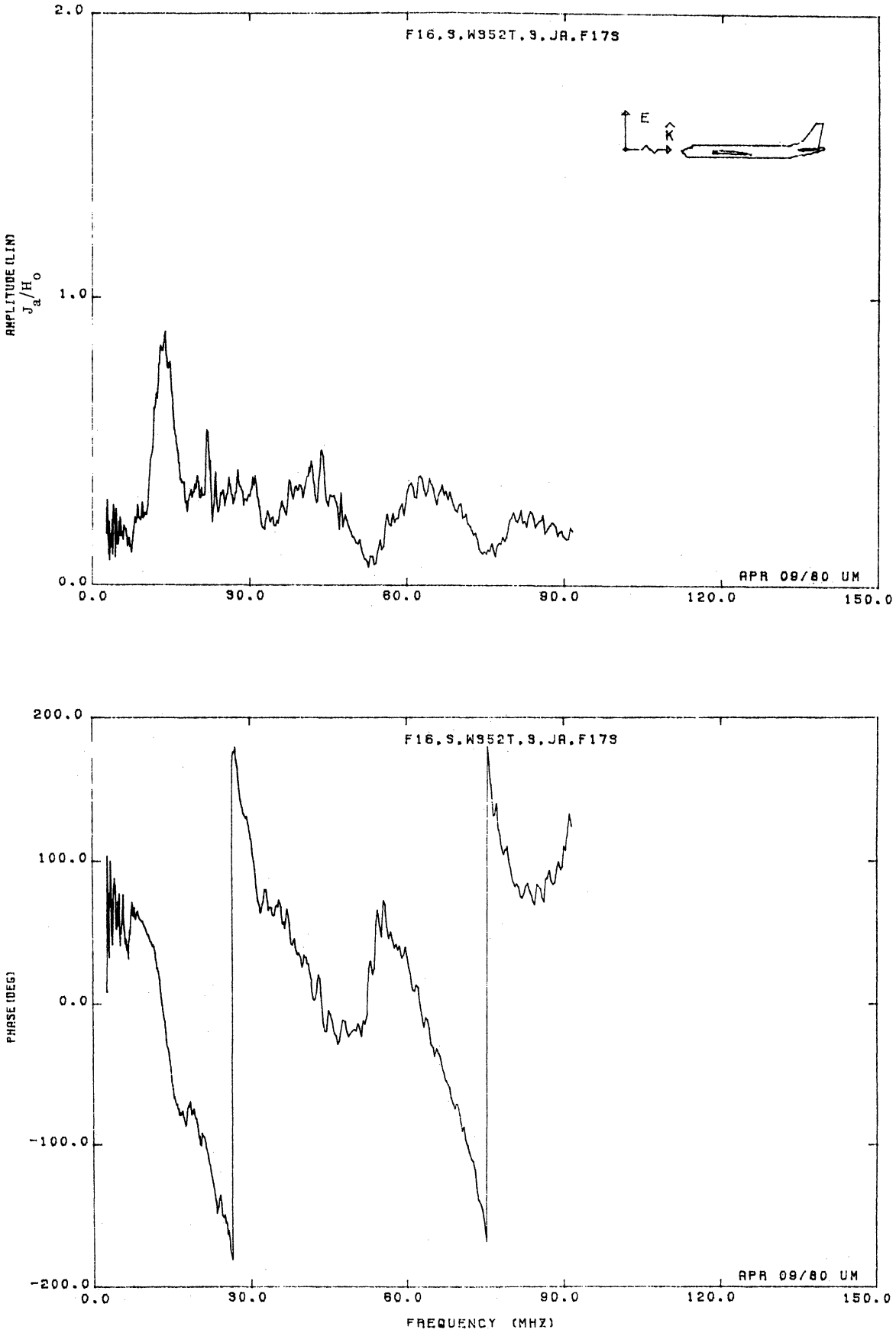

Figure 17S. Axial Current at STA:W352T, Excitation 3, 1/48 Model.

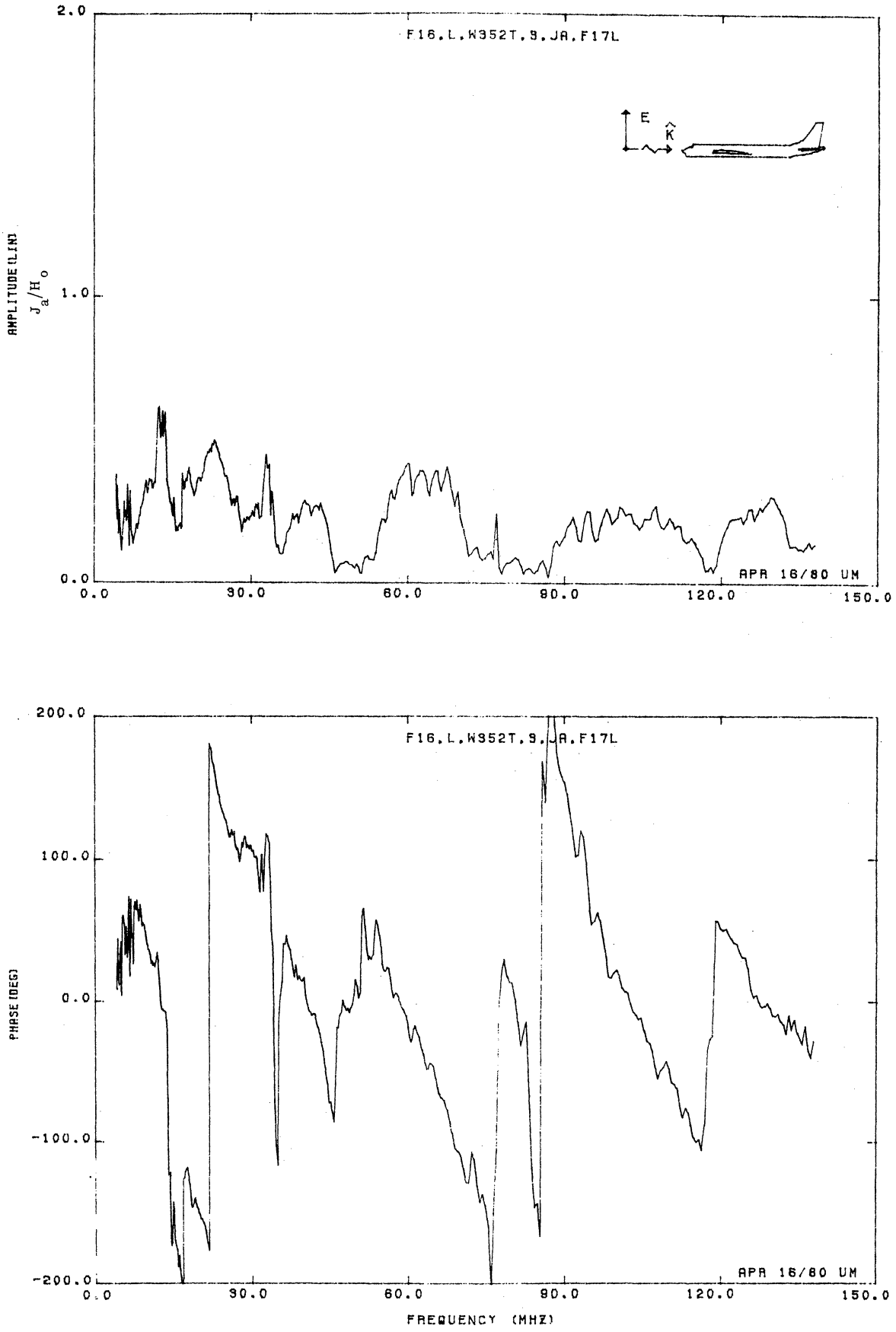

Figure 17L. Axial Current at STA:W352T, Excitation 3, 1/32 Model.

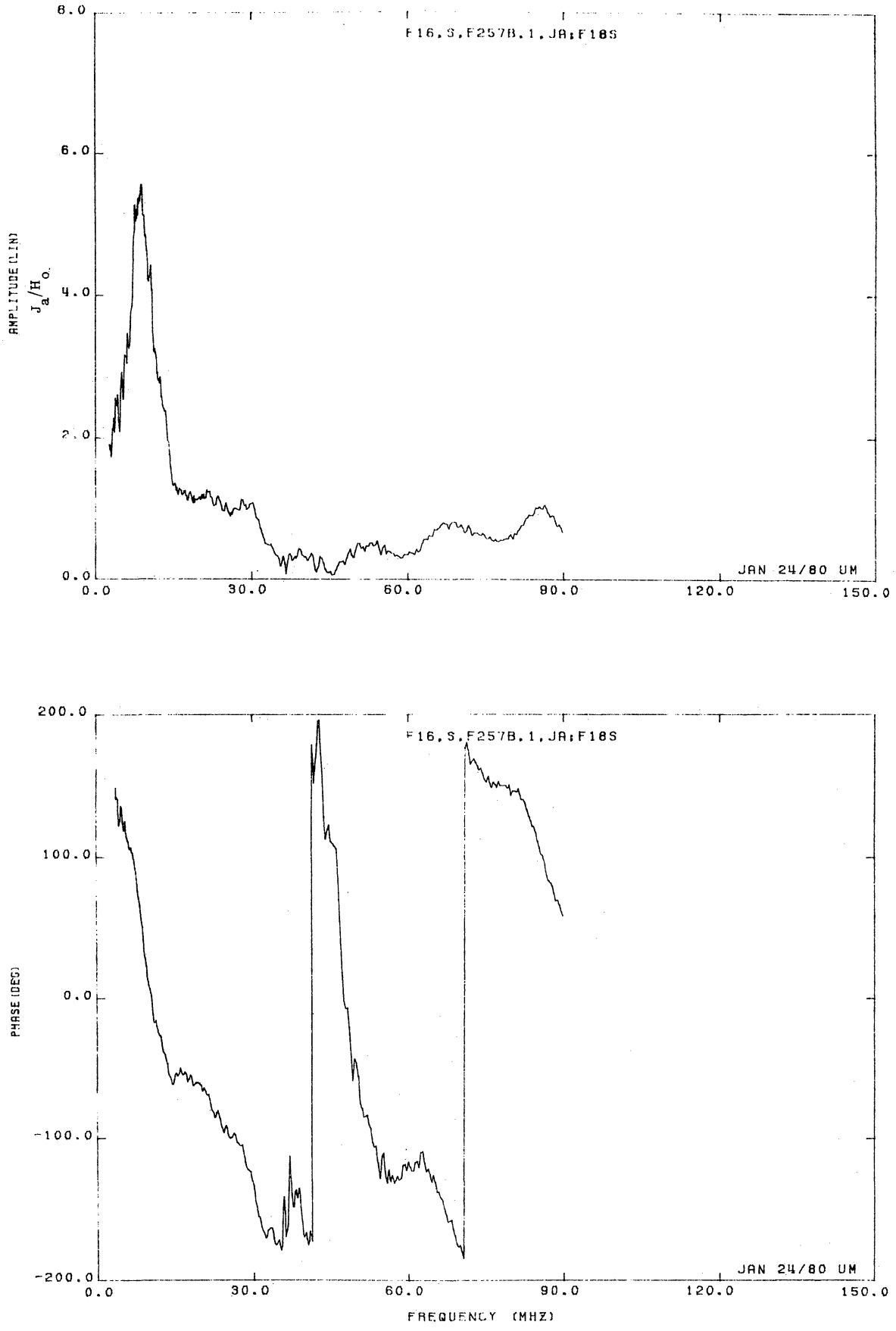

Figure 18S. Axial Current at STA:F257B, Excitation 1, 1/48 Model.

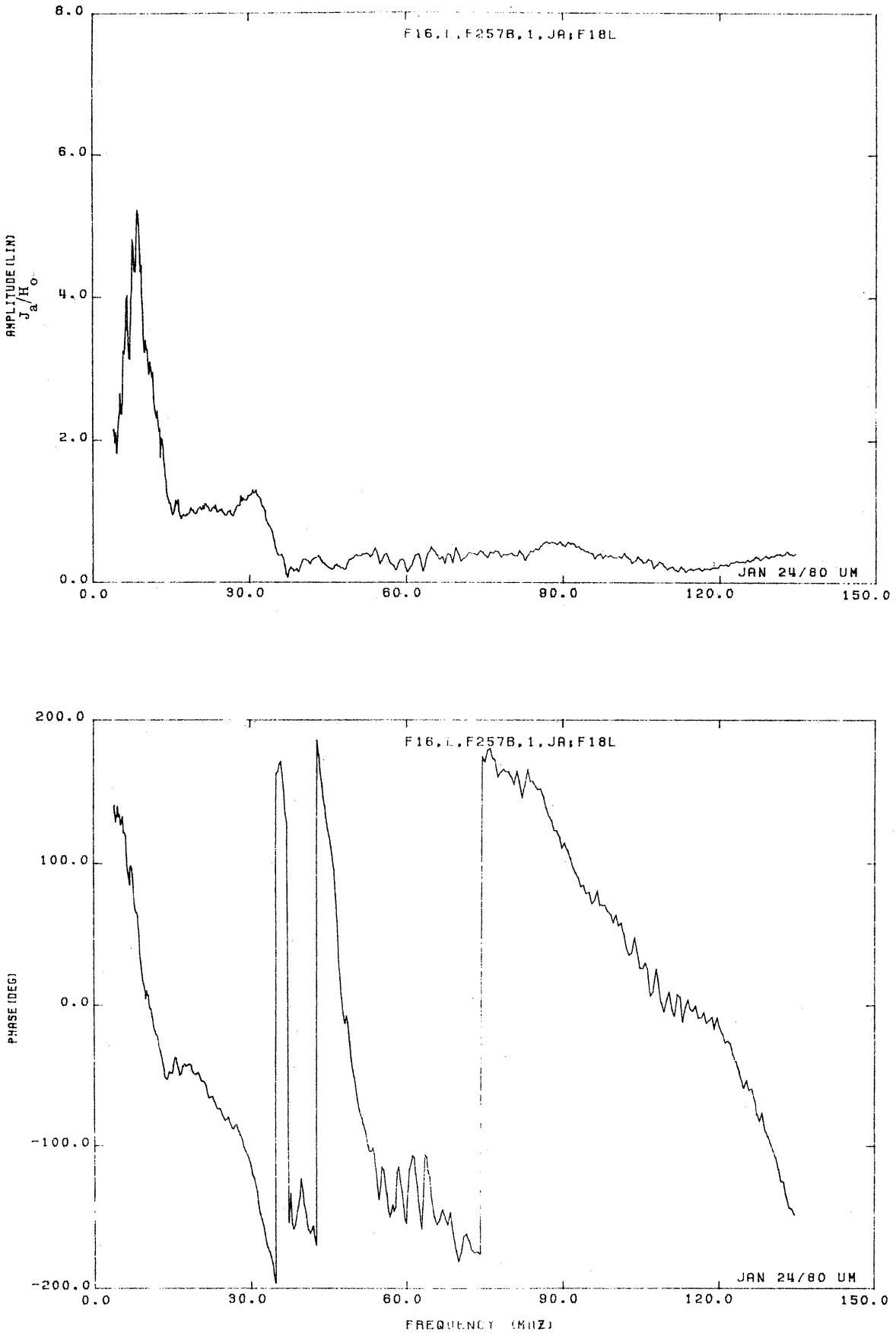

Figure 18L. Axial Current at STA:F257B, Excitation 1, 1/32 Model.

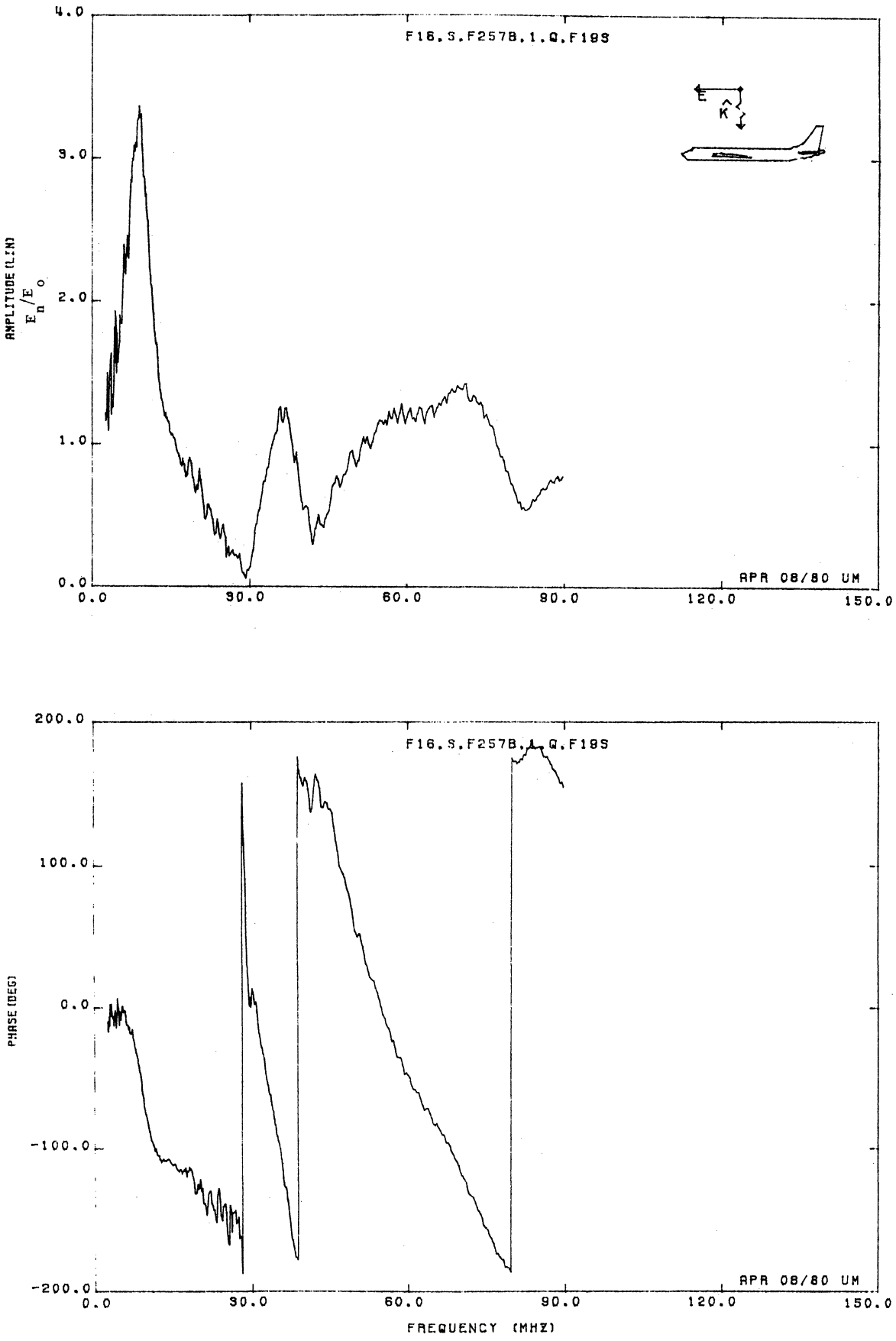

Figure 19S. Normal Electric Field at STA:F257B, Excitation 1, 1/48 Model.

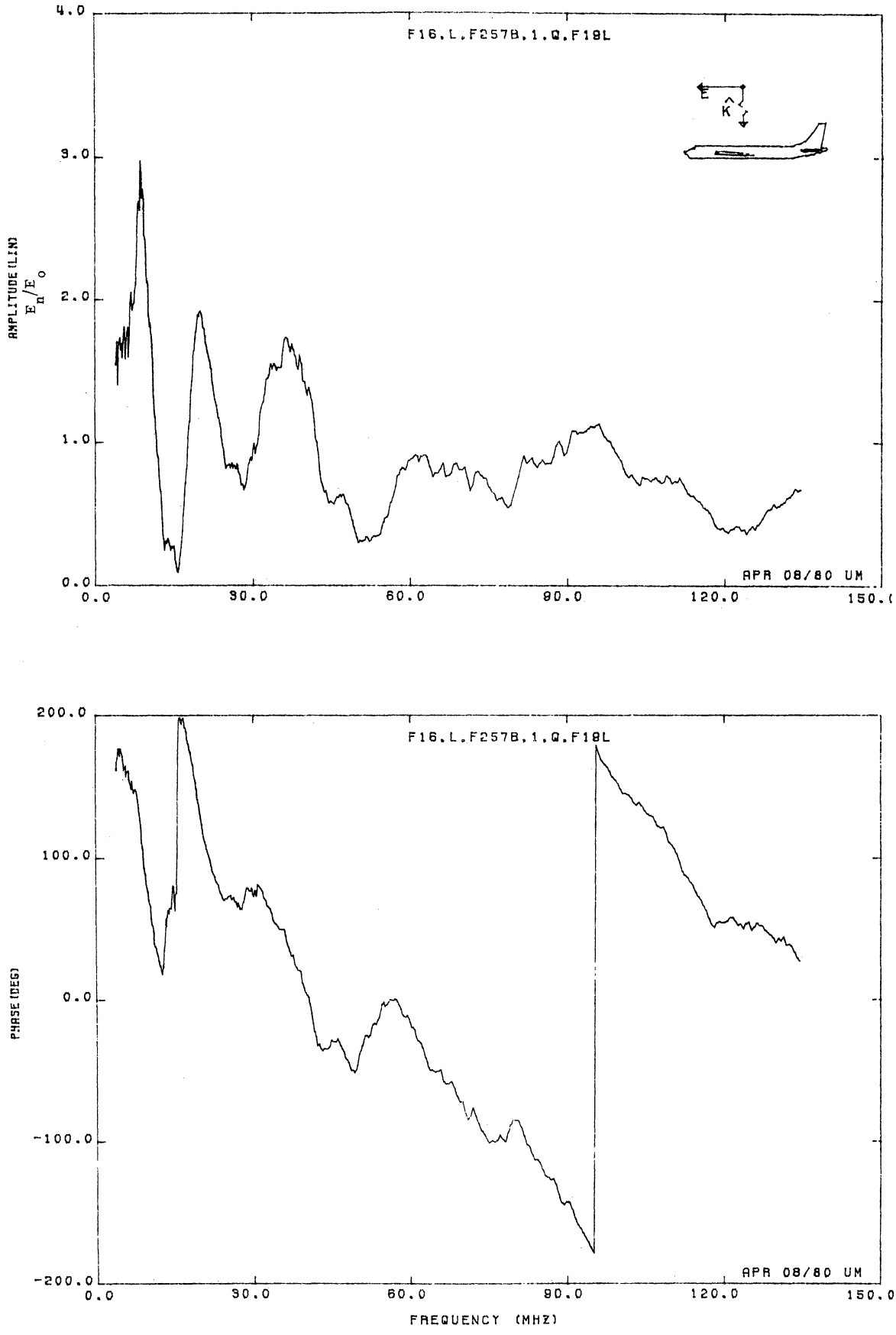

Figure 19L. Normal Electric Field at STA:F257B, Excitation 1, 1/32 Model.

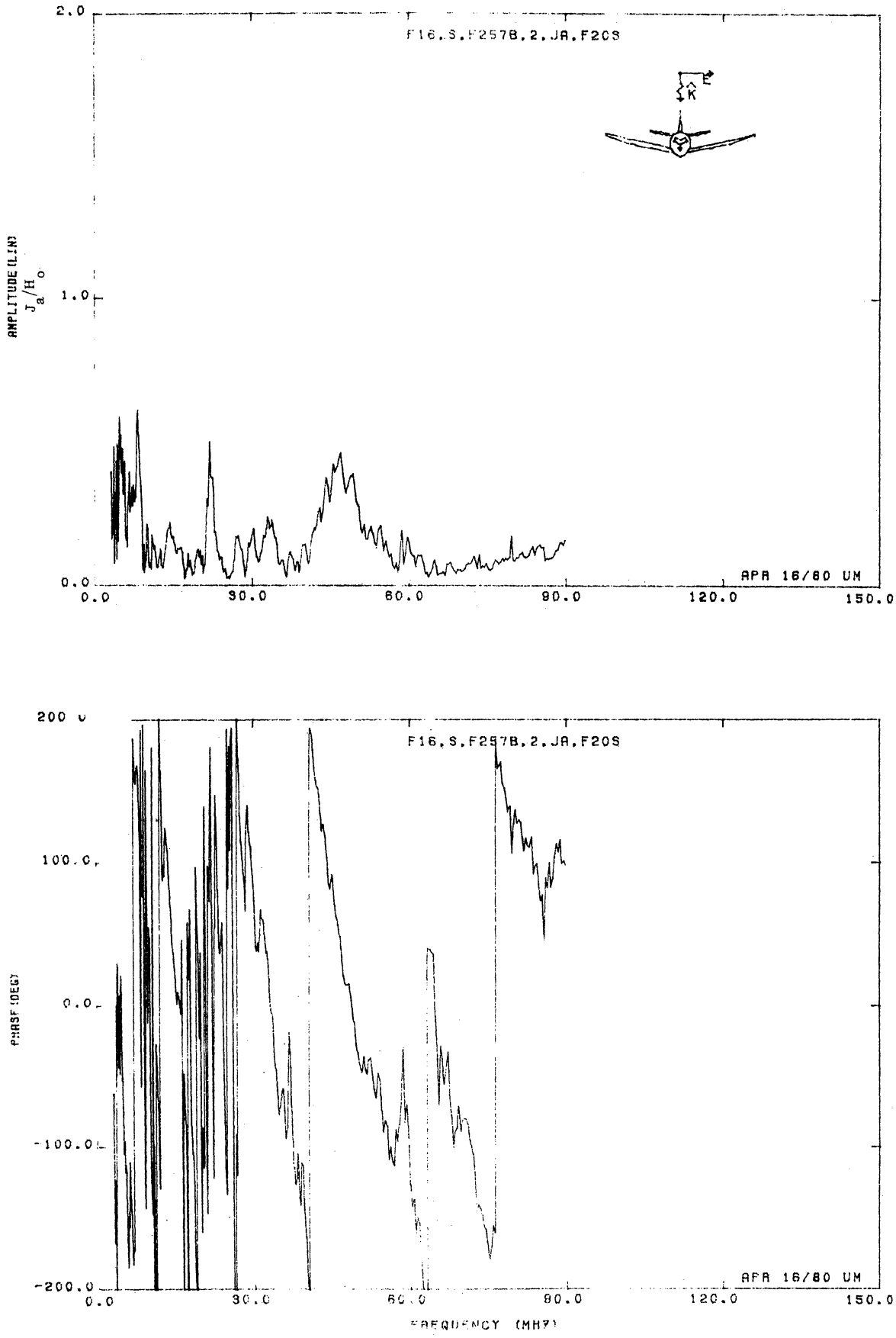

Figure 20S. Axial Current at STA:F257B, Excitation 2, 1/48 Model.

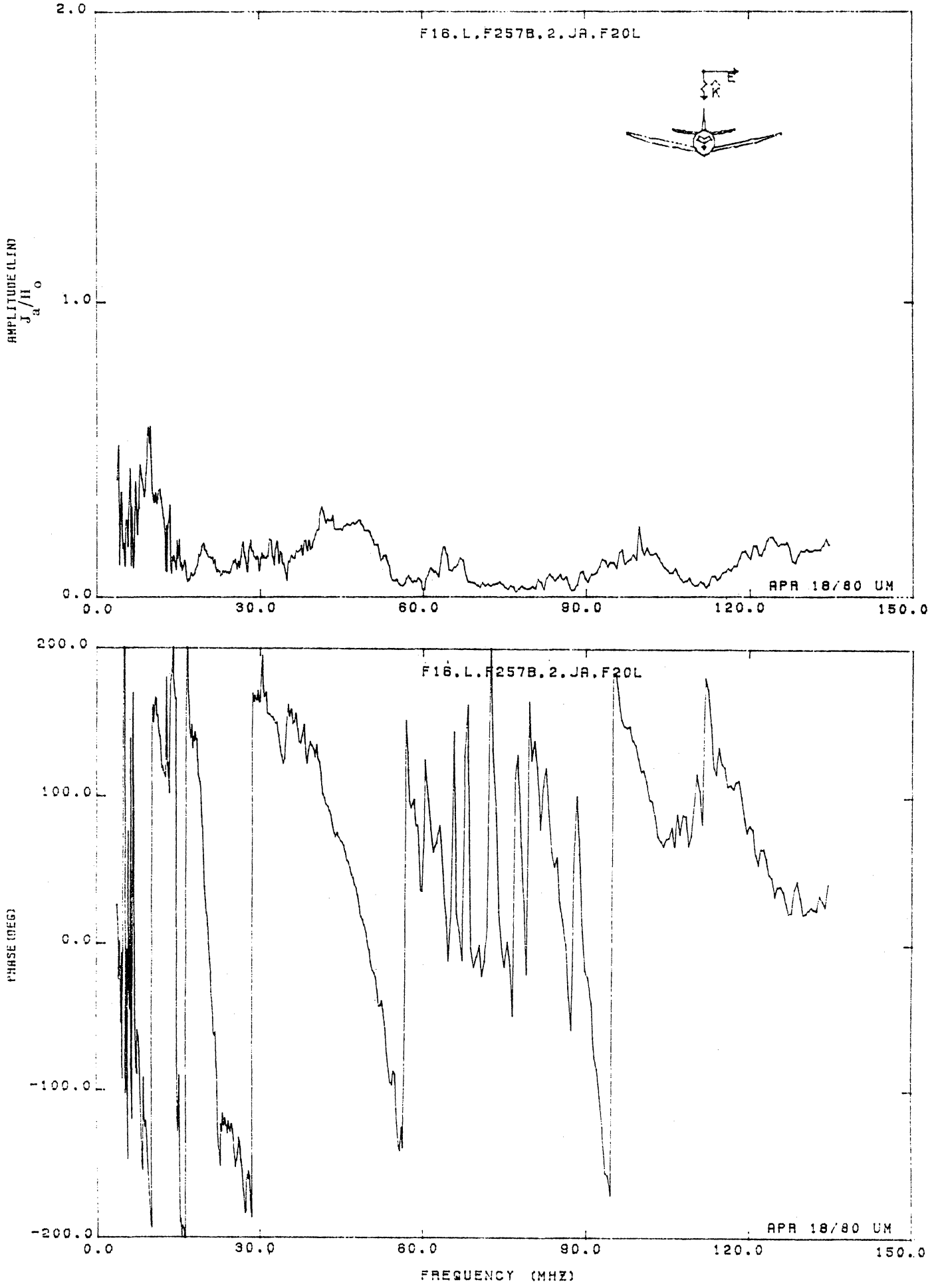

Figure 20L. Axial Current at STA:F257B, Excitation 2, 1/32 Model.

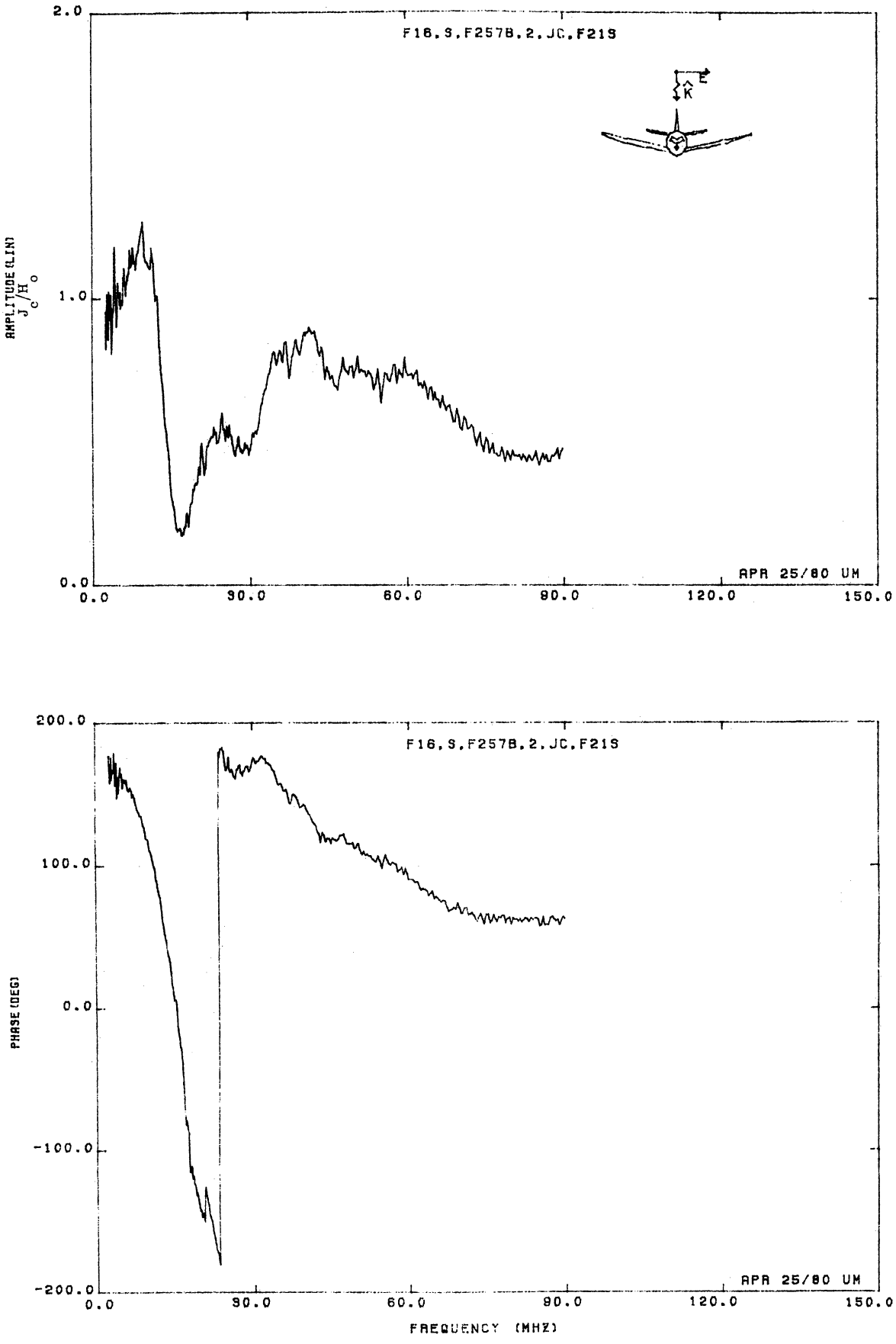

Figure 21S. Circumferential Current at STA:F257B, Excitation 2, 1/48 Model.

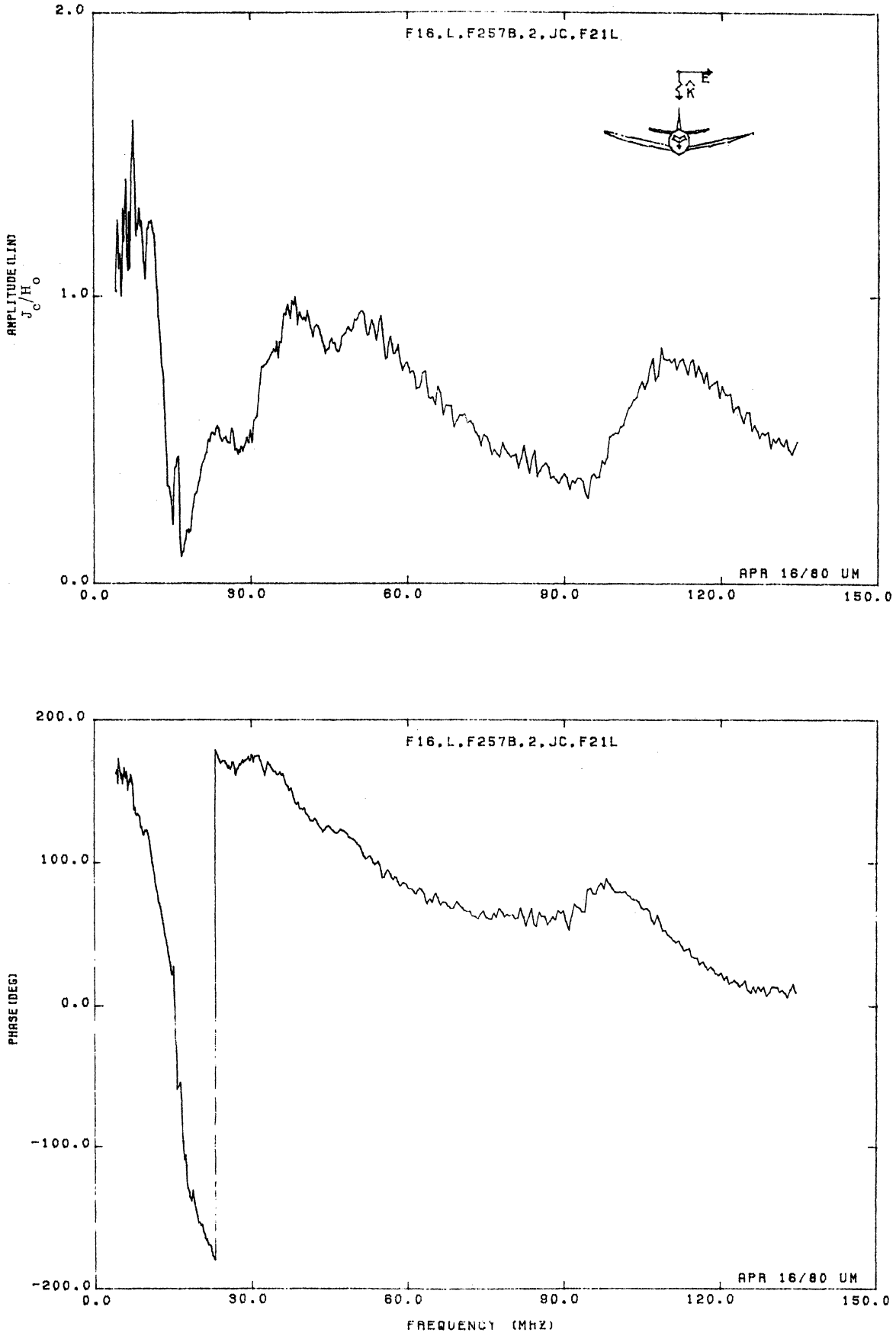

Figure 21L. Circumferential Current at STA:F257B, Excitation 2, 1/32 Model.

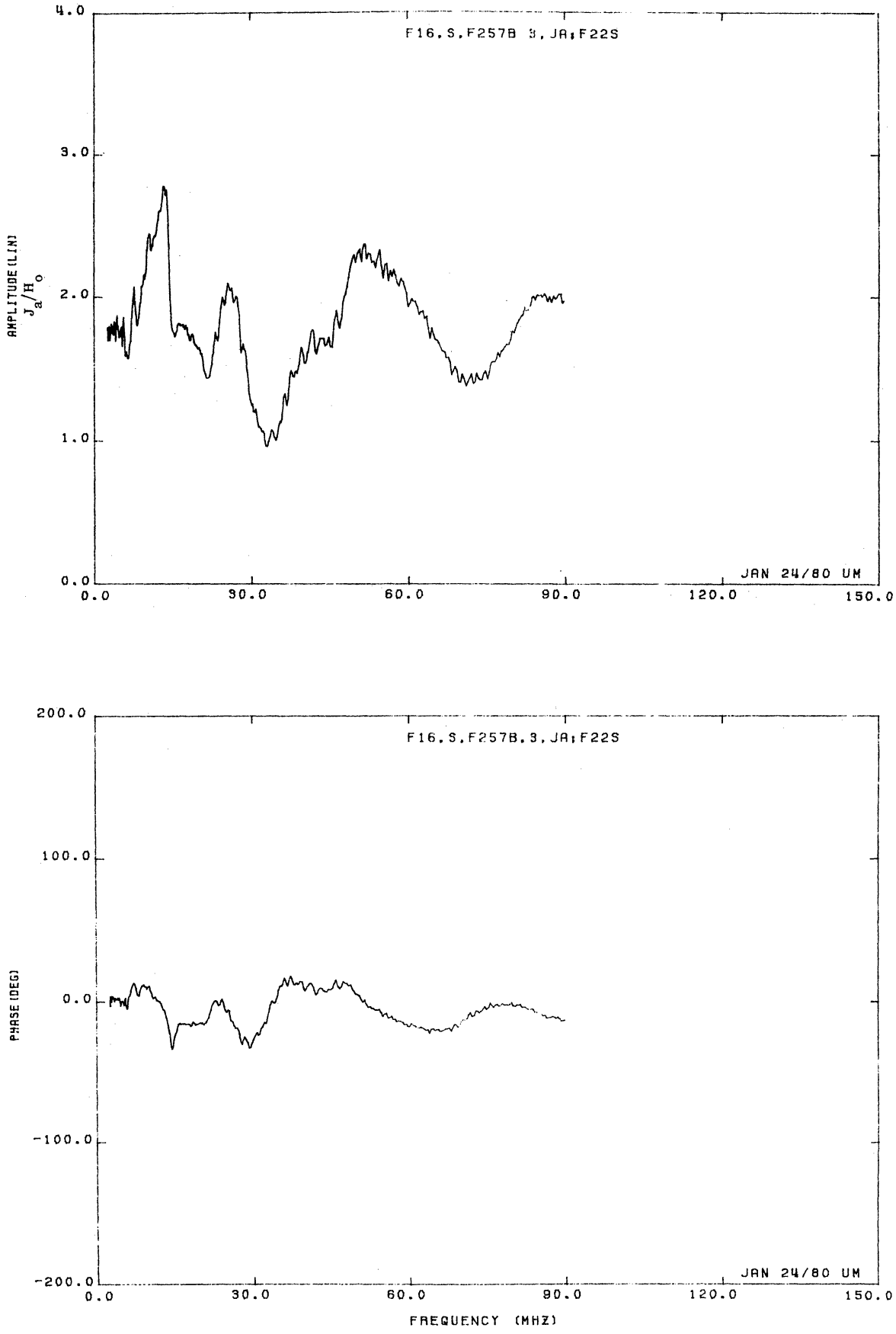

Figure 22S. Axial Current at STA:F257B, Excitation 3, 1/48 Model.

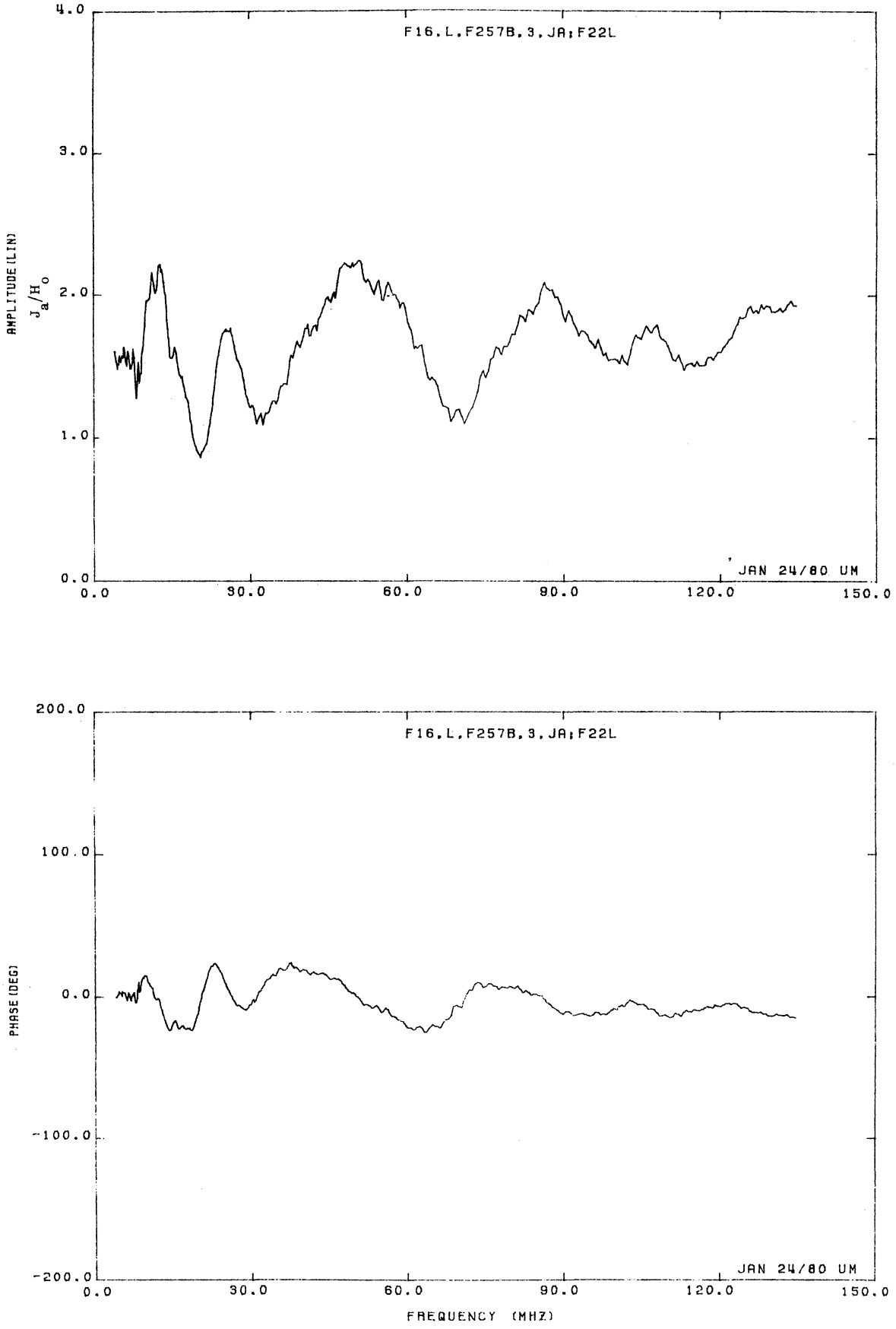

Figure 22L. Axial Current at STA:F257B, Excitation 3, 1/32 Model.

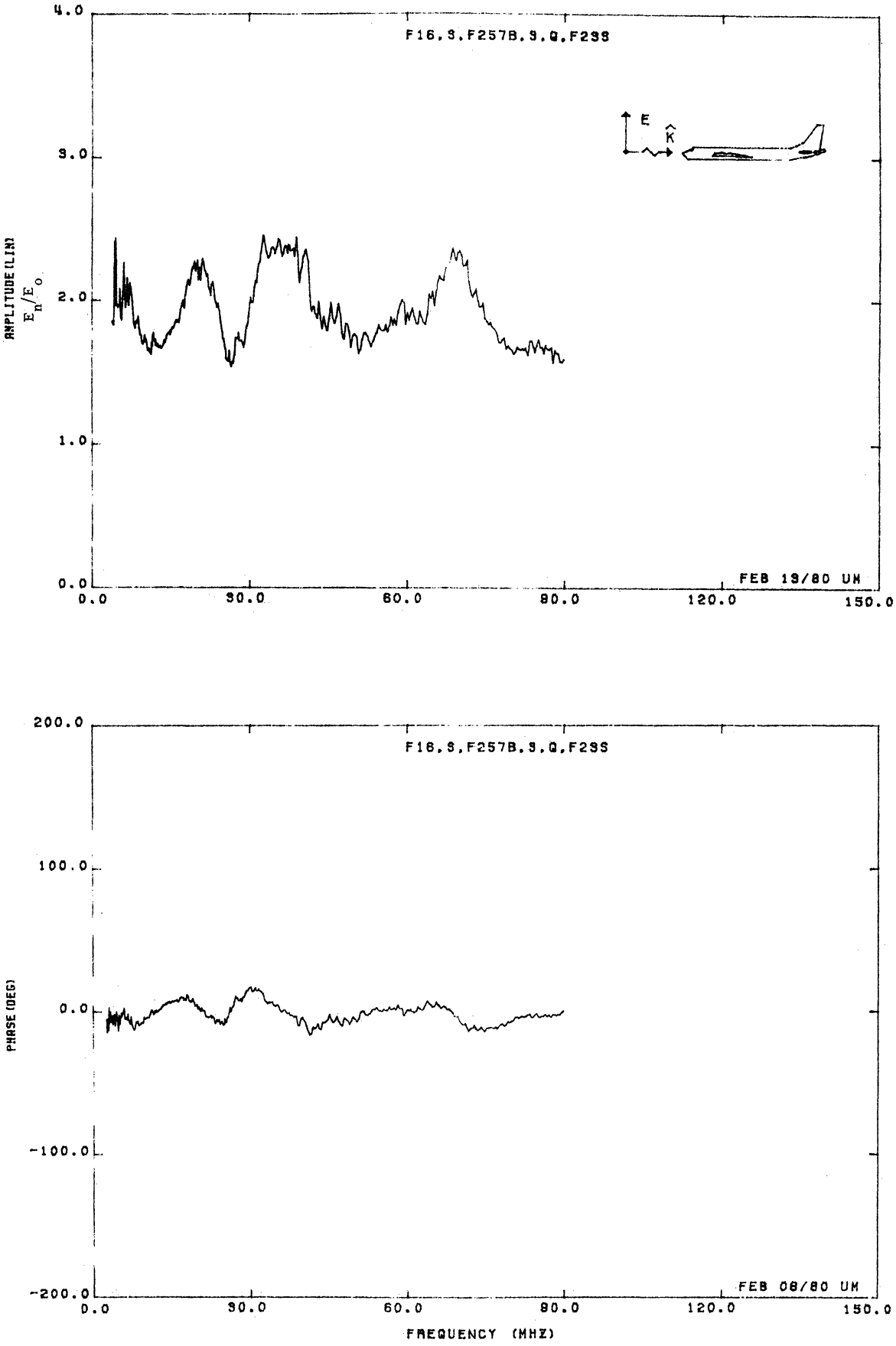

Figure 23S. Normal Electric Field at STA:F257B, Excitation 3, 1/48 Model.

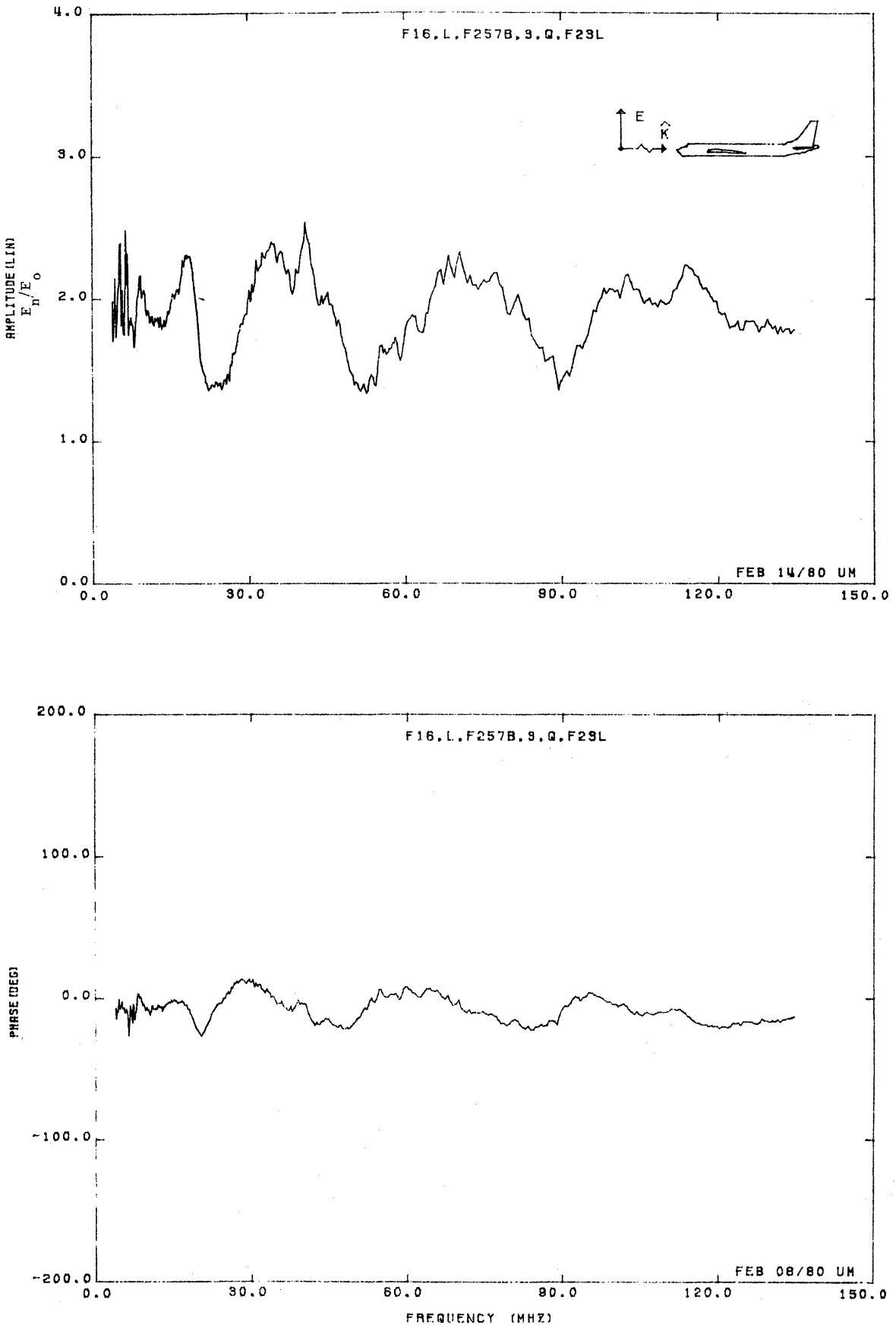

Figure 23L. Normal Electric Field at STA:F257B, Excitation 3, 1/32 Model.

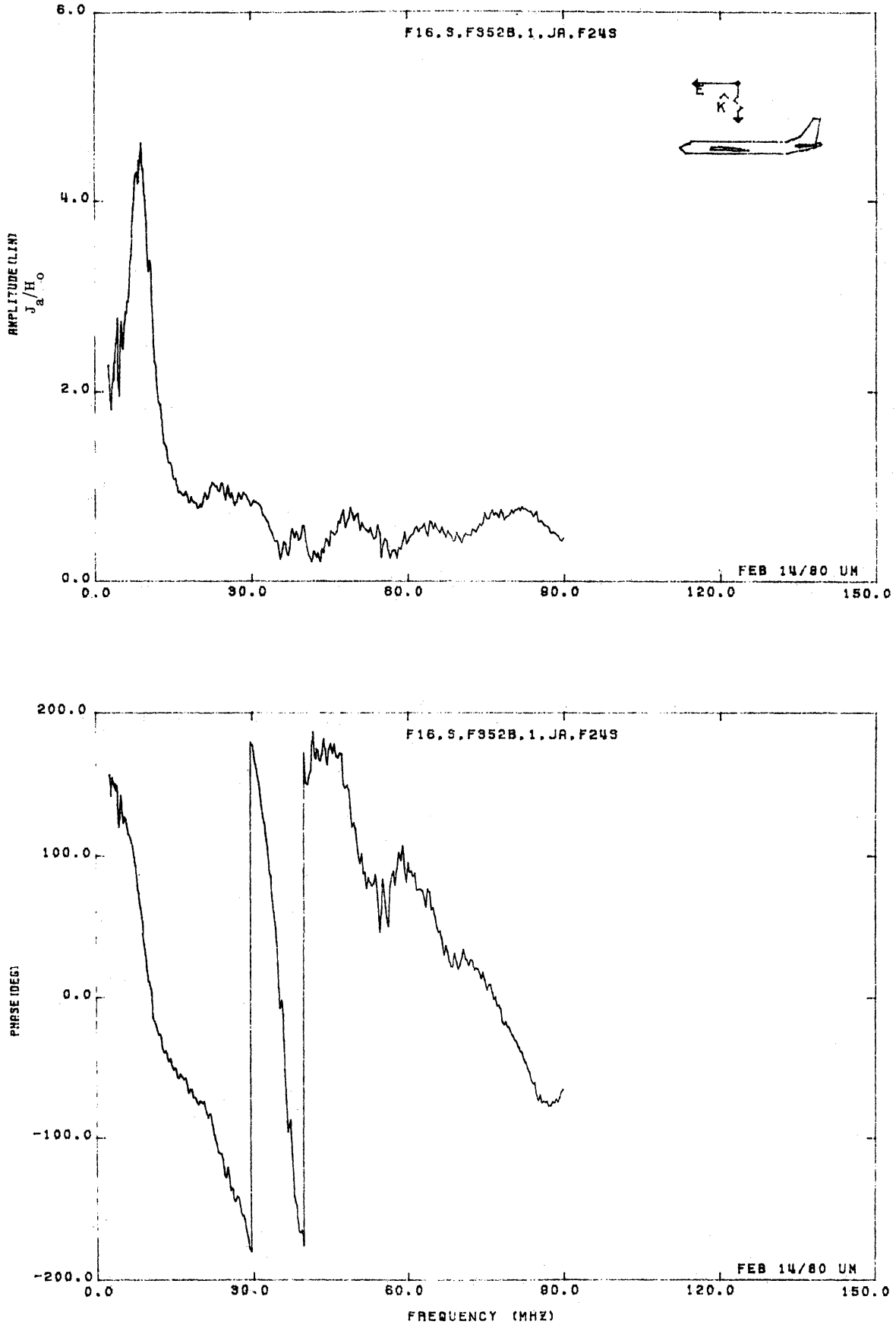

Figure 24S. Axial Current at STA:F352B, Excitation 1, 1/48 Model.

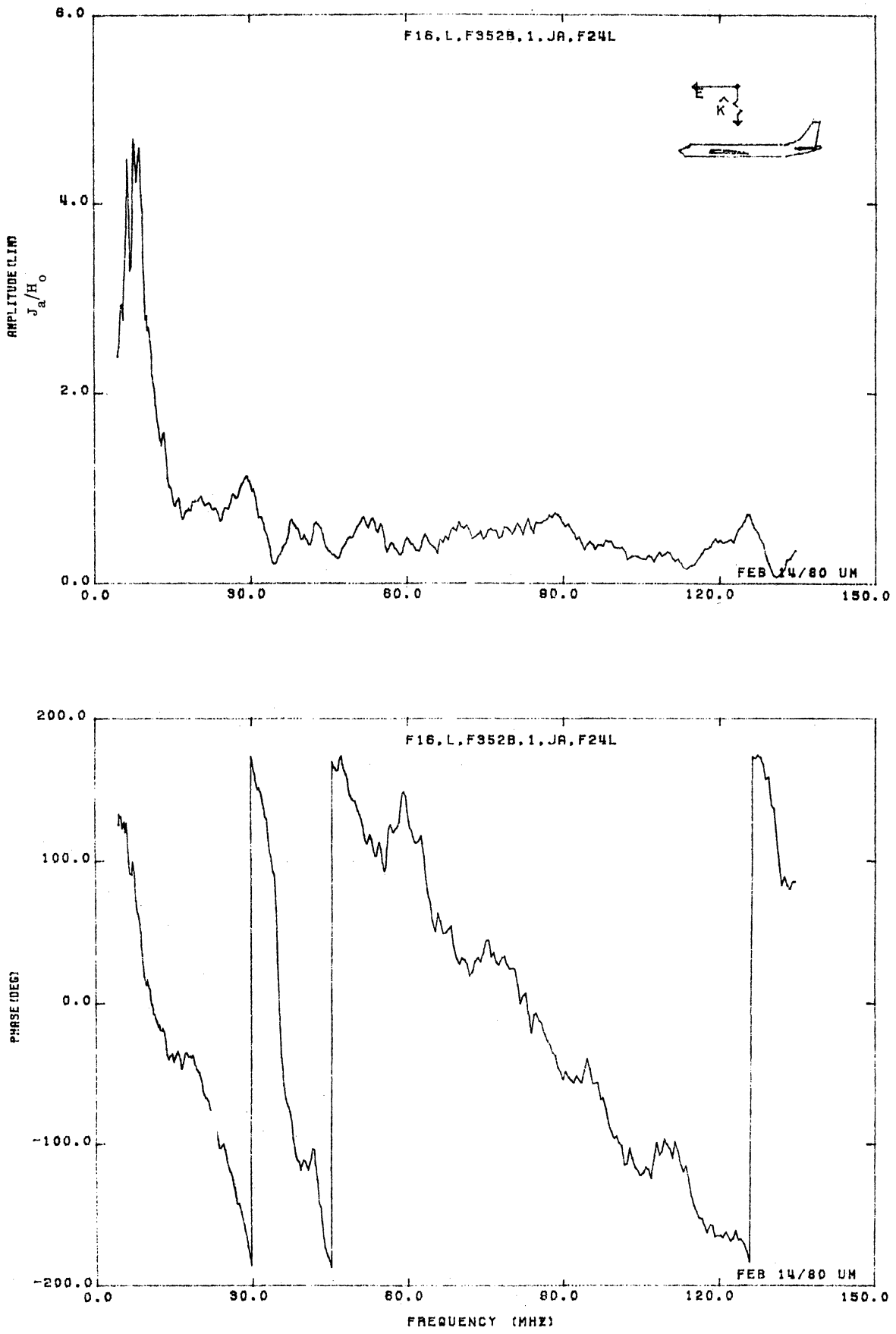

Figure 24L. Axial Current at STA:F352B, Excitation 1, 1/32 Model.

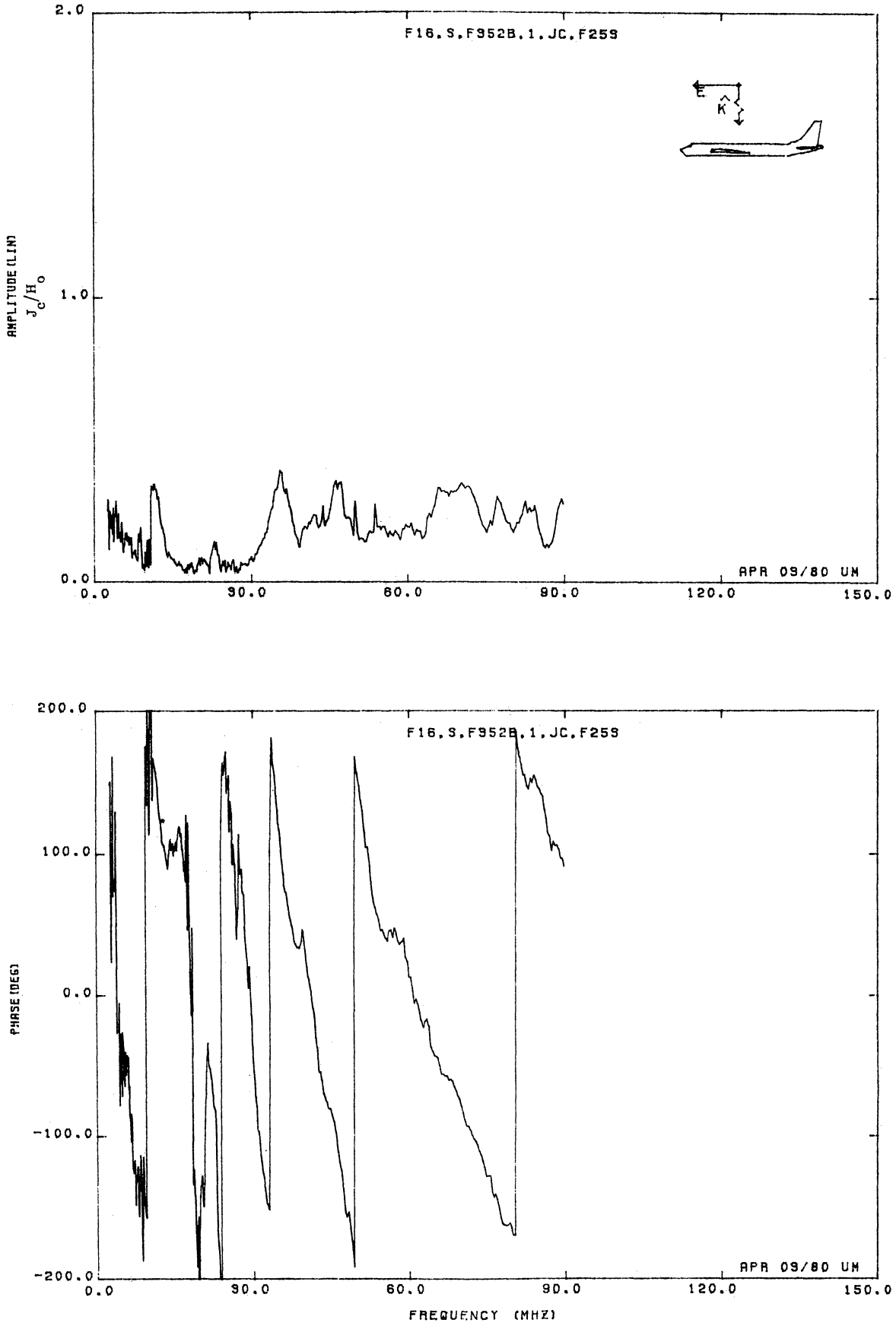

Figure 25S. Circumferential Current at STA:F352B, Excitation 1, 1/48 Model.

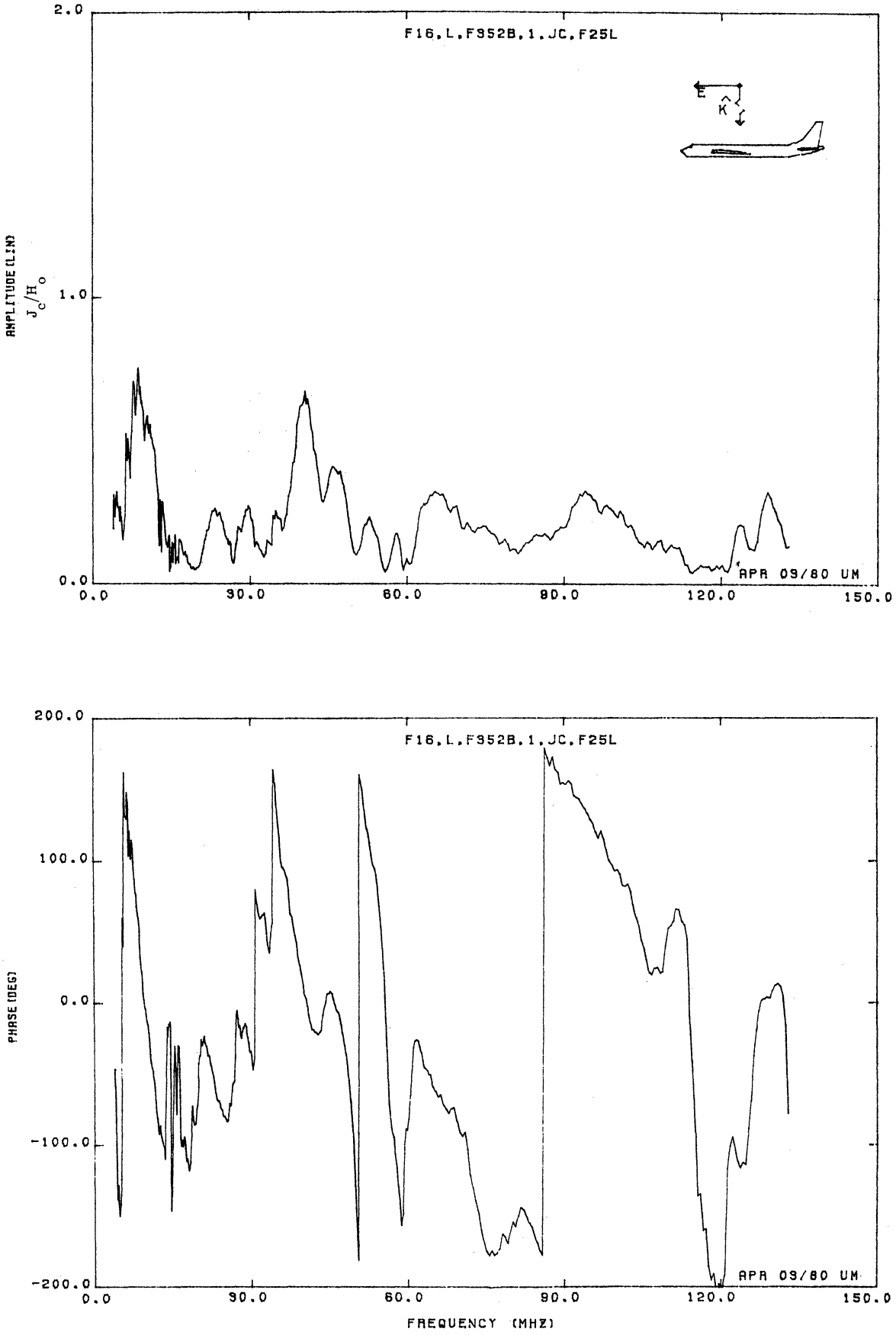

Figure 25L. Circumferential Current at STA:F352B, Excitation 1, 1/32 Model.

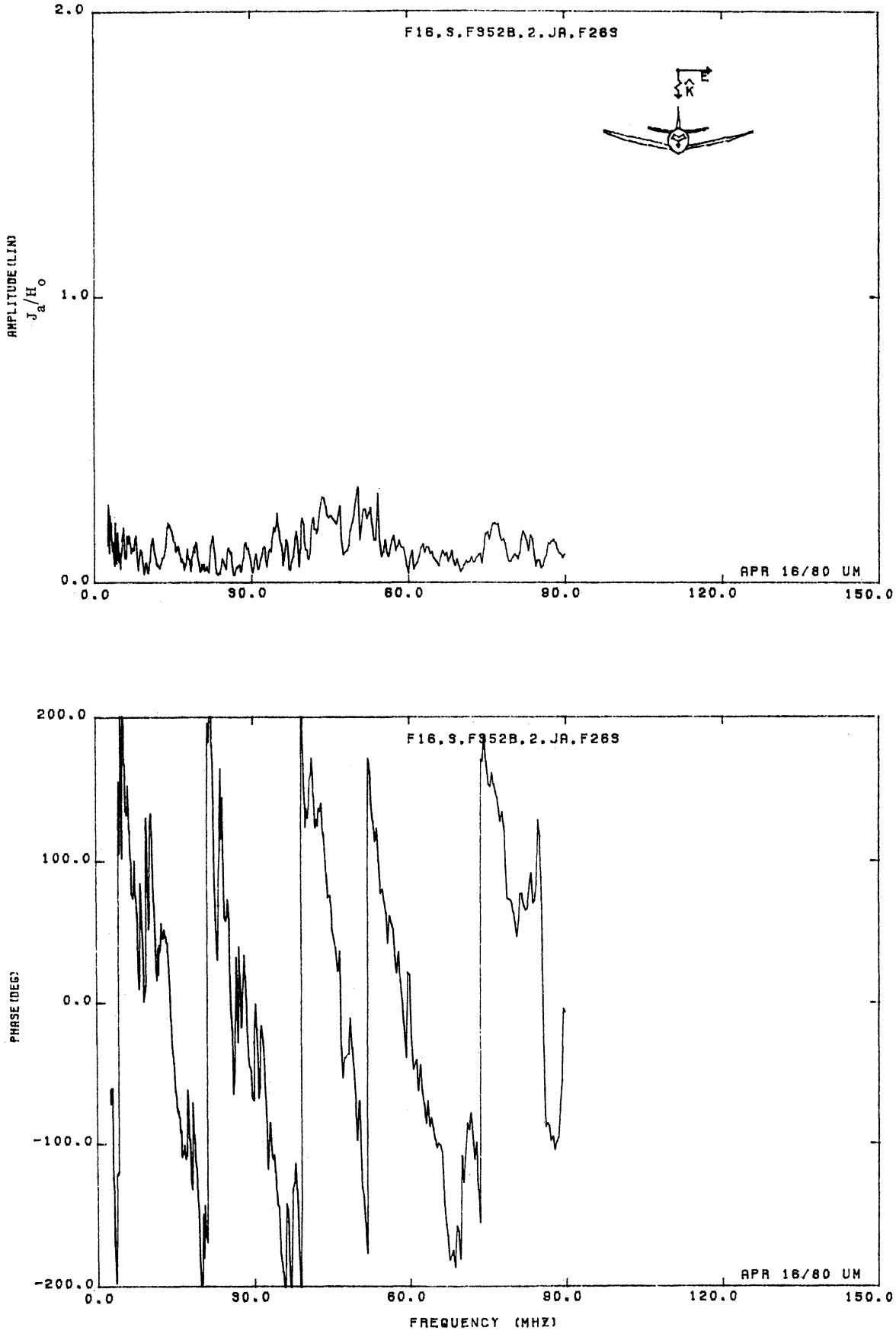

Figure 26S. Axial Current at STA:F352B, Excitation 2, 1/48 Model.

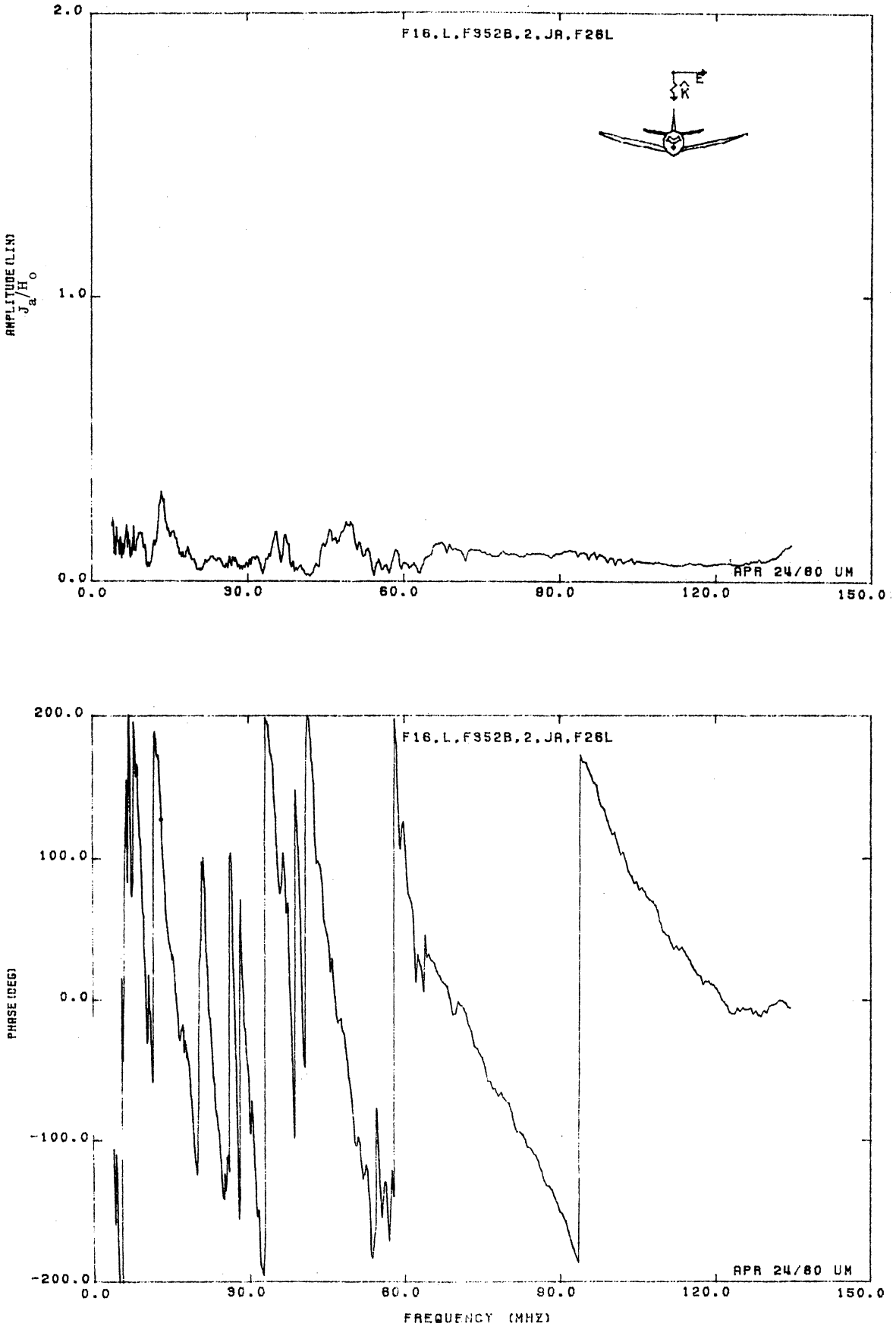

Figure 26L. Axial Current at STA:F352B, Excitation 2, 1/32 Model.

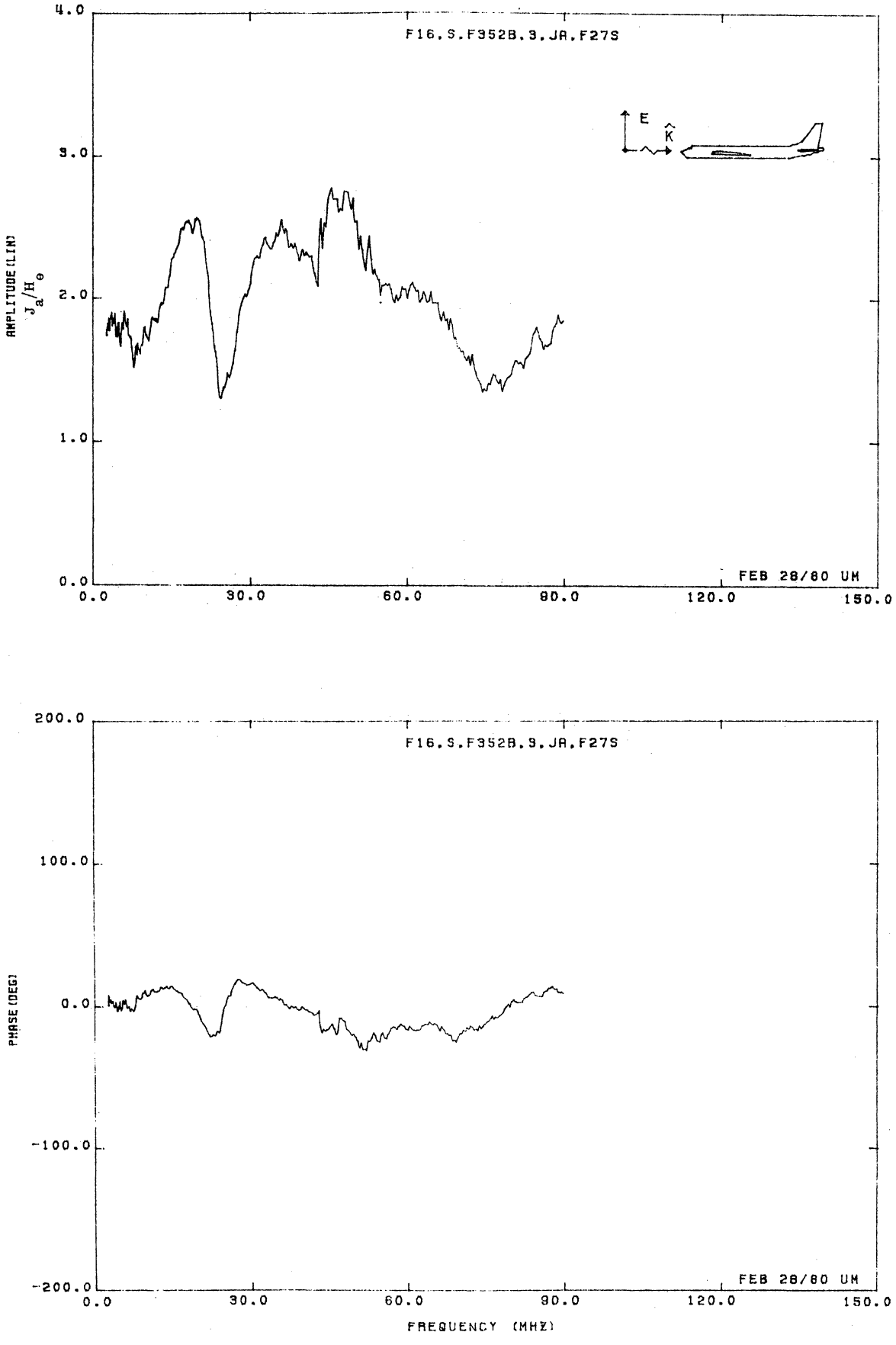

Figure 27S. Axial Current at STA:F352B, Excitation 3, 1/48 Model.

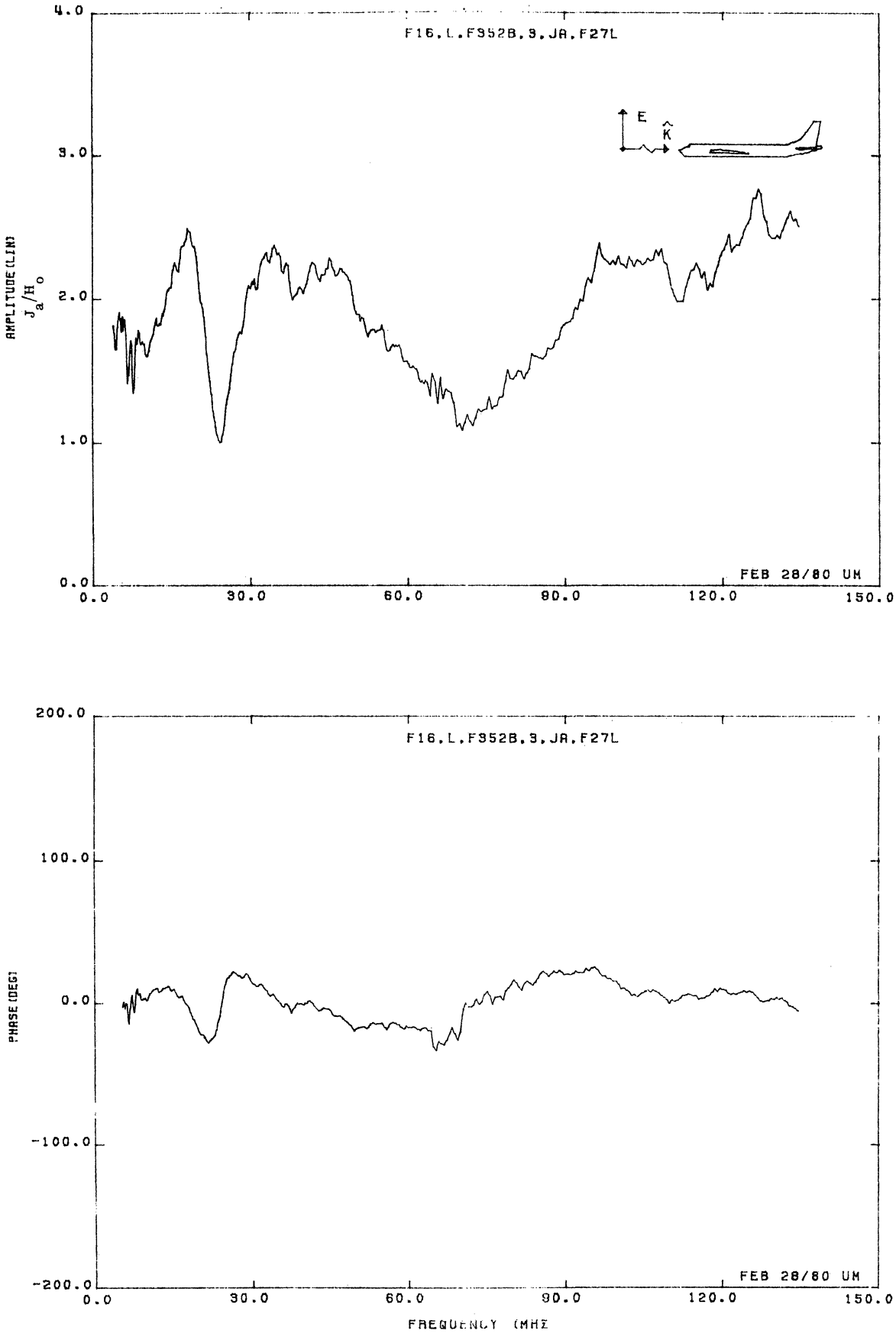

Figure 27L. Axial Current at STA:F352B, Excitation 3, 1/32 Model.

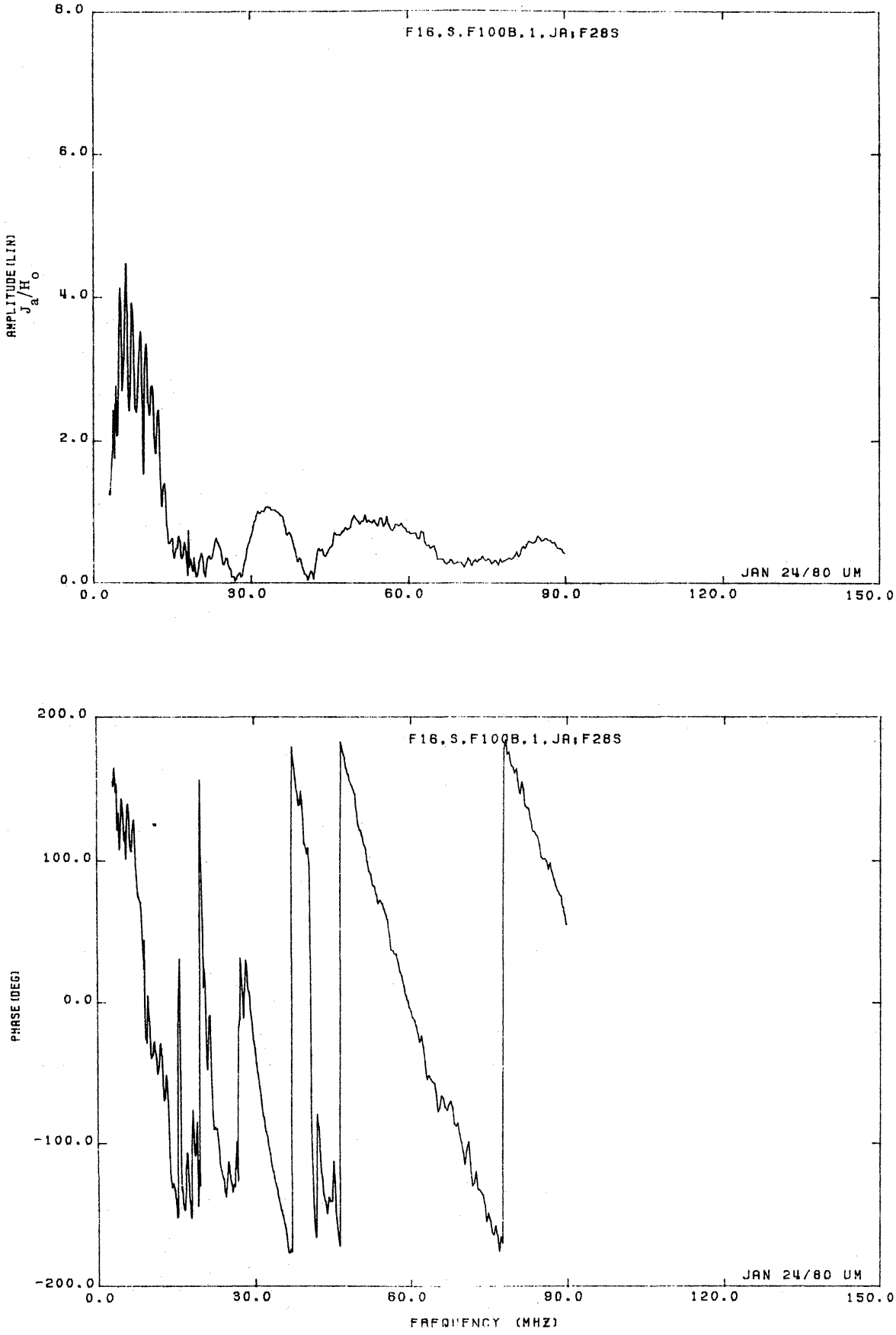

Figure 28S. Axial Current at STA:F100B, Excitation 1, 1/48 Model.

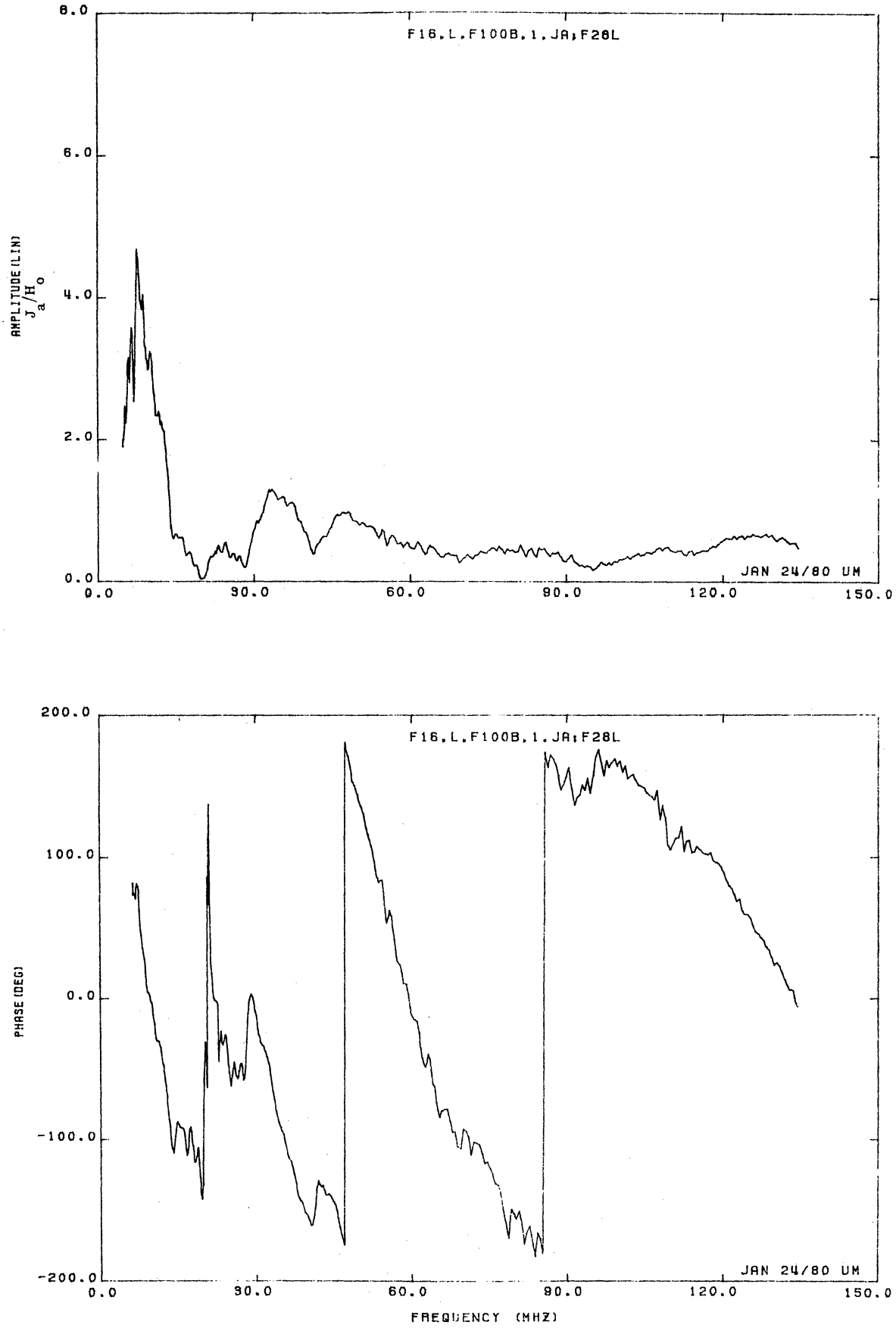

Figure 28L. Axial Current at STA:F100B, Excitation 1, 1/32 Model.

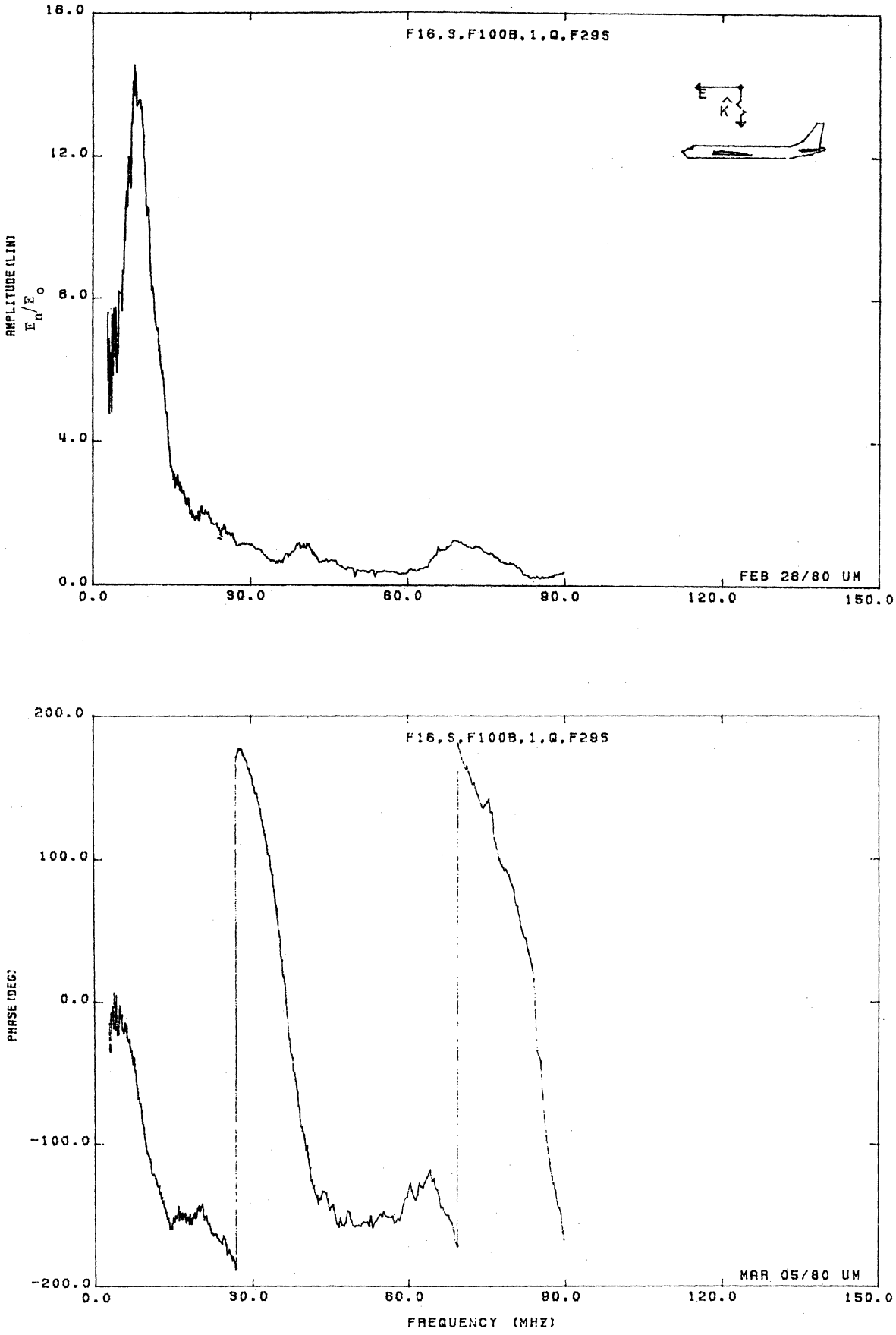

Figure 29S. Normal Electric Field at STA:F100B, Excitation 1, 1/48 Model.

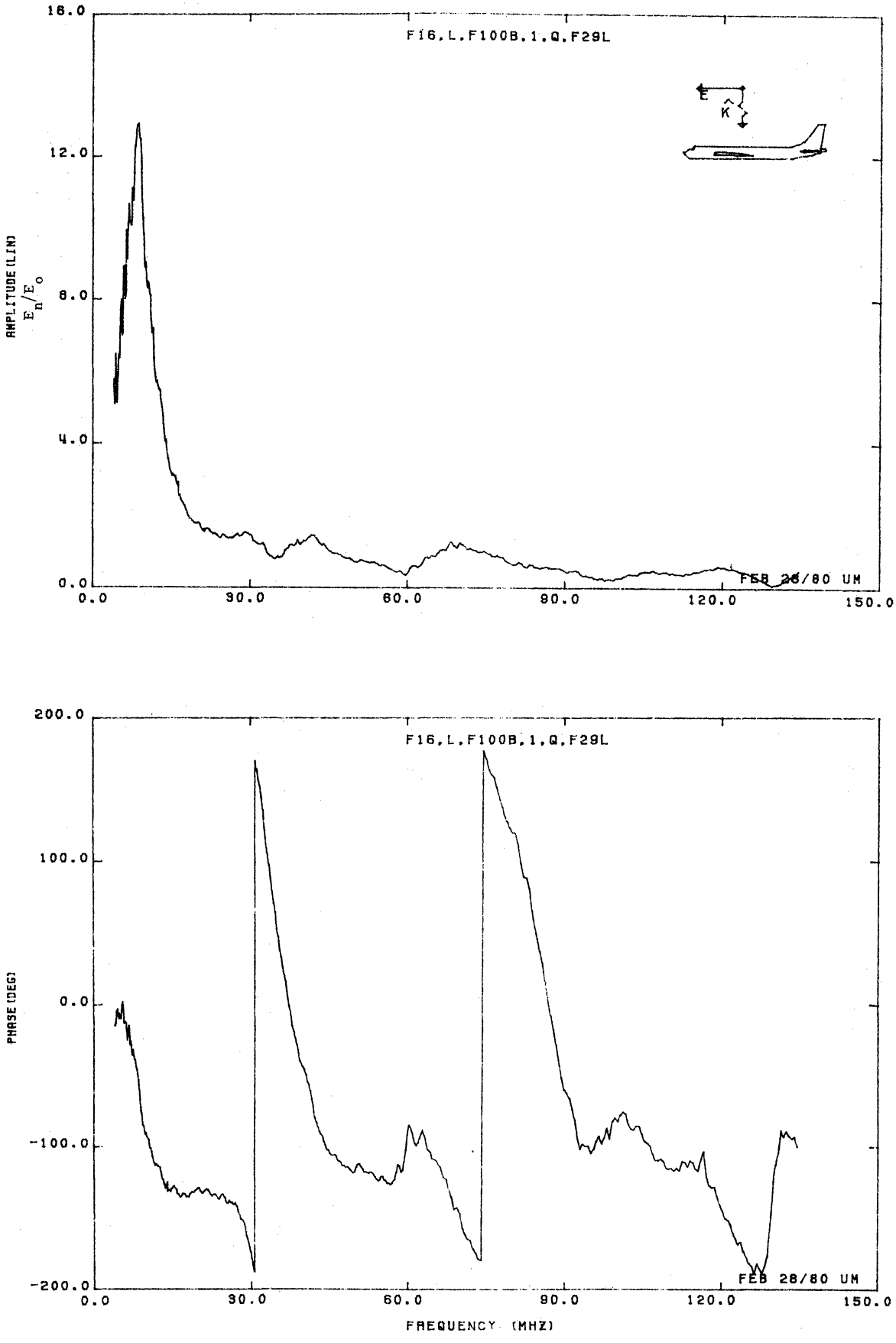

Figure 29L. Normal Electric Field at STA:F100B, Excitation 1, 1/32 Model.

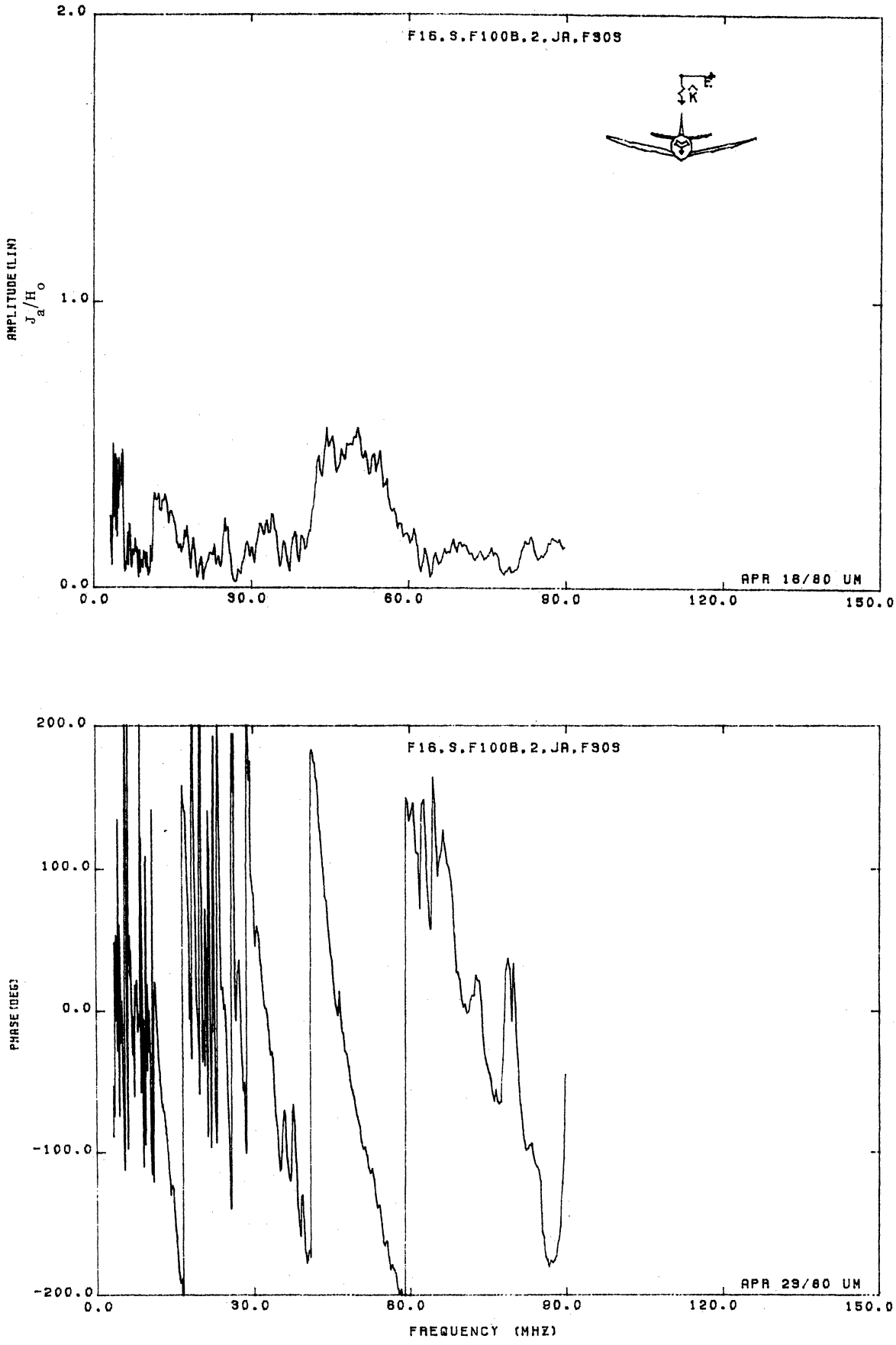

Figure 30S. Axial Current at STA:F100B, Excitation 2, 1/48 Model.

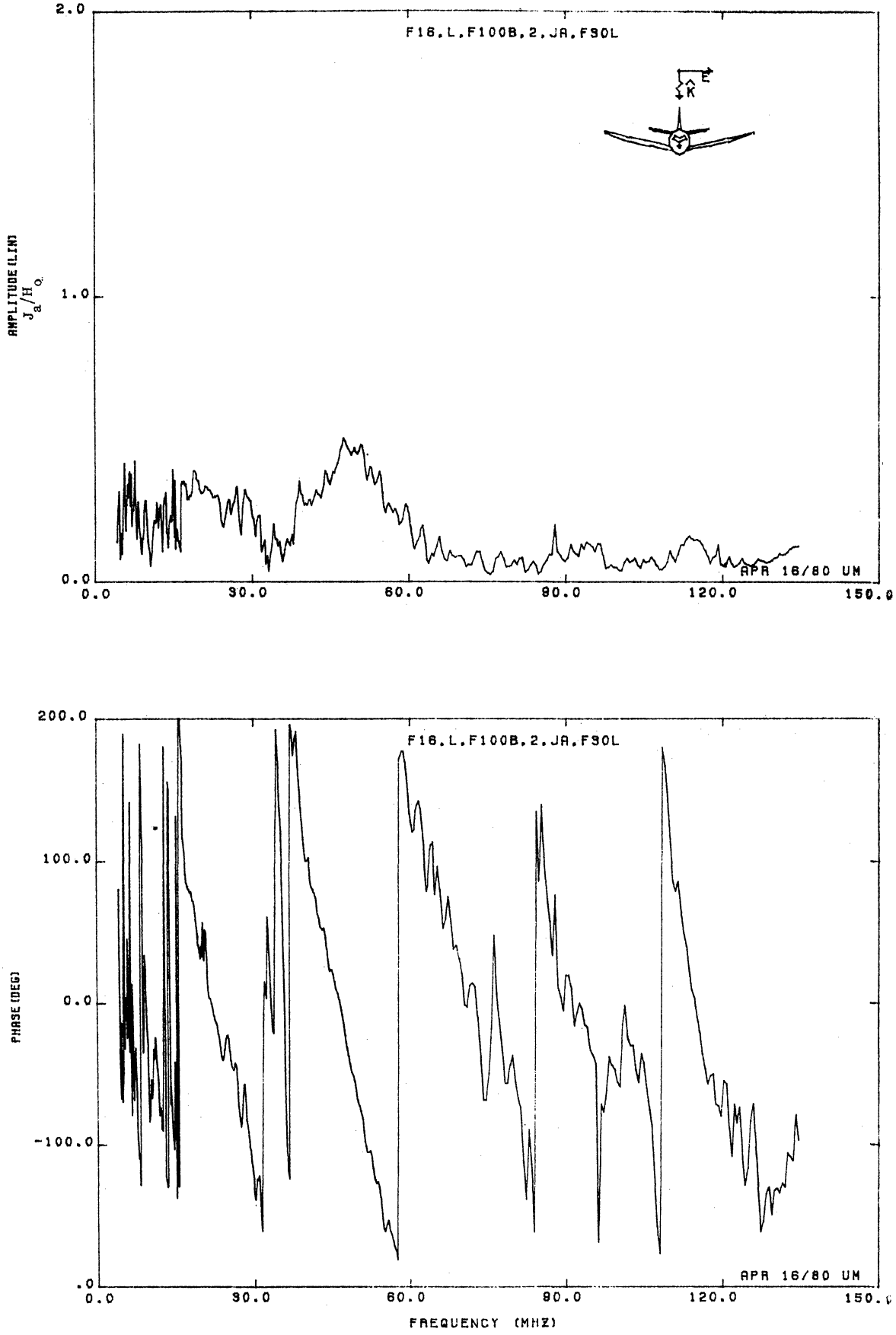

Figure 30L. Axial Current at STA:F100B, Excitation 2, 1/32 Model.

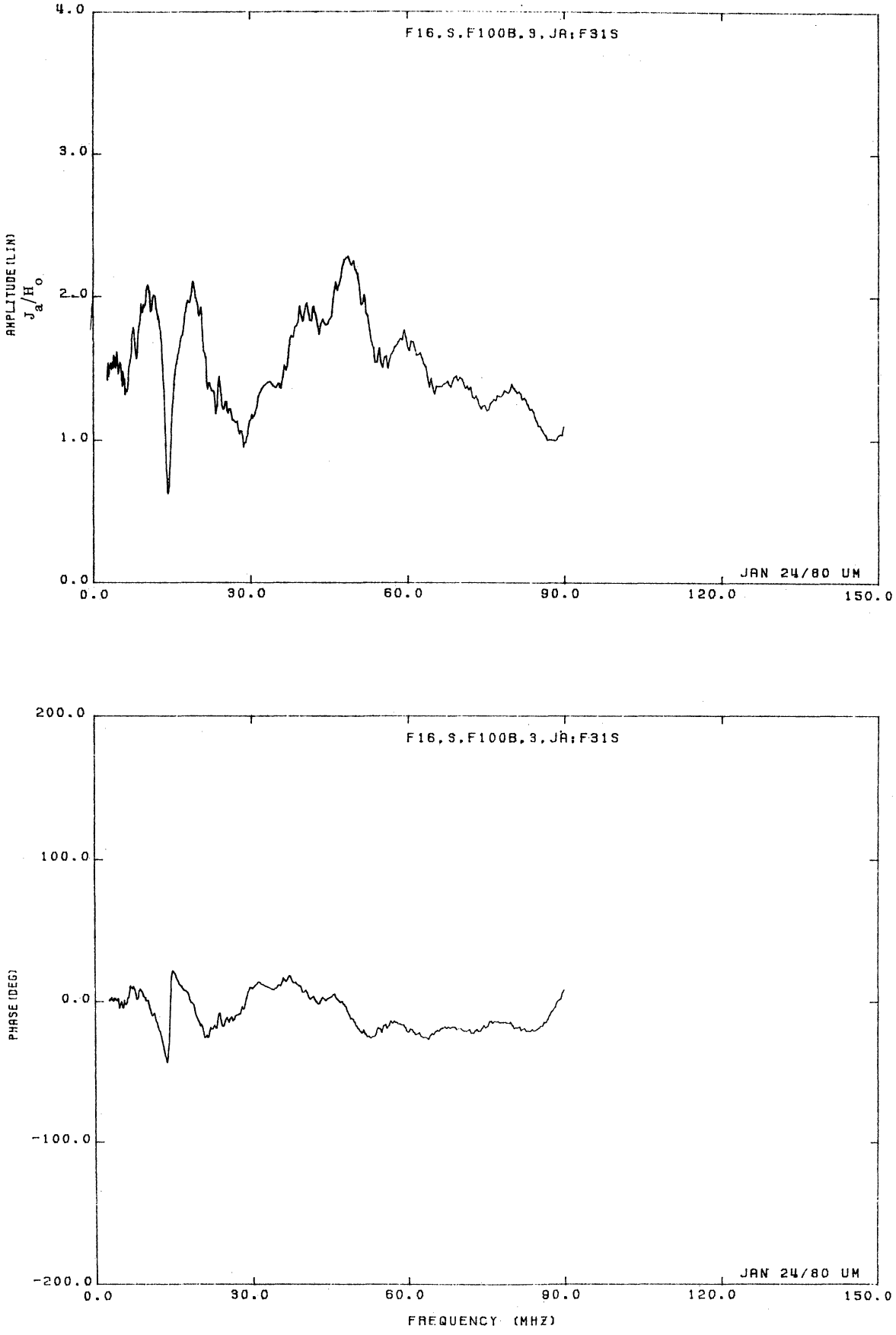

Figure 31S. Axial Current at STA:F100B, Excitation 3, 1/48 Model.

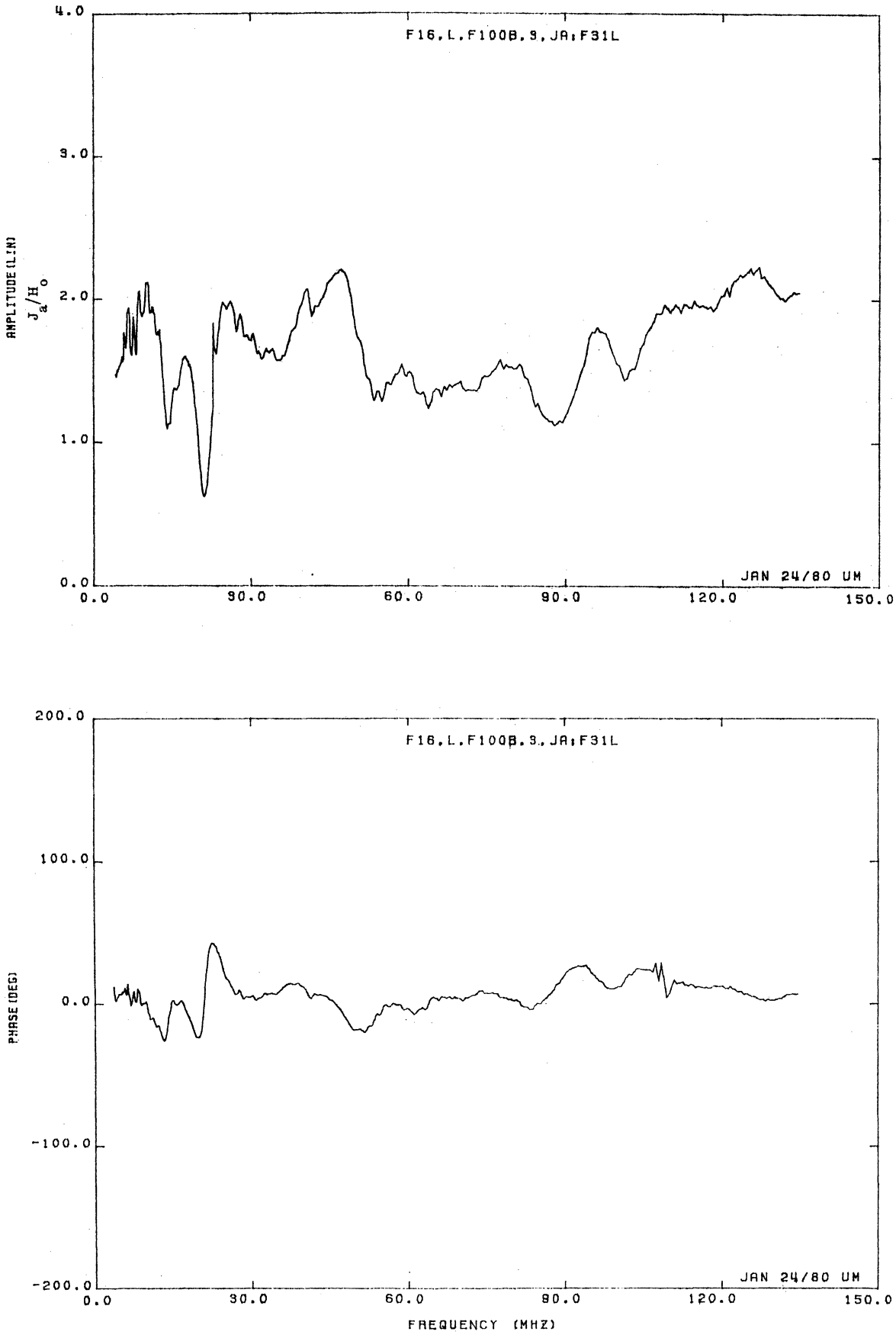

Figure 31L. Axial Current at STA:F100B, Excitation 3, 1/32 Model.

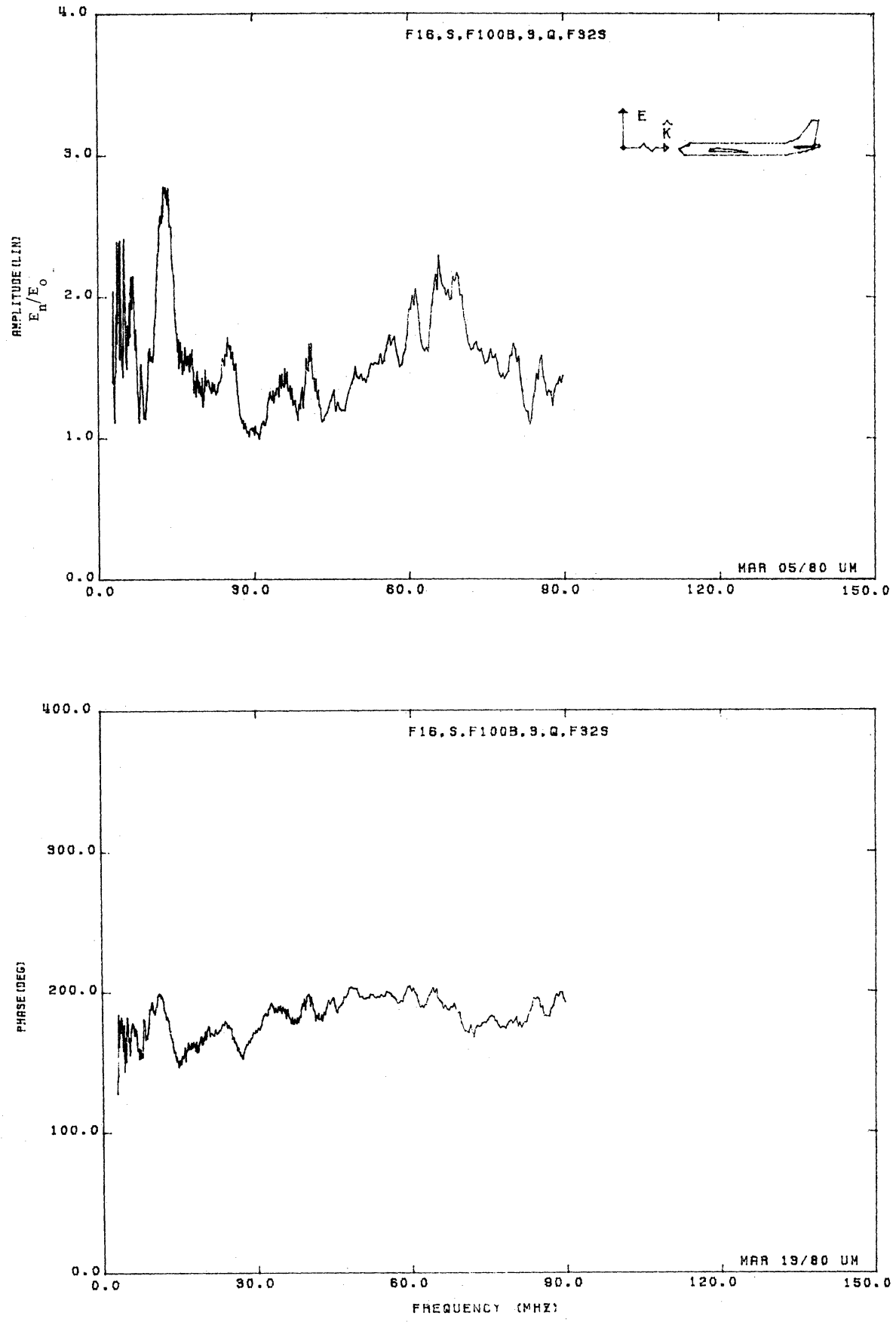

Figure 32S. Normal Electric Field at STA:F100B, Excitation 3, 1/48 Model.

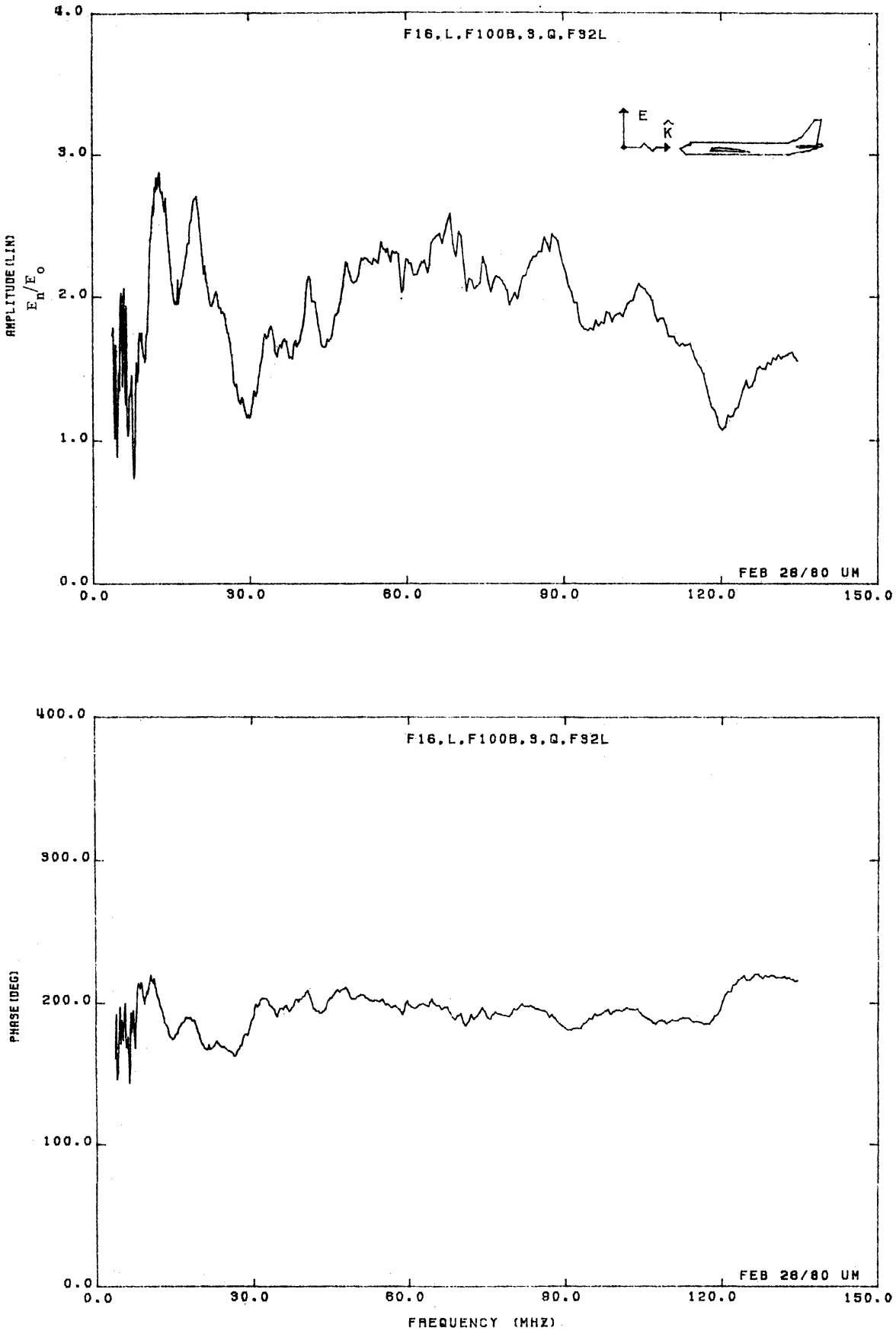

Figure 32L. Normal Electric Field at STA:F100B, Excitation 3, 1/32 Model.

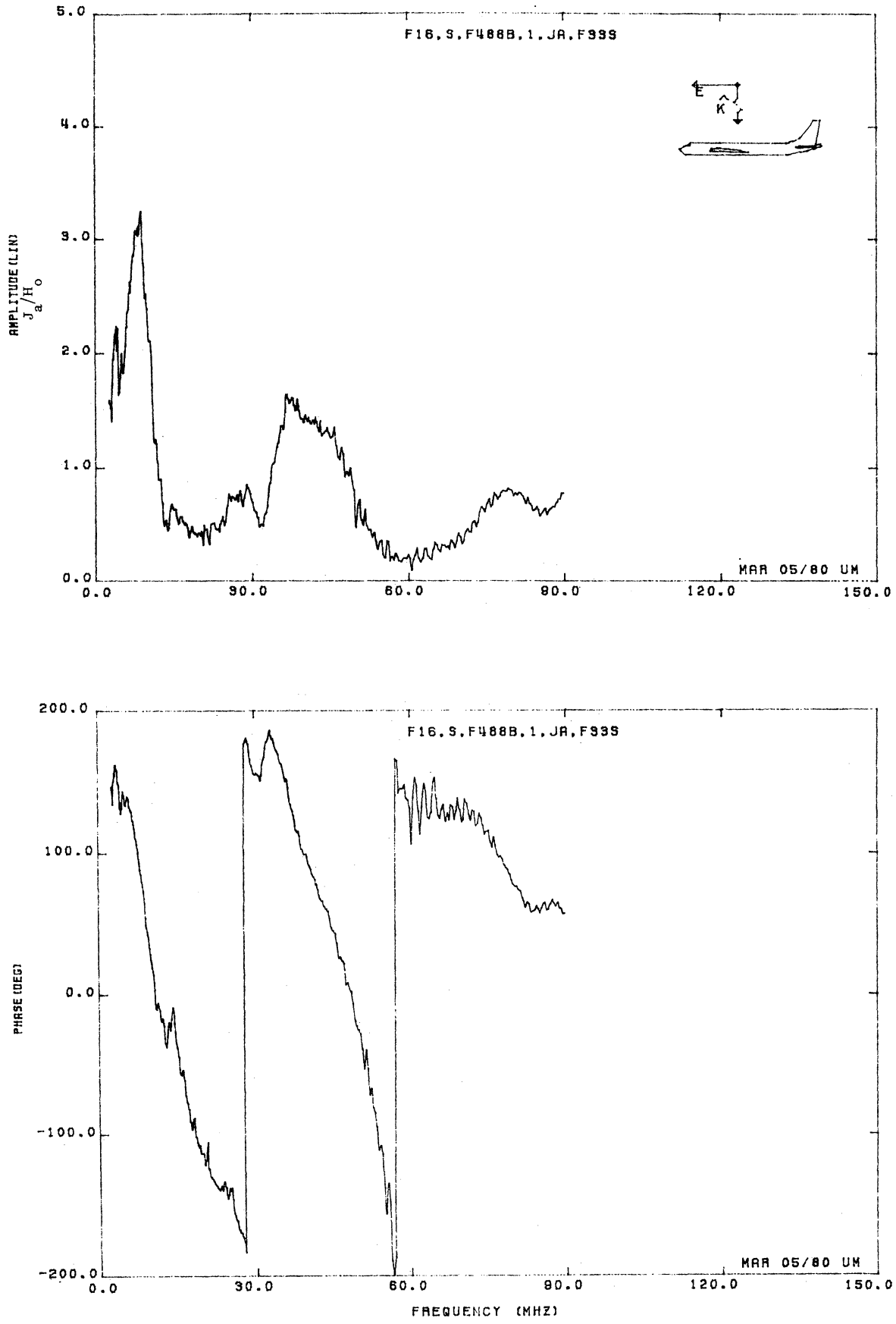

Figure 33S. Axial Current at STA:F488B, Excitation 1, 1/48 Model.

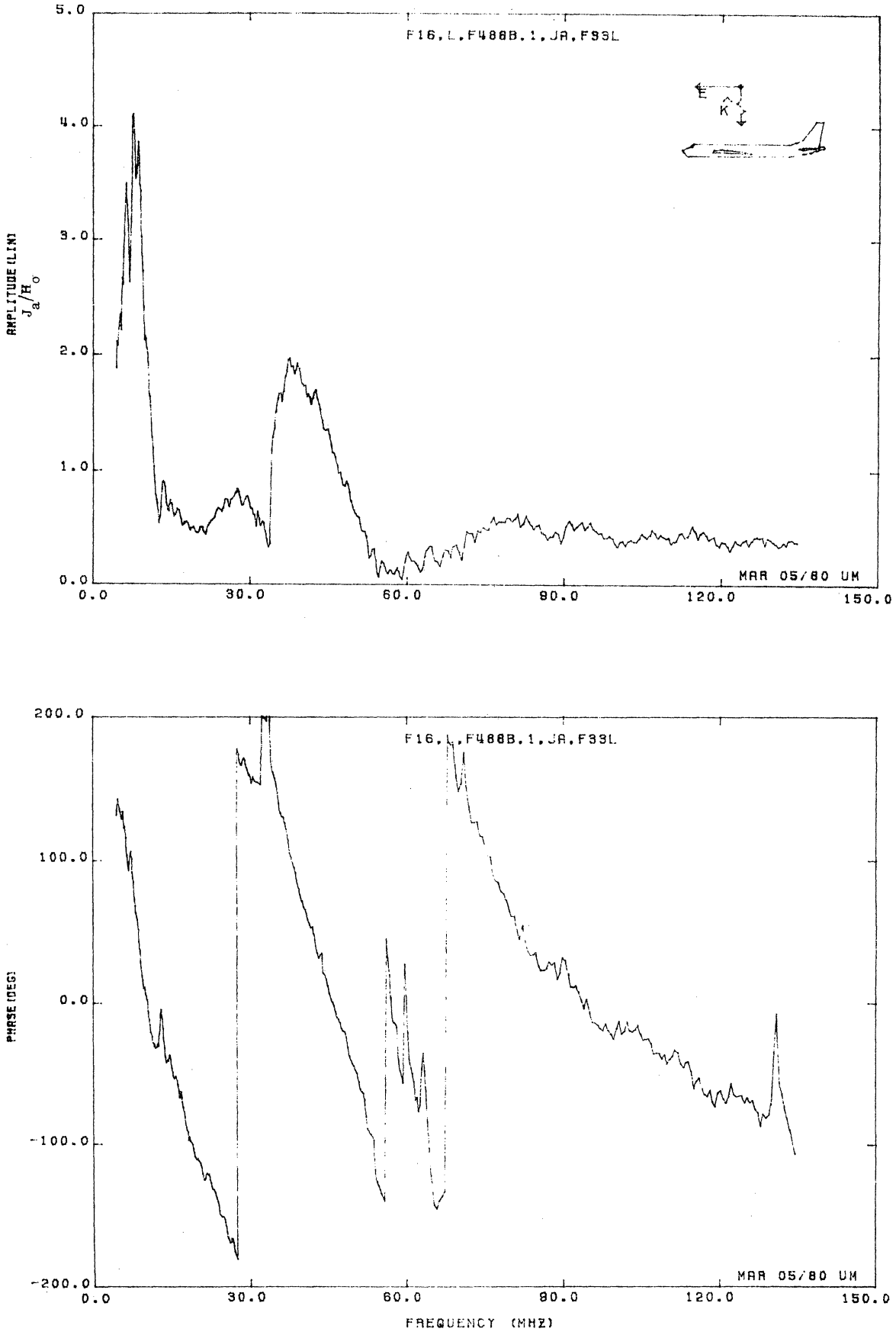

Figure 33L. Axial Current at STA:F488B, Excitation 1, 1/32 Model.

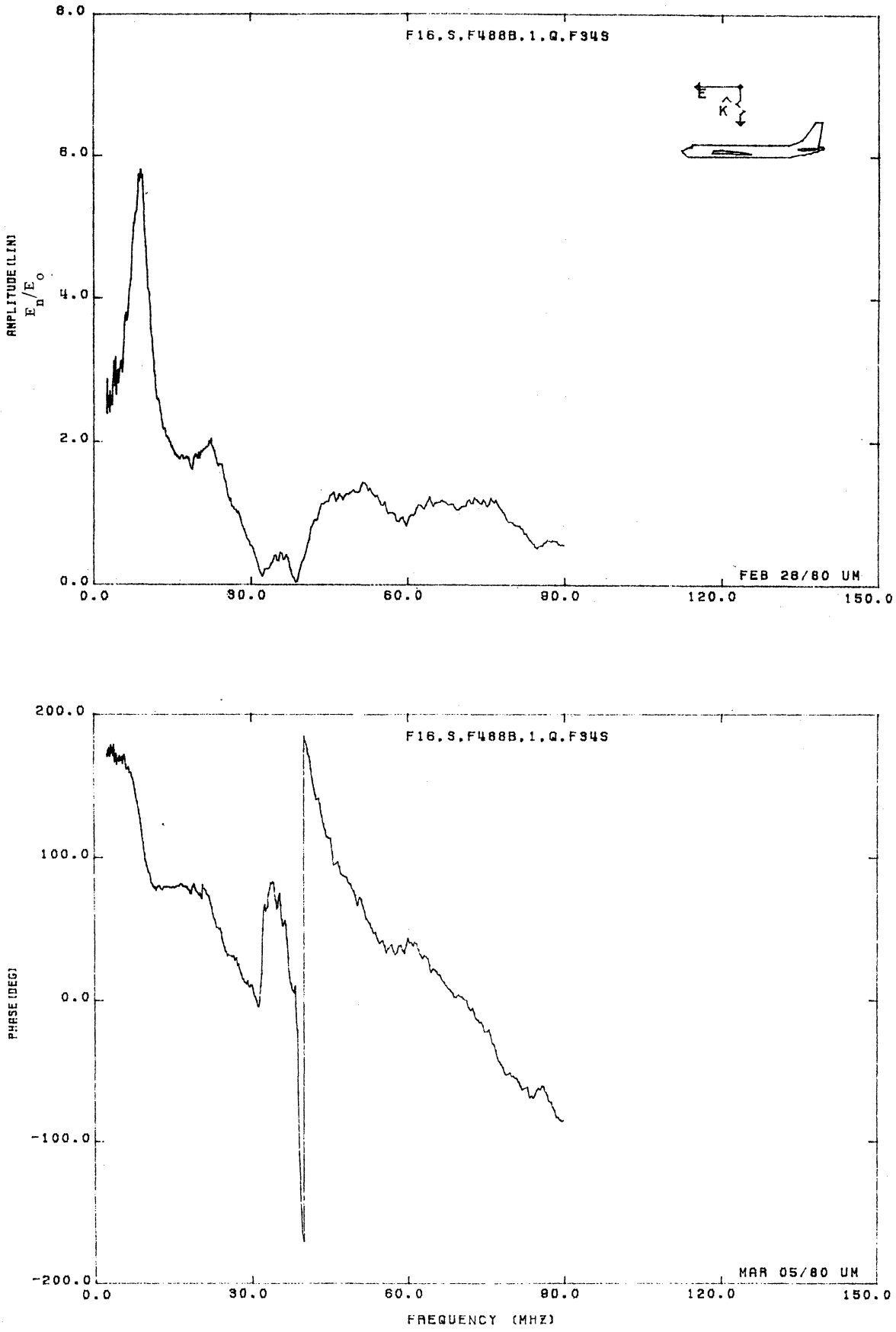

Figure 34S. Normal Electric Field at STA:F488B, Excitation 1, 1/48 Model.

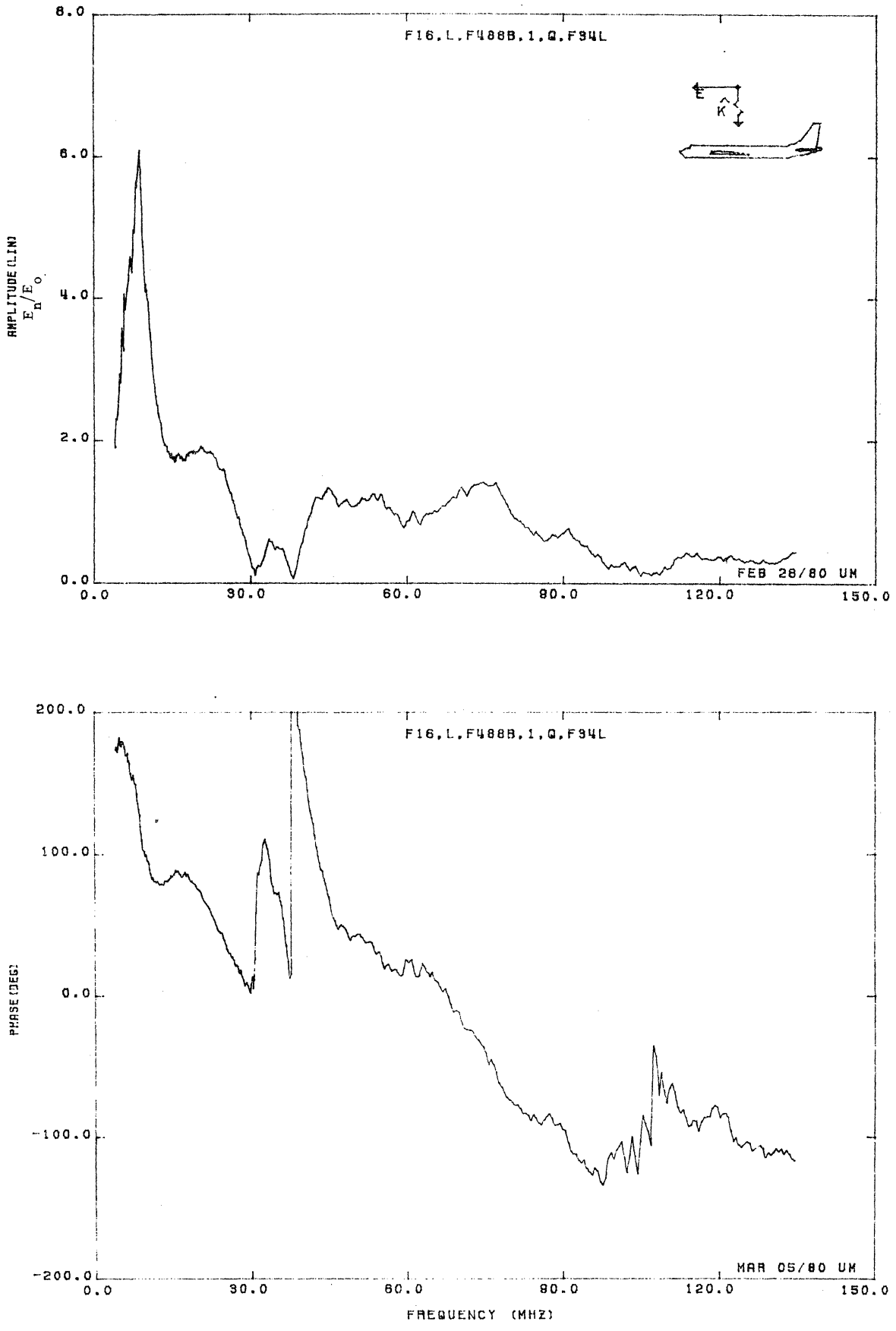

Figure 34L. Normal Electric Field at STA:F488B, Excitation 1, 1/32 Model.

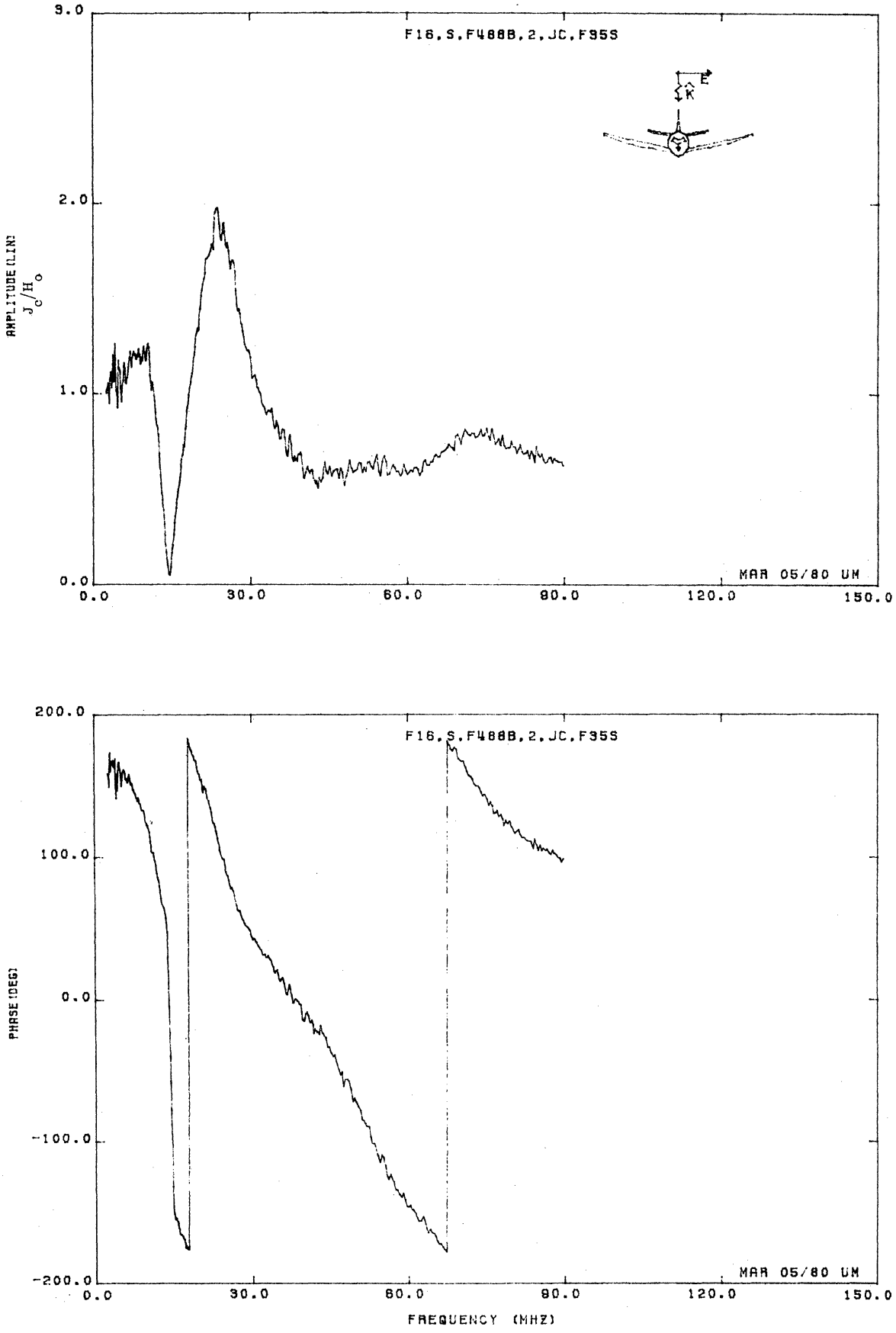

Figure 35S. Circumferential Current at STA:F488B, Excitation 2, 1/48 Model.

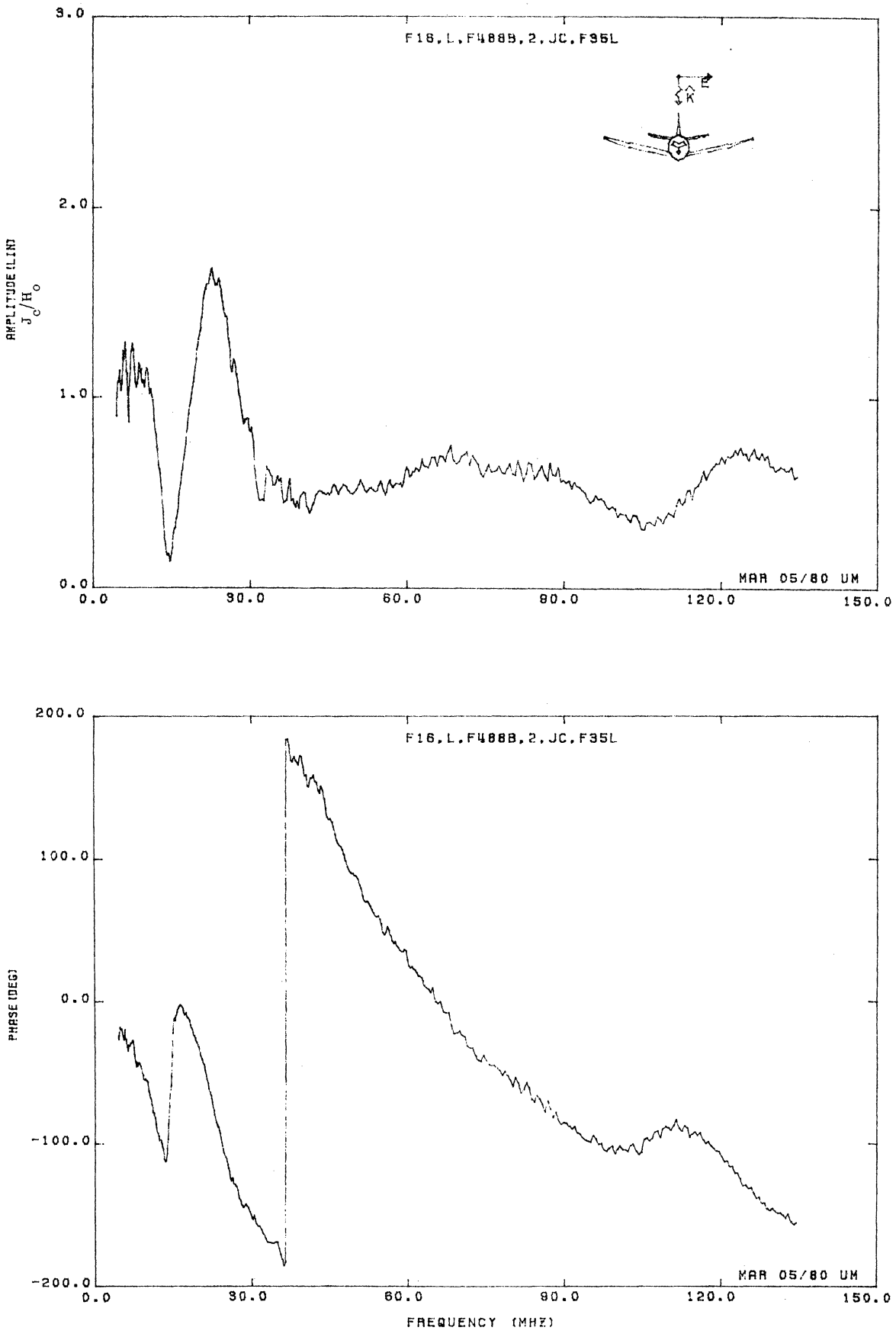

Figure 35L. Circumferential Current at STA:488B, Excitation 2, 1/32 Model.

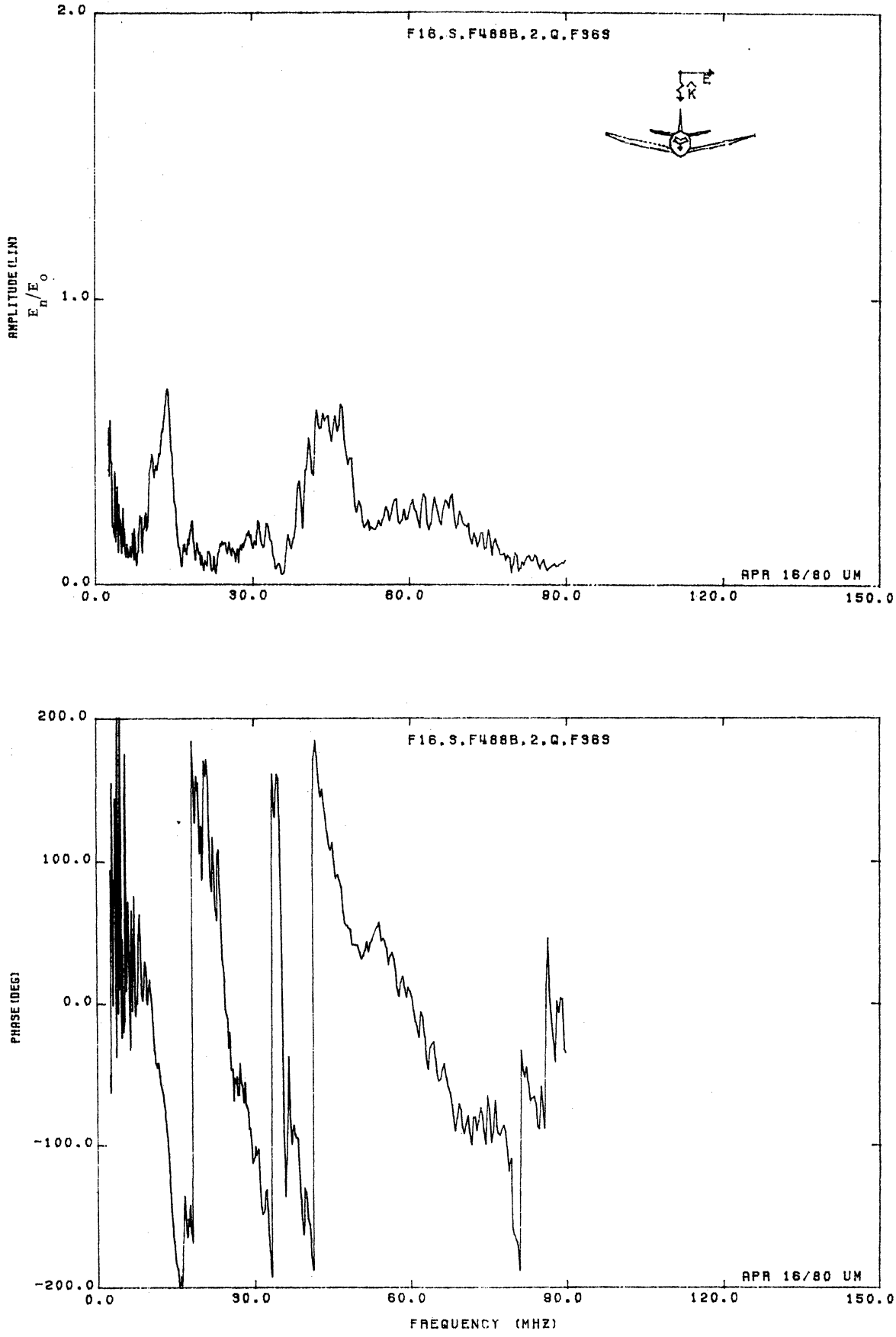

Figure 36S. Normal Electric Field at STA:F488B, Excitation 2, 1/48 Model.

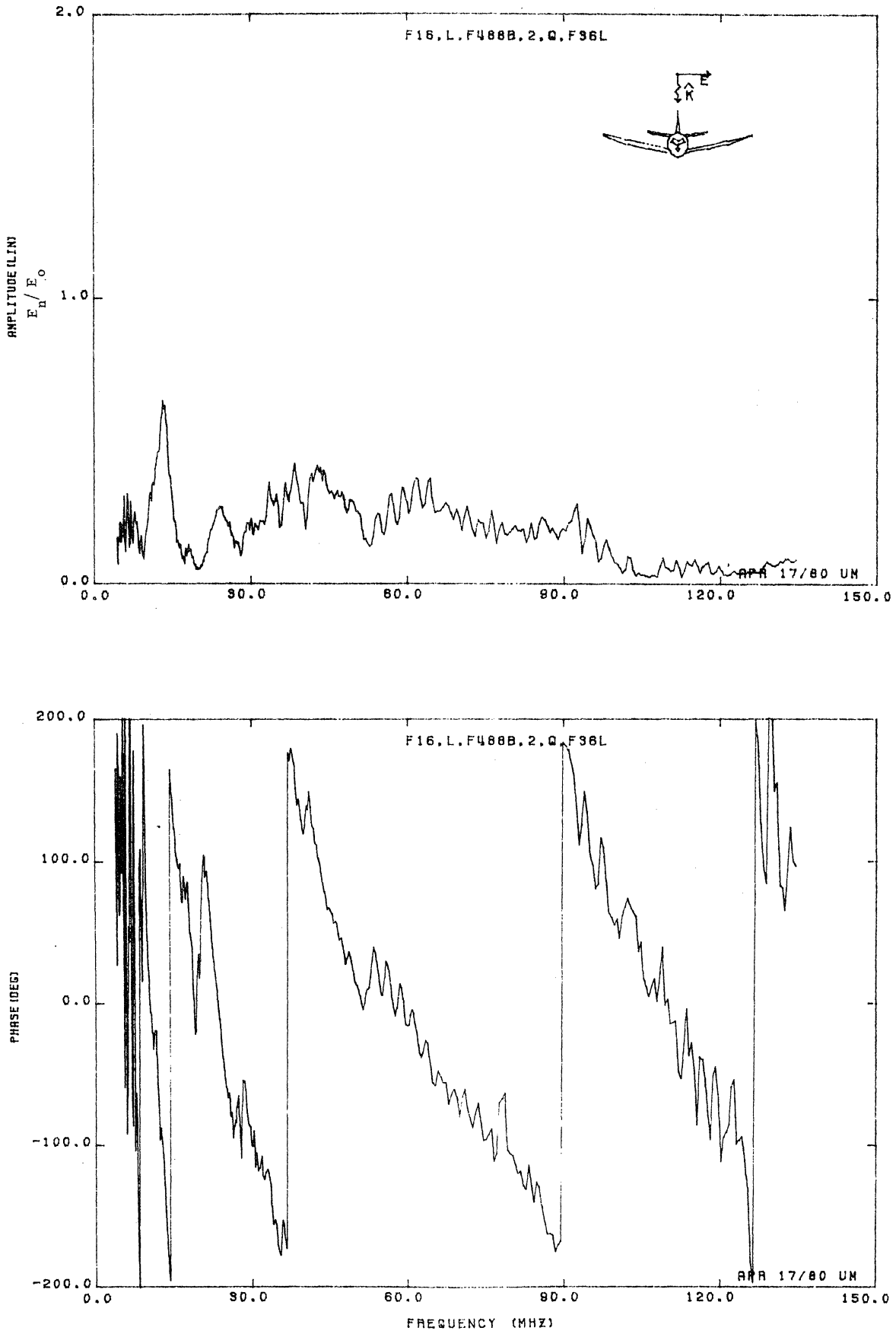

Figure 36L. Normal Electric Field at STA:F488B, Excitation 2, 1/32 Model.

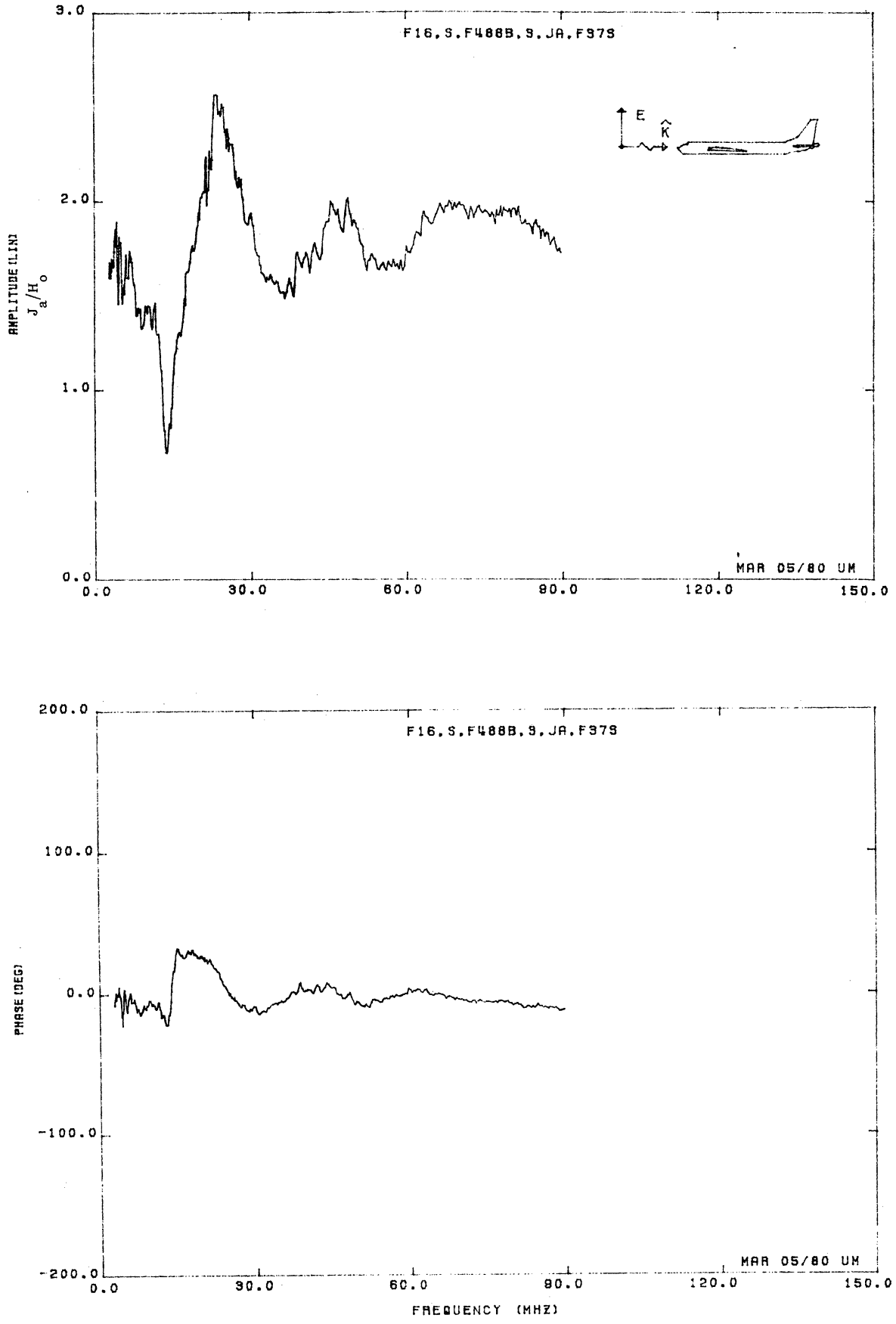

Figure 37S. Axial Current at STA:F488B, Excitation 3, 1/48 Model.

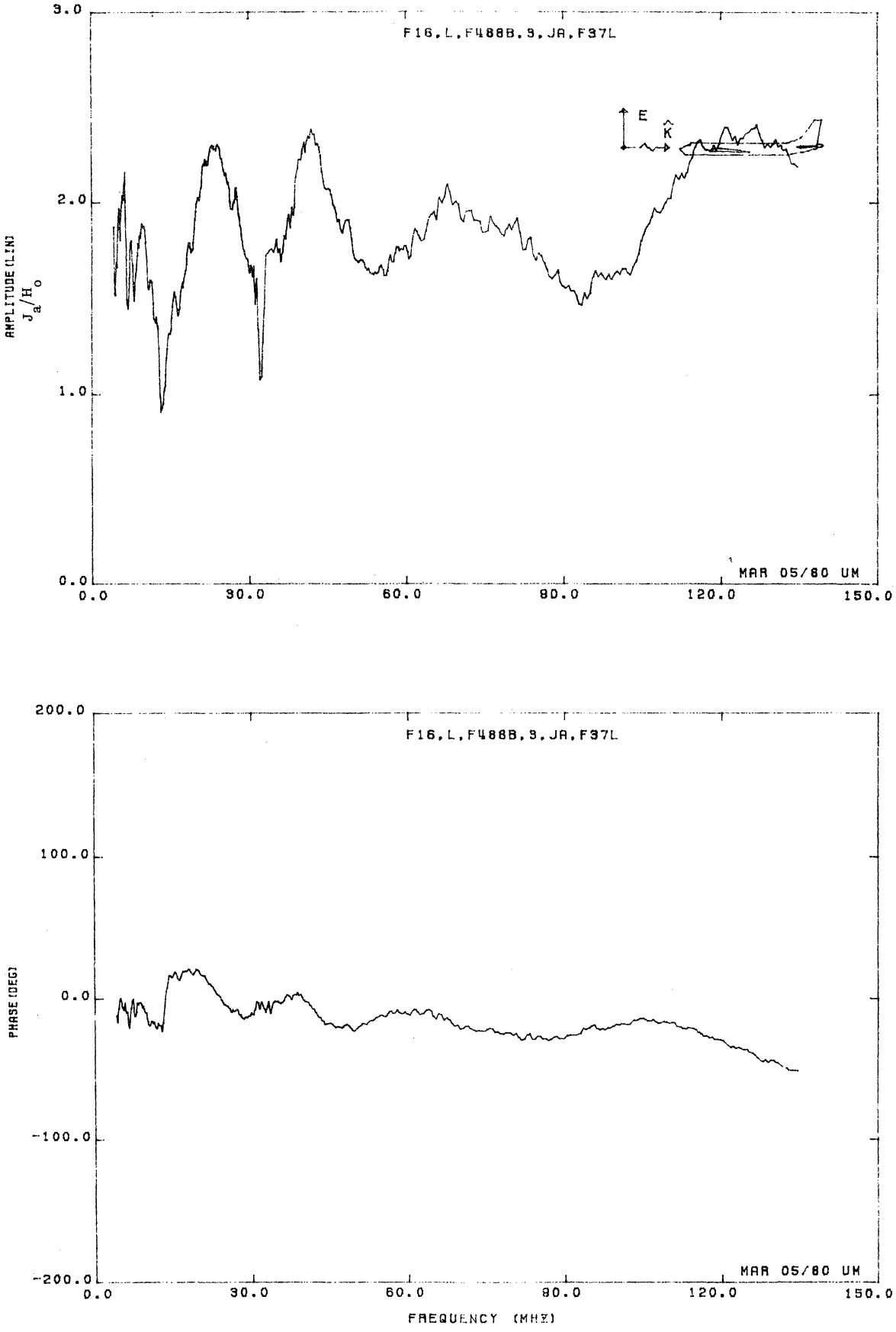

Figure 37L. Axial Current at STA:F488B, Excitation 3, 1/32 Model.

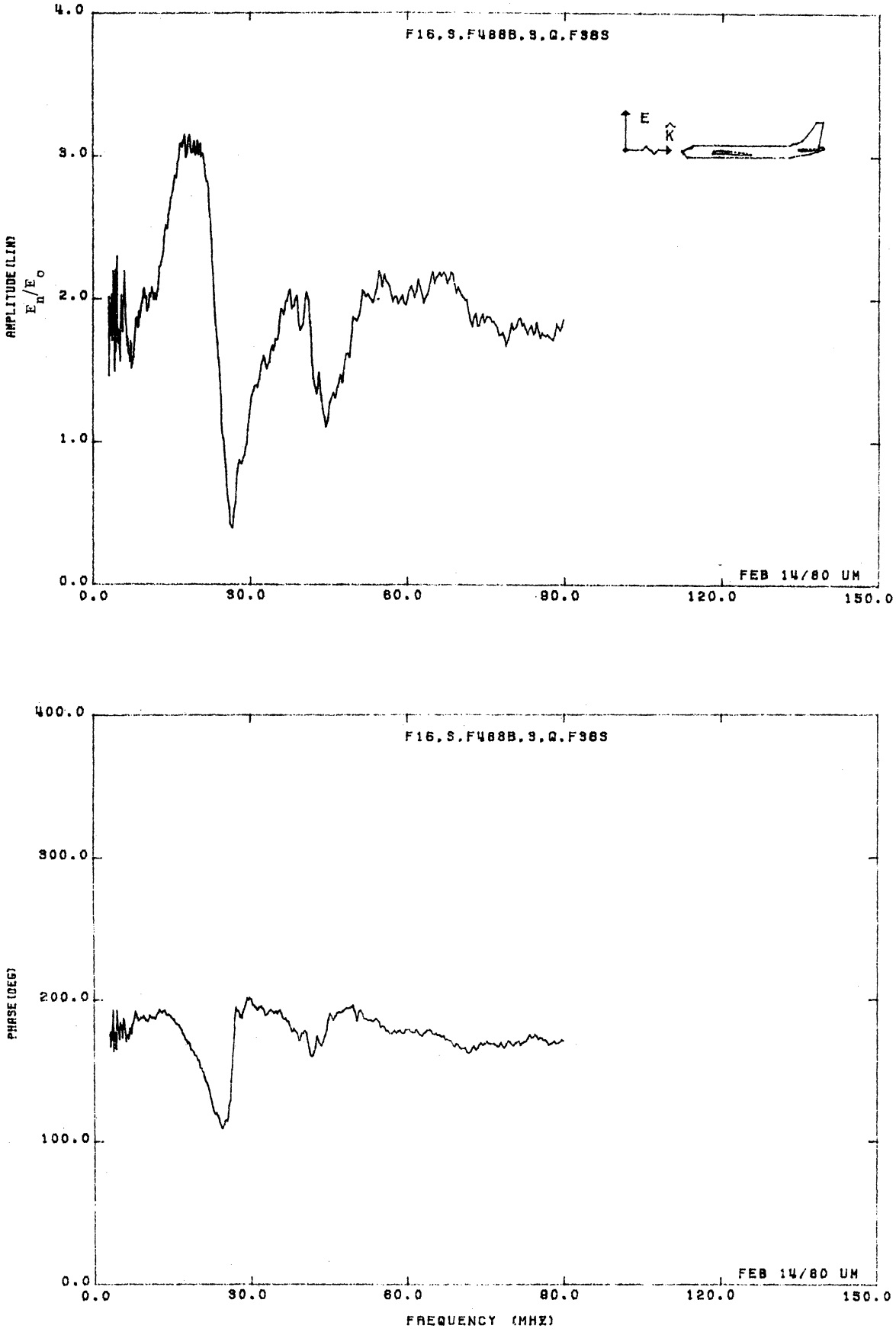

Figure 38S. Normal Electric Field at STA:F488B, Excitation 3, 1/48 Model.

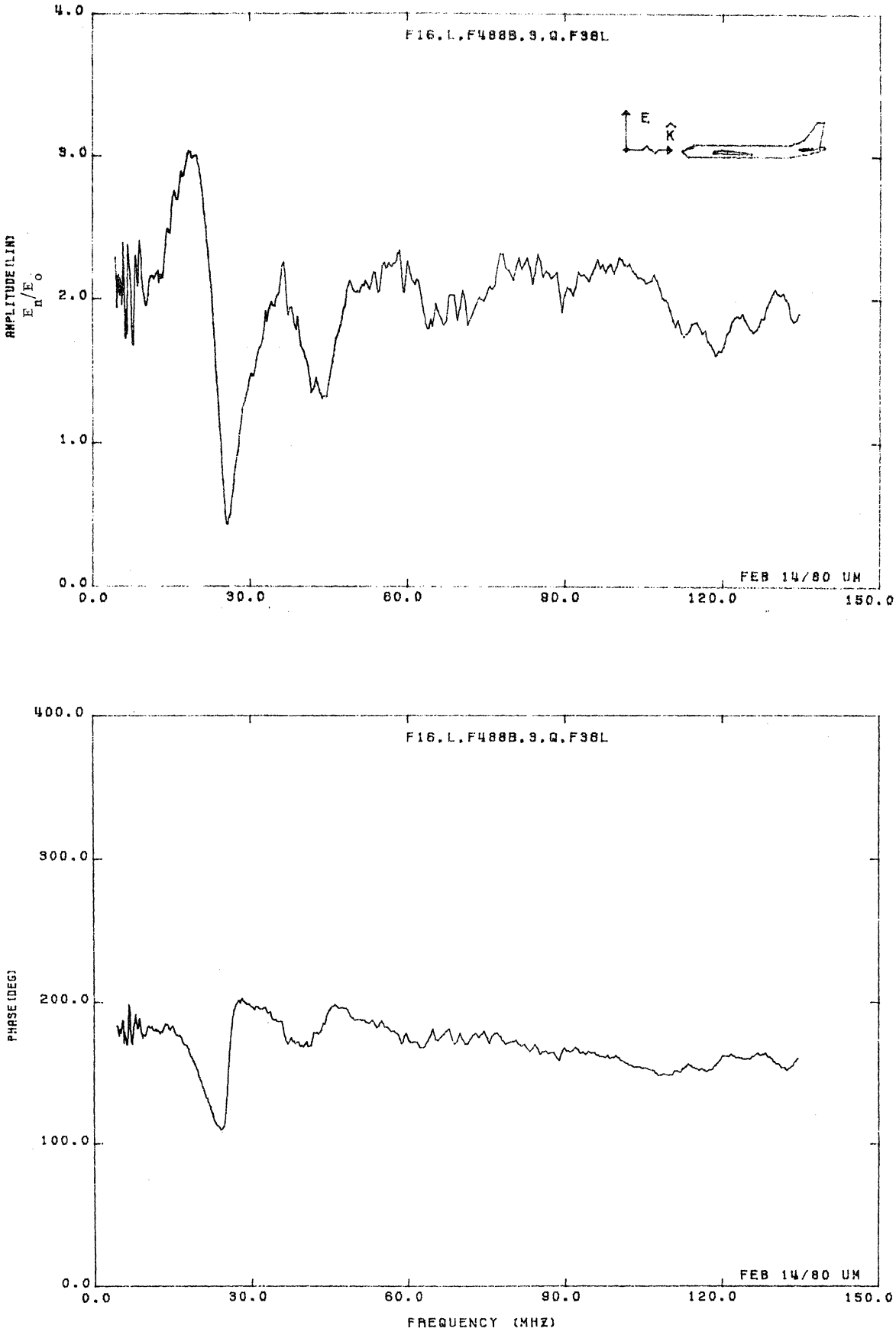

Figure 38L. Normal Electric Field at STA:F488B, Excitation 3, 1/32 Model.

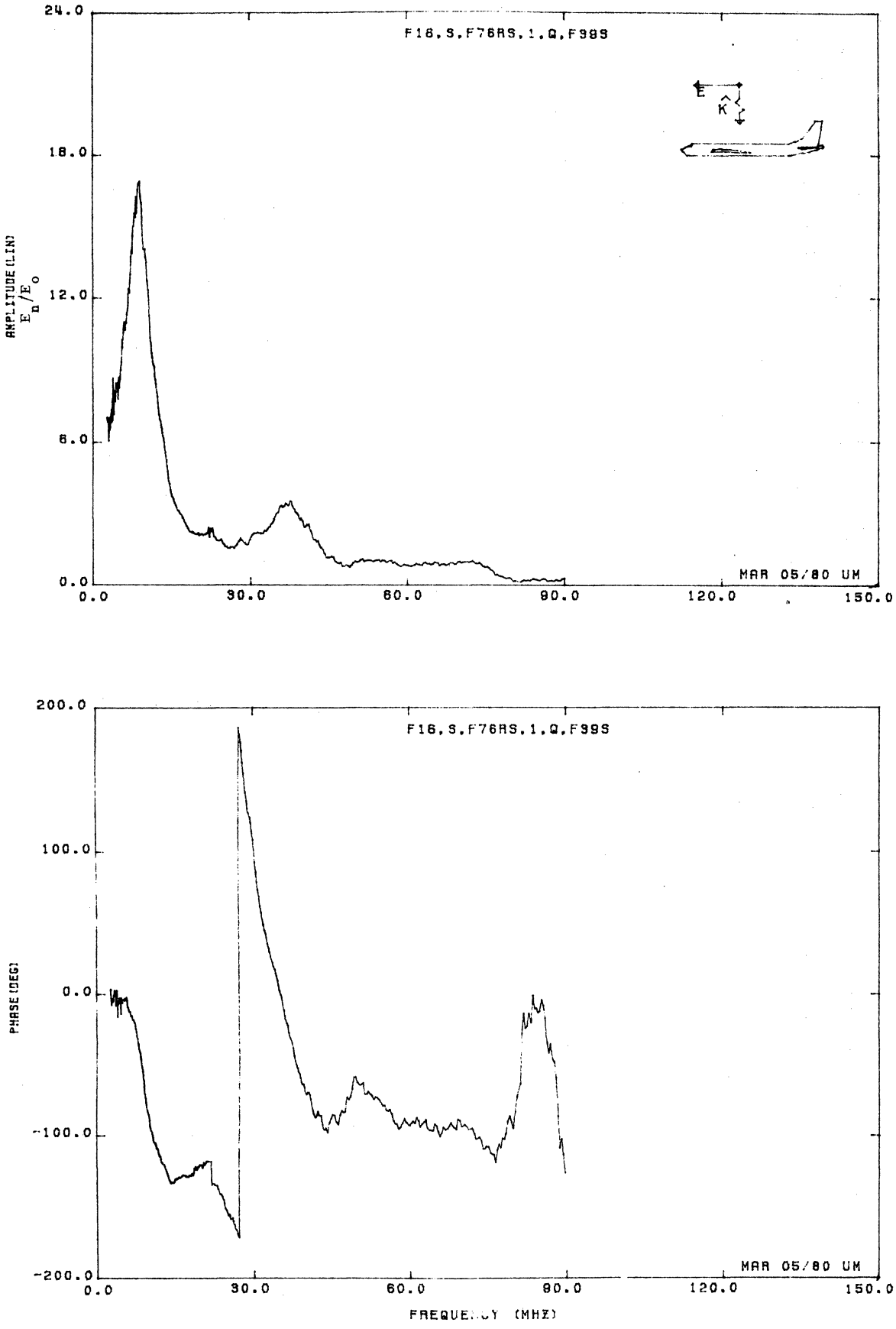

Figure 39S. Normal Electric Field at STA:F76RS, Excitation 1, 1/48 Model.

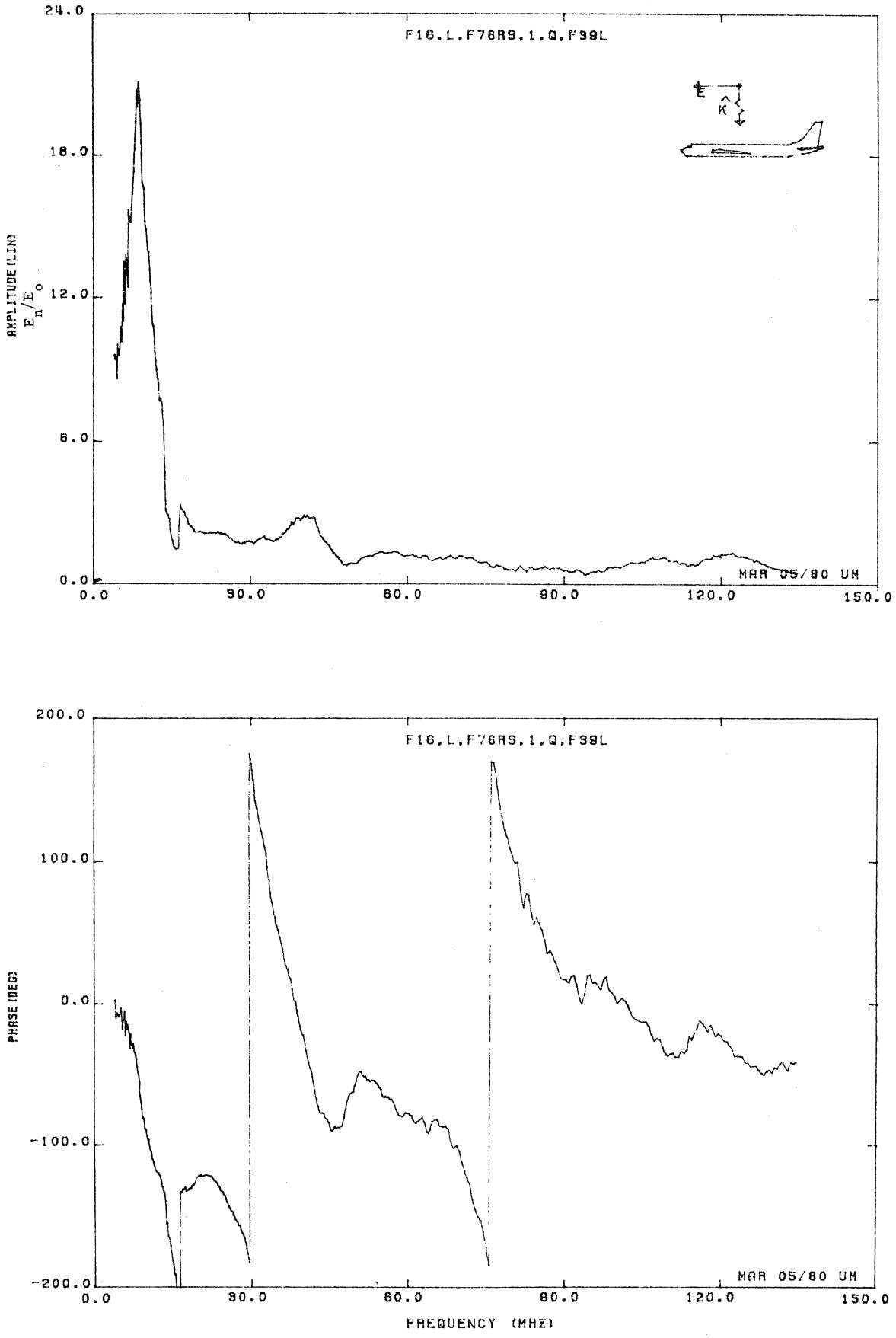

Figure 39L. Normal Electric Field at STA:F76RS, Excitation 1, 1/32 Model.

UNIVERSITY OF MICHIGAN
3 9015 03483 7271